UNIVERSITY OF READING

# A Survey of Operator Splitting Applied to Upwind Differencing

J.J. Barley

Numerical Analysis Report 2/88

Department of Mathematics

# A Survey of Operator Splitting Applied to Upwind Differencing

J.J. Barley

Numerical Analysis Report 2/88

The work reported here forms part of the Research Programme of the Oxford/Reading Institute for Computational Fluid Dynamics.

Contents

Abstract

A study is made of operator splitting methods for two-dimensional hyperbolic problems with application to various test problems. Particular emphasis is given to upwind differencing schemes for non-linear systems of equations and some analysis is given for simple cases. The results presented give insight into the feasibility of using split schemes for two-dimensional conservation laws and the circumstances in which genuinely two-dimensional schemes may be necessary.

## §1 Introduction

In a paper by Strang [1] a procedure for solving two-dimensional systems of partial differential equations is presented. This procedure, often called operator splitting, has been a tool commonly used in solving multi-dimensional fluid flow problems such as those governed by the inviscid Euler equations.

The underlying strategy involved in operator splitting is to replace the system of equations in n dimensions by n one-dimensional systems. Each one-dimensional system is solved by some suitable method and the solutions recombined in a suitable manner to yield an approximate solution to the full problem.

In this report we consider three different techniques of applying operator splitting and compare the application of these techniques to several two-dimensional test problems. Section 2 reviews Strang's paper in which two of the operator split methods are presented. The third split method being considered in this report is introduced in Section 4.

In Section 3 we consider upwinding methods in one-dimension and their use in solving the Euler equations. An analysis of various splitting strategies is given in Section 4. The test problems are stated in Section 5 and the results set out in the following section. A discussion of the results is given in Section 7.

## §2 The Technique of Operator Splitting

In a paper by Strang [1] a technique for solving, to second order accuracy, a stystem of linear first order hyperbolic partial differential equations was proposed. He dubbed the resulting methods as 'alternating direction schemes' and carried out an analysis of these schemes on the model problem

$$\left.\begin{aligned} \underset{\sim}{u}_t &= A\underset{\sim}{u}_x + B\underset{\sim}{u}_y \\ \underset{\sim}{u}(x,y,0) &= \underset{\sim}{u}_0(x,y) \end{aligned}\right\} \tag{2.1}$$

where A and B are symmetric constant matrices which do not necessarily commute.

The underlying philosophy of such schemes is that the two-dimensional equation (2.1), may be split into two one-dimensional equations, namely

$$\underset{\sim}{u}_t = A\underset{\sim}{u}_x \tag{2.2a}$$

$$\underset{\sim}{u}_t = B\underset{\sim}{u}_y \tag{2.2b}$$

and that solving both of these one-dimensional equations simultaneously is equivalent in some approximate sense to solving the two-dimensional equation (2.1). To demonstrate this in the linear case we recall the two-dimensional linear advection equation

$$\left.\begin{aligned} u_t + au_x + bu_y &= 0 \\ u(x,y,t) &= u_o(x,y) \end{aligned}\right\} \qquad (2.3)$$

which has solution

$$u(x,y,t) = u_o(x - at\ ,\ y - bt)\ ,$$

can be split into two sibling equations

$$u_t + au_x = 0 \qquad (2.4a)$$

$$u_t + bu_y = 0\ . \qquad (2.4b)$$

If we now simultaneously integrate (2.4a) and (2.4b), remembering that (2.4a) is independent of y and (2.4b) is independent of x, along all lines y = constant and x = constant respectively (c.f. Section 4), then we arrive at the solutions

$$u(x,y,t) = u_o(x-at,\tilde{y}) \qquad (2.5a)$$

$$u(x,y,t) = u_o(\tilde{x},y-bt) \qquad (2.5b)$$

respectively, where

$$\tilde{x} = \tilde{x}(x,t)$$

$$\tilde{y} = \tilde{y}(y,t)$$

are two independent functions.

In obtaining these solutions, we have used the fact that data is preserved along the one-dimensional characteristics of (2.4a) and (2.4b) given by

$$x - at = \text{constant}$$

$$y - bt = \text{constant}$$

respectively. However, since the integrations are performed simultaneously, both characteristic equations are satisfied in solving (2.4a) and (2.4b). Hence

$$\tilde{x} = x - at$$

$$\tilde{y} = y - bt$$

and the solution is

$$u(x,y,t) = u_o(x-at,\ y-bt)$$

which is the solution of (2.3). This justifies the splitting in the linear case.

It is worth noting that if we split equation (2.3) such that its two sibling equation, when summed together, yield the original equation (2.3), i.e.

$$\tfrac{1}{2}u_t + au_x = 0 \qquad (2.6a)$$

$$\tfrac{1}{2}u_t + bu_y = 0 \qquad (2.6b)$$

then solving these two equations *simultaneously* yields the solution

$$u(x,y,t) = u(x-2at,\ y-2bt)$$

which is, of course, incorrect. In many places the sibling equations are written in the form of (2.6) rather than (2.4) indicating that the sibling equations are to be solved sequentially, which is then (in the linear case) equivalent to solving the full equation.

Returning now to Strang's paper, we look at the specific type of problem considered there and two of the operator split methods described.

As stated previously, the model problem is a first order linear system of hyperbolic partial differential equations

$$\left.\begin{aligned} \underset{\sim}{u}_t &= A\underset{\sim}{u}_x + B\underset{\sim}{u}_y \\ \underset{\sim}{u}(x,y,0) &= \underset{\sim}{u}_o(x,y) \end{aligned}\right\} \qquad (2.7)$$

The matrices A and B considered are constant and symmetric, but not necessarily commutable.

We shall require difference approximations to the partial differential equations to be second order (in the case of smooth data

without non-linear features such as discontinuities or shocks). Given a difference operator, $S_k$, which is a weighted sum of translations,

$$(S_k \underset{\sim}{f})(x,y) = \sum_{i,j} C_{i,j} \underset{\sim}{f}(x+ih, y+jh) \tag{2.8}$$

where $C_{i,j}$ are constant coeffficent matrices, we can define the order of accuracy by comparing $S_k \underset{\sim}{u}$ with the Taylor expansion of $\underset{\sim}{u}(x,y,t+k)$. For second order accuracy, given that $\underset{\sim}{u}$ is a smooth solution, we shall require that

$$S_k \underset{\sim}{u} = \underset{\sim}{u} + k\underset{\sim}{u}_t + \frac{k^2}{2} \underset{\sim}{u}_{tt} + O(k^3) \ . \tag{2.9}$$

Thus writing $\underset{\sim}{u}(x,y,t) = \underset{\sim}{f}(x,y)$ and determining $\underset{\sim}{u}_t$ and $\underset{\sim}{u}_{tt}$ from the partial differential equation (2.7), we require that for all smooth functions $\underset{\sim}{f} = \underset{\sim}{f}(x,y)$

$$S_k \underset{\sim}{f} = \underset{\sim}{f} + k(A\underset{\sim}{f}_x + B\underset{\sim}{f}_y) + \frac{k^2}{2} (A^2 \underset{\sim}{f}_{xx} + (AB+BA) \underset{\sim}{f}_{xy} + B^2 \underset{\sim}{f}_{yy})$$

$$+ O(k^3) \ . \tag{2.10}$$

Attention is now focussed on the Lax-Wendroff operator, which in one spatial dimension is given by

$$L_k^x = I + rA\Delta + \frac{r^2}{2} A^2 \delta^2 \tag{2.11}$$

where $r = \frac{k}{h}$ , (2.12)

$$\Delta f(x) = \frac{1}{2}\,(f(x+h) - f(x-h)) = hf_x(x) + O(h^3) \qquad (2.13)$$

and

$$\delta^2 f(x) = f(x+h) - 2f(x) + f(x-h) = h^2 f_{xx}(x) + O(h^4) \qquad (2.14)$$

This scheme has been the subject of much literature (see e.g.[3]) and it suffices to state that the scheme is linearly stable if the eigenvalues of A satisfy

$$\max_j |\lambda_j(A)| \leq \frac{1}{r} \qquad (2.15)$$

and that it is of second order accuracy in both space and time (given the above definition of a second order approximation).

Strang [1] considered several methods of combining and adjusting the one-dimensional operators $L_k^x$ and $L_k^y$ to yield second order methods for solving the model problem, two of which are analysed here, namely:

(i) The "symmetric sum" of one-dimensional Lax-Wendroff operators:-

$$S_k^{(1)} = \frac{1}{2}(L_k^x L_k^y + L_k^y L_k^x) \qquad (2.16)$$

and

(ii) The sequential method

$$S_k^{(2)} = L_{\frac{k}{2}}^x L_k^y L_{\frac{k}{2}}^x . \tag{2.17}$$

The second method, $S_k^{(2)}$, is also known as the 'fractional step method' and is associated with Yanenko [2].

Following Strang, if we substitute the difference scheme into (2.16), then $S_k^{(1)}$ is the difference operator

$$S_k^{(1)} = \frac{1}{2}\left\{(I + rA\Delta_x + \frac{r^2}{2}A^2\delta_x^2)(I + rB\Delta_y + \frac{r^2}{2}B^2\delta^2{}_y)\right.$$

$$\left.+(I + rB\Delta_y + \frac{r^2}{2}B^2\delta_y^2)(I + rA\Delta_x + \frac{r^2}{2}A^2\delta_x^2)\right\}$$

$$= I + r(A\Delta_x + B\Delta_y) + \frac{r^2}{2}(A^2\delta_x^2 + (AB + BA)\Delta_x\Delta_y + B^2\delta_y^2)$$

$$+ O(r^3) . \tag{2.18}$$

Hence

$$(S_k^{(1)}\underset{\sim}{f})(x,y) = \underset{\sim}{f}(x,y) + k(A\underset{\sim}{f}_x + B\underset{\sim}{f}_y) + \frac{k^2}{2}(A^2\underset{\sim}{f}_{xx} + (AB + BA)\underset{\sim}{f}_{xy}$$

$$+ B^2\underset{\sim}{f}_{yy}) + O(k^3) , \tag{2.19}$$

and so $S_k^{(1)}$ is a second order accurate approximate solution operator to equation (2.7). Carrying out the same analysis of $S_k^{(2)}$, we find that this is also a second order approximate solution operator to

equation (2.7).

In a paper by Yanenko [2] and elsewhere in the book by Sod [3], $S_k^{(2)}$ is reviewed and the same conclusion about accuracy is reached without reference to the symmetry of the matrices A and B .

In principle, $S_k^{(2)}$ can compute solutions faster than $S_k^{(1)}$ and thus $S_k^{(2)}$ was favoured by Strang. However, the author has found that with careful programming, the difference in computation speed can be made negligible.

In recent years many advances have been made in the study of hyperbolic partial differential equations and in the theory of one-dimensional difference operators applied to hyperbolic partial differential equations, especially application of such operators to one-dimensional fluid flows. For example, much is now known about numerical techniques for solving conservation laws, i.e. equations of the form

$$u_t + f(u)_x = 0 \ . \tag{2.20}$$

Solutions of such equations produce discontinuities in general (unless f is a linear function of u) and numerical techniques have been developed that can handle these non-linear features. Indeed the classical schemes, such as the Lax-Wendroff scheme, have become less widely used following the advent of adaptive TVD schemes, such as those of Osher [15], Roe [4], Van Leer [12], which are able to successfully generate sharp solution profiles near shocks and contact discontinuities

(as well as being accurate in regions of smooth data). It is near these discontinuities that classical schemes produce oscillatory behaviour and require the addition of artificial viscosity. Many difficult problems in computational fluid dynamics, governed by the Euler equations, have been solved very successfully (in one-dimension) by such schemes. In particular, Roe's decomposition [4], in which flux limiters have been incorporated, is particularly successful.

However, all the theory concerning conservation laws and flux limiters has been developed only in one spatial dimension. What, then happens when we are faced with a two-dimensional problem in computational fluid dynamics? There are only a few truly two-dimensional approaches to solving such problems and, as a compromise, such problems are generally solved using operator splitting. For example, the Euler equations in two-dimensions can be written as

$$\underset{\sim}{u}_t + A\underset{\sim}{u}_x + B\underset{\sim}{u}_y = 0 \ , \tag{2.21}$$

a non-linear system of hyperbolic partial differential equations. The Jacobian matrices A and B are asymmetric and certainly do not commute. However, given that we can solve the one-dimensional sibling equations

$$\underset{\sim}{u}_t + A\underset{\sim}{u}_x = 0 \tag{2.22a}$$

$$\underset{\sim}{u}_t + B\underset{\sim}{u}_y = 0 \tag{2.22b}$$

we may attack the full parental problem (2.21) by employing operator splitting.

Despite excellent results obtained via operator splitting, certain questions do arise about the validity of employing operator splitting when solving the two-dimensional Euler equations, since the Jacobian matrices, $A$ and $B$, are not constant, in fact they vary not only spatially but temporally. This difficulty is generally ignored when applying operator splitting to the Euler equations.

Since the analysis of splitting methods is incomplete, as we shall see in section 4, and since no analysis has been done with respect to non-linear systems of equations, the question of the validity of operator splitting remains unanswered. This report is a contribution to the evidence for and against operator splitting.

## §3 A Brief Review of One-Dimensional Techniques

In this section we briefly review the techniques used in solving one-dimensional non-linear hyperbolic problems of the form

$$\left.\begin{aligned} u_t + f(u)_x &= 0 \\ u(x,0) &= u_o(x) \end{aligned}\right\} \qquad (3.1)$$

and show how these techniques can be extended to solving the inviscid compressible Euler equations in one-dimension. We begin by considering some analytic results concerning the solution of (3.1).

### 3.1 Analytic Considerations

It is well known that equation (3.1) can be solved by the method of characteristics. By writing

$$f(u)_x = a(u)u_x \qquad (3.2)$$

where

$$a(u) = f'(u)$$

(3.1) becomes

$$u_t + a(u)u_x = 0 \qquad (3.3)$$

the characteristic curves of which are given by

$$x - a(u)t = \text{constant} \tag{3.4}$$

Since (3.1) is a conservation law, information is propagated along the characteristics, i.e. in this case u = constant along the characteristics, and so a solution of (3.1) is

$$u(x,t) = u_o(x-a(u)t) \ .$$

This solution holds as long as the characteristics remain well-defined and do not cross or diverge from a point. If the characteristics do cross then the solution becomes double valued and a shock or discontinuity is produced. We can then continue the solution by considering weak solutions and by including the Rankine-Hugoniot relationship

$$\frac{[f]}{[u]} = s \tag{3.5}$$

where s is the shock speed and

$$[(\cdot)] = (\cdot)_R - (\cdot)_L \tag{3.6}$$

is the jump in states of $f$ and $u$ across the discontinuity.

If the characteristics diverge then there is an infinity of possible weak solutions. For example, consider Burger's equation

$$u_t + (\tfrac{1}{2}u^2)_x = 0 \tag{3.7}$$

with the following initial data:

$$u_o(x) = \begin{cases} 1 & x > 0 \\ 0 & x < 0 \end{cases} . \tag{3.8}$$

Two possible solutions are

$$\text{a)} \qquad u(x,t) = \begin{cases} 1 & x > t/2 \\ 0 & x < t/2 \end{cases} \tag{3.9}$$

$$\text{b)} \qquad u(x,t) = \begin{cases} 1 & x > t \\ x/t & 0 < x < t \\ 0 & x < 0 \end{cases}$$

solution (a) representing a rightward travelling shock and solution (b) representing an expansion ramp. To obtain the correct physical solution we call upon the entropy condition (Lax [7], Oleinik [5]) which is derived from consideration of the limiting equation

$$u_t + f(u)_x = \epsilon u_{xx} \tag{3.10}$$

as $\epsilon \downarrow 0$ .

In simple terms, the entropy condition tells us that, for a convex flux function $f(u)$ $(f''(u) > 0)$ and a fixed time $t$, the solution of (3.1), in traversing the x-axis from $-\infty$ to $+\infty$, can only jump down at discontinuities. In the above example the correct physical solution is (b).

The above analytic results have been useful in developing high resolution upwind algorithms for solving scalar conservation laws.

For a fuller account of the treatment of hyperbolic conservation laws see Smoller [6].

## 3.2 Upwinding in One-Dimension

Having described some analytic results for scalar hyperbolic conservation laws, we now briefly outline some numerical techniques developed for solving such equations.

Consider the linear advection problem

$$\left.\begin{aligned} &u_t + a u_x = 0 \\ &u(x,0) = u_0(x) \end{aligned}\right\} \qquad (3.11)$$

with $a > 0$ .

The simplest upwind scheme for solving this equation is that attributed to Cole and Murman [27] and can be written as

$$u^k = u_k - \lambda a(u_k - u_{k-1}) \tag{3.12}$$

or

$$u^k = u_k - \nu \Delta u_{k-\frac{1}{2}} \tag{3.13}$$

where

$$\lambda = \frac{\Delta t}{\Delta x} \quad , \qquad \nu = a\lambda$$

$$u_k = u_k^n \quad , \qquad u^k = u_k^{n+1}$$

and $\quad \Delta(\cdot)_{k+\frac{1}{2}} = (\cdot)_{k+1} - (\cdot)_k \ .$

This can be thought of as the advection of the linear interpolant of the data and thus can be seen to be highly diffusive (see figure 1), as is the case with most first order schemes.

On the other hand, second order schemes, such as Lax-Wendroff [8] or Warming and Beam [9], are known to produce oscillations when the solution varies rapidly (see figures 2 and 3). These two schemes can be written

$$\text{L-W:} \quad u^k = u_k - \nu \Delta u_{k-\frac{1}{2}} - \frac{\nu}{2}(1-\nu)\ \Delta_-(\Delta u_{k+\frac{1}{2}}) \tag{3.14}$$

$$\text{W-B:} \quad u^k = u_k - \nu \Delta u_{k-\frac{1}{2}} - \frac{\nu}{2}(1-\nu)\ \Delta_-(\Delta u_{k-\frac{1}{2}}) \tag{3.15}$$

where

$$\Delta_-\ (\cdot)_k = (\cdot)_k - (\cdot)_{k-1} \ .$$

Both of the above schemes can be regarded as the advection of quadratic interpolation of data, which accounts for the production of spurious oscillations around regions of rapidly varying data due to the underlying quadratic interpolation. Various techniques have been constructed for the approximate solution of scalar conservation laws which are both high resolution and non-oscillatory (e.g. Woodward and Collella's PPM [10], Boris and Book's FCT [11], Van Leer's MUSCL [12], Harten, Enquist, Osher, and Chakravarthy's ENO Schemes [14] and Roe and Sweby's Flux Limiter Schemes [13]). These schemes all work by limiting the amount of second order flux in such a way that oscillations are suppressed. We give here a brief description of how the Flux Limiter methods succeeds in preventing oscillations.

Following Sweby [13] we can view the Lax-Wendroff scheme as a first order scheme,

$$u^k = u_k - \nu \Delta u_{k-\frac{1}{2}} \tag{3.16}$$

with the additional second order flux (or anti-diffusive flux)

$$-\Delta_- \{\tfrac{1}{2}\nu(1-\nu)\ \Delta u_{k+\frac{1}{2}}\} \ . \tag{3.17}$$

This anti-diffusive flux is then modified in such a way as to prevent oscillations, i.e. it is replaced by

$$-\ \Delta_-\{\phi_k \tfrac{1}{2}\nu(1-\nu)\Delta u_{k+\frac{1}{2}}\} \tag{3.18}$$

where $\phi_k$ is a function of consecutive gradients

$$\phi_k = \phi(r_k)$$

$$r_k = \frac{\Delta u_{k-\frac{1}{2}}}{\Delta u_{k+\frac{1}{2}}} \quad . \tag{3.19}$$

We now call upon the notion of Total Variation Diminishing Solutions (TVD) to place bounds on $\phi_k$ .

The TVD property is based upon the fact that the analytic solution of a conservation law satisfies the inequality (in one-dimension)

$$\frac{d}{dt} \int |u_x| dx \quad \leq 0 \quad . \tag{3.20}$$

i.e. the variation of u does not increase (see [7]). The discrete analogue of this result is

$$TV(u^{n+1}) \quad \leq \quad TV(u^n) \tag{3.21}$$

where the discrete TV is defined as

$$TV(u^n) = \sum_k |u_k^n - u_{k-1}^n| \quad . \tag{3.22}$$

From Sweby [13] we know that any scheme written in the form

$$u^k = u_k - C_{k-\frac{1}{2}} \Delta u_{k-\frac{1}{2}} + D_{k+\frac{1}{2}} \Delta u_{k+\frac{1}{2}} \tag{3.23}$$

is TVD iff

$$\left.\begin{aligned} C_{k+\frac{1}{2}} &\geq 0 \\ D_{k+\frac{1}{2}} &\geq 0 \\ C_{k+\frac{1}{2}} + D_{k+\frac{1}{2}} &\leq 1 \end{aligned}\right\} . \tag{3.24}$$

Writing the flux limited scheme as a single difference scheme we have

$$u^k = u_k - \nu\Delta_{k-\frac{1}{2}} - \Delta_- \{\phi_k{}^{\frac{1}{2}}(1-\nu)\nu\Delta u_{k+\frac{1}{2}}\} . \tag{3.25}$$

Equation (3.25) can be manipulated to yield

$$u^k = u_k - \nu\left\{1 + \tfrac{1}{2}(1-\nu)\left[\frac{\phi_k}{r_k} - \phi_{k-1}\right]\right\} \Delta u_{k-\frac{1}{2}} \tag{3.26}$$

from which we can apply the TVD criteria to produce bounds on $\phi_k$ . This leaves freedom to choose $\phi_k$ to be such that (3.26) is 'as second order as possible'. The second order TVD region is shown in figure 5.

In practice flux limiter schemes are highly successful (see

figure 4) and easy to extend to non-linear problems and systems of hyperbolic conservation laws.

We now turn our attention to entropy satisfaction within numerical schemes (q.v. Section 2). It is alarmingly easy to produce entropy violating solution via numerical methods, for example, if we apply the Cole-Murman scheme (3.12) to the inviscid Burgers equation (3.7) with the initial data

$$u_o(x,0) = \begin{cases} 0.5 & |x - 3.75| \leq 1.25 \\ -0.5 & |x - 3.75| > 1.25 \end{cases} \tag{3.27}$$

then the wrong solution is produced (see figure 6).

The reason for this is that the scheme is dispersing the solution around the sonic point of the equation i.e. where $f'(u) = 0$ . To remedy this discrepency Osher [15] devised a criteria for semi-discrete schemes approximating (3.1) to be entropy satisfying and thus to be able to converge to the correct physical solution. These schemes, dubbed E-schemes, have the form

$$\frac{\partial u}{\partial t} = - \frac{1}{\Delta x}(h^E_{k+\frac{1}{2}} - h^E_{k-\frac{1}{2}}) \tag{3.28}$$

where $h^E$ is a consistent numerical entropy satisfying flux function

$$h^E_{k+\frac{1}{2}} = h^E(u_{k+1} , u_k , \ldots , u_{k-m}) \tag{3.29}$$

$$h^E(u , u , \ldots , u) = f(u) \tag{3.30}$$

and

$$\mathrm{sgn}(u_{k+1} - u_k)\left[h^E_{k+\frac{1}{2}} - f(u)\right] \leq 0 \ . \tag{3.31}$$

Schemes of this form (e.g. Enquist-Osher [15]) are at most first order accurate. However they can be used as a basis on which to add flux limiters (see Sweby [13]) and produce very good (and physically correct) results (see figures 7 and 8).

We now turn our attention to the Euler Equations.

## 3.3 The Euler Equations and Roe's Scheme

The Euler equations arise when modelling an inviscid compressible fluid and take the form of three conservation equations, namely conservation of mass, momentum and energy. To complete the system an equation of state is also required. We can write the conservation equations in a form similar to (3.1), i.e.

$$\underset{\sim}{u}_t + \underset{\sim}{f}(\underset{\sim}{u})_x = 0 \tag{3.32}$$

where

$$\underset{\sim}{u} = (\rho,\ \rho u,\ e)^T$$

$$\underset{\sim}{f} = (\rho u,\ p+\rho u^2\ ,\ u(e+p))^T$$

and where $\rho$, u, e, p are the density, velocity, total energy and pressure respectively. The equation of state takes the form

$$p = p(\rho, i)$$

where i is the internal energy.

As in the analytic case, we can write this as

$$\underset{\sim}{u}_t + A\underset{\sim}{u}_x = 0 \tag{3.33}$$

Where A is the Jacobian matrix, defined as

$$A = A(\underset{\sim}{u}) = \frac{\partial \underset{\sim}{f}}{\partial \underset{\sim}{u}} . \tag{3.34}$$

A popular method of solving the Euler equation numerically is Roe's scheme, a linearised approximate Riemann solver (Roe [4], Roe and Pike [16], Glaister [19]). The basic idea behind this approach is that we locally linearise A over a computational cell to give an approximation to the Jacobian. This approximate Jacobian, $\tilde{A}$, is then used to obtain approximate eigenvalues and eigen-vectors $\tilde{\lambda}_i$ , $\underset{\sim}{\tilde{e}}_i$ . An increment $\Delta\underset{\sim}{u}$ is then decomposed onto the eigenvectors $\underset{\sim}{\tilde{e}}_i$ with wavestrengths $\tilde{\alpha}_i$ given by

$$\Delta\underset{\sim}{u} = \sum \tilde{\alpha}_i \, \underset{\sim}{\tilde{e}}_i \tag{3.35}$$

The averages $\tilde{\alpha}_i$ are then calculated solving (3.35) together with

$$\Delta \underset{\sim}{f} = \sum \tilde{\lambda}_i \, \tilde{\alpha}_i \, \underset{\sim}{\tilde{e}}_i \tag{3.36}$$

which forms a discrete analogue of the spatial differencing of the Euler equations.

Each wave is represented by

$$\underset{\sim}{\phi}_i = \Delta \underset{\sim}{f}_i \, \frac{\Delta t}{\Delta x} = \tilde{\lambda}_i \, \tilde{\alpha}_i \, \underset{\sim}{\tilde{e}}_i \, \frac{\Delta t}{\Delta x} \tag{3.37}$$

which is then used to update $\underset{\sim}{u}$ in time in an upwind manner, i.e. added to the appropriate end of the computational cell according to the sign of $\tilde{\lambda}_i$ .

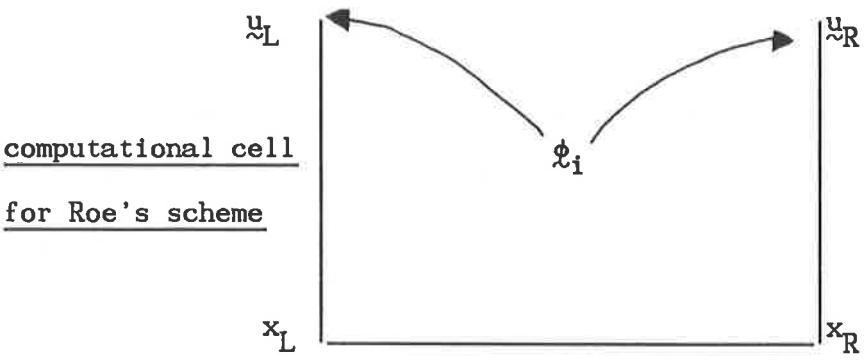


figure A

i.e. $$\underset{\sim}{u}^{L} = \underset{\sim}{u}_{L} - \phi_i \qquad \forall i : \tilde{\lambda}_i < 0 \tag{3.38}$$

$$\underset{\sim}{u}^{R} = \underset{\sim}{u}_{R} - \phi_i \qquad \forall i : \tilde{\lambda}_i > 0 \; . \tag{3.39}$$

This method assumes a piecewise constant form for $\underset{\sim}{u}$ within each computational cell and in effect solves the Riemann problem at the jump interface. Roe's scheme is a first order method, although a seconder order version with flux-limiters can be easily applied (Sweby [13]) and it is also possible to embed an entropy 'fix' in the scheme to prevent backward facing shocks by considering the sign of the eigenvalues at the left and right hand ends of the computational cell $\lambda_L$ , $\lambda_R$ . A second order version of Roe's scheme has been shown to be convergent (Sweby and Baines [17]) for scalar non-linear hyperbolic p.d.e.'s. Results for this scheme applied to the shock tube problem of Sod [25] are shown in figures 9 through to 11. Further extensions have been made to this scheme, see for example Glaister [18], [19], who has adapted the scheme to give a linearised approximate Riemann solver for non-cartesian geometries with a general equation of state. The scheme can also be used to solve the two-dimensional Euler equations via operator splitting (see for example Barley [20]) although, recently, Roe himself has pointed out difficulties associated with this extension (Roe [21]). Despite this objection, operator splitting has proved to be a very useful tool in solving multi-dimensional fluid flows, and in the next section we shall consider some simple analysis of operator splitting.

## §4 An Analysis of Splitting Strategies

In this section we give a comparative analysis of three splitting techniques. We start by describing the three methods.

### 4.1 Description of Methods

In Section 2 we saw how Strang compared two different splitting strategies. The assumptions made there about his model problem do not hold for the equations we are interested in here, namely the Euler equations, which are non-linear and have non-constant asymmetric Jacobian matrices.

Since we are interested in the difference in resloution of split schemes, it seems sensible to take the underlying one-dimensional solution operator to be of first order in the hope that when extended to higher order, the most successful first order split method will also succeed at being the highest resolution method when flux limiters are applied.

We start by clarifying some notation. Considering the scalar conservation law

$$u_t + f(u)_x + g(u)_y = 0 \ , \tag{4.1}$$

then use of a splitting technique implies that we solve the two sibling equations

$$u_t + f(u)_x = 0 \qquad (4.2a)$$

$$u_t + g(u)_y = 0 \qquad (4.2b)$$

via some one-dimensional solution operators.

We let $L_x$ be the one-dimensional solution operator which solves (4.2a) using only x-variations throughout the computational domain, i.e.

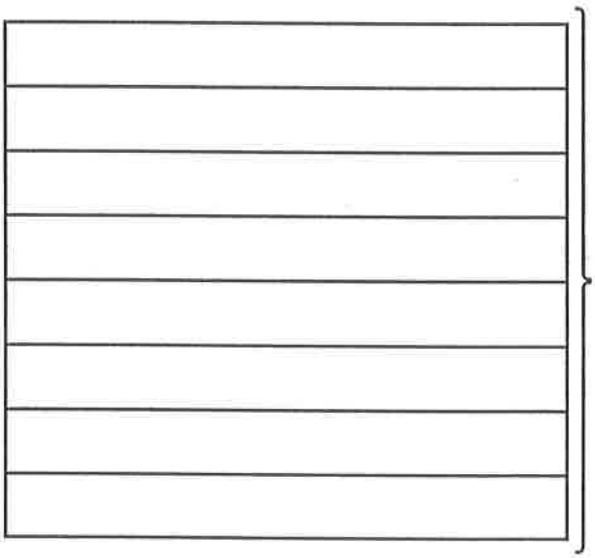


Figure B

Similarly, we let $L_y$ be the one-dimensional solution operator which solves (4.2b) using only y-variations throughout the computational domain.

Using this notation we can write down the three splitting strategies refered to in Section 2 as follows:

a) $S^{(1)} = \frac{1}{2}(L_x L_y + L_y L_x)$ - Strang's original method

b) $S^{(2)} = L_x^{\frac{1}{2}} L_y^{\frac{1}{2}} L_y^{\frac{1}{2}} L_x^{\frac{1}{2}}$ - Yanenko's method of fractional steps

c) $S^{(3)} = L_x + L_y - I$ - "genuinely two-dimensional" for first order solution operators.

We note that $S^{(2)}$ is slightly different to the operator considered by Strang, since he combined the two $L_y^{\frac{1}{2}}$ operators to yield $L_y$ ; however, since we are concerned with solving a non-linear system, we can no longer do this since the Jacobian matrices are solution dependent.

It is worth noting that if the three methods are programmed naively, $S^{(2)}$ will take twice as long to advance from one time level to the next as $S^{(3)}$ , whereas $S^{(3)}$ will need twice as much storage since the solution at the next time level is based on both operators $L_x$ and $L_y$ operating on the solution at the previous time level. $S^{(1)}$ comes off even worse in this respect since it needs the storage associated with $S^{(3)}$ while taking the time to advance one time-step associated with $S^{(2)}$ .

For most of the analysis given here we will be considering $L_x$ and $L_y$ as first-order upwind difference operators, i.e.

$$L_x = u^n_{i,j} - v_{i-\frac{1}{2},j} \, \Delta_x \, u_{i-\frac{1}{2},j} \qquad (4.3)$$

$$L_y = u^n_{i,j} - v_{i,j-\frac{1}{2}} \Delta_y u_{i,j-\frac{1}{2}} \tag{4.4}$$

where $$v_{i-\frac{1}{2},j} = \frac{\Delta_x f_{i-\frac{1}{2},j}}{\Delta_x u_{i-\frac{1}{2},j}} \cdot \frac{\Delta t}{\Delta x} \tag{4.5}$$

$$v_{i,j-\frac{1}{2}} = \frac{\Delta_y g_{i,j-\frac{1}{2}}}{\Delta_y u_{i,j-\frac{1}{2}}} \cdot \frac{\Delta t}{\Delta y} \tag{4.6}$$

$$\Delta_x(\cdot)_{i-\frac{1}{2},j} = (\cdot)_{i,j} - (\cdot)_{i-1,j} \tag{4.7}$$

$$\Delta_y(\cdot)_{i,j-\frac{1}{2}} = (\cdot)_{i,j} - (\cdot)_{i,j-1} \tag{4.8}$$

and $\frac{\Delta t}{\Delta x}$ , $\frac{\Delta t}{\Delta y}$ are the mesh ratio's parallel to the x and y axes respectively. We will consider only situations where wavespeeds are positive ($v_{i,j} > 0$) , although the analysis carries through, with simple modification, for any wave speed.

## 4.2 Numerical Stencils

If we consider updating the mesh point (i,j) , then, by consider the stencils of the three splitting techniques with $L_x$ and $L_y$ defined by (4.3) and (4.4), we have an indication of which points are influencing the updating procedure.

Diagrammatically the stencils for $S^{(1)}$, $S^{(2)}$, $S^{(3)}$ are as

follows:-

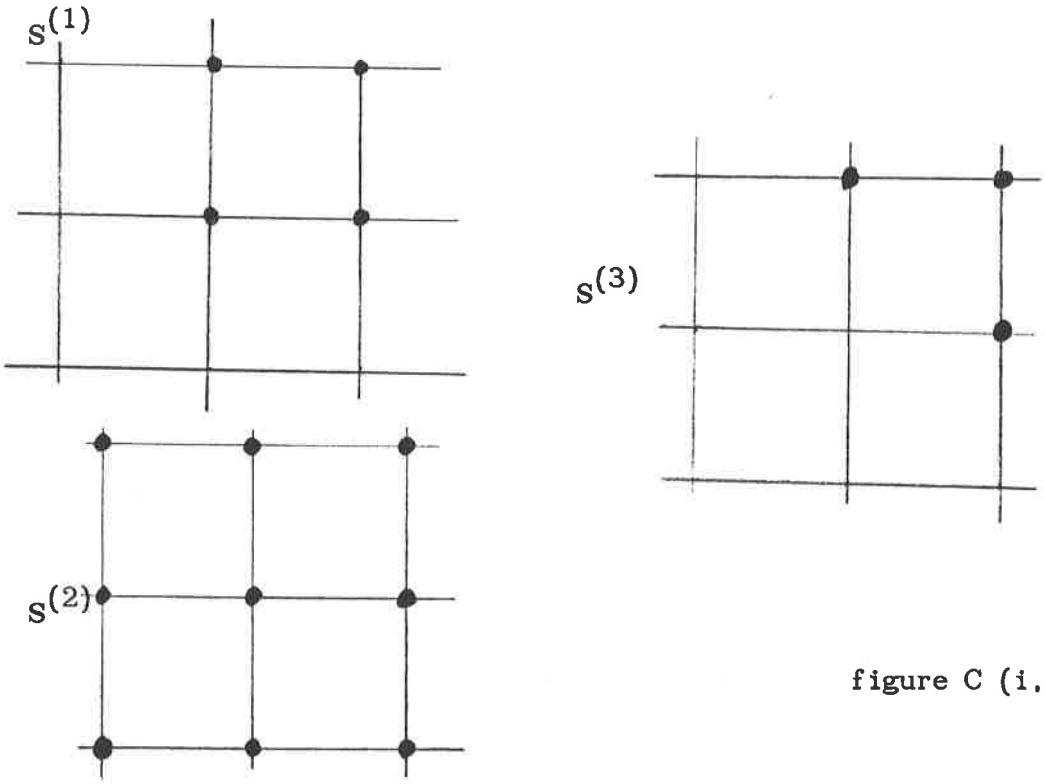


figure C (i,ii,iii)

4.3 Numerical Schemes

If we consider solving the two-dimensional linear advection equation, then we can write down the three different split schemes explicitly, i.e. for solving

$$u_t + au_x + bu_y = 0 \qquad (4.9)$$
$$a,b > 0$$

we have

$$L_x(u^n) \equiv u^n_{i,j} - a\frac{\Delta t}{\Delta x}(u^n_{i,j} - u^n_{i-1,j}) \qquad (4.10)$$

$$L_y(u^n) \equiv u^n_{i,j} - b\frac{\Delta t}{\Delta y}\,(u^n_{i,j} - u^n_{i,j-1}) \quad . \tag{4.11}$$

After a little manipulation, the three schemes can be written explicitly as

$$S^{(1)}_{\Delta t} = (1-\nu_x)(1-\nu_y)u^n_{i,j} + (1-\nu_x)\,\nu_y u^n_{i,j-1} + (1-\nu_y)\nu_x\,u^n_{i-1,j} + \nu_x\,\nu_y\,u^n_{i-1,j-1}$$

$$S^{(2)}_{\Delta t} = (1-\mu_x)^2(1-\mu_y)^2u^n_{i,j} + 2\mu_x(1-\mu_x)(1-\mu_y)^2u^n_{i-1,j} + 2\mu_y(1-\mu_y)(1-\mu_x)^2u^n_{i,j-1}$$

$$+ 4\mu_x\mu_y(1-\mu_x)(1-\mu_y)u^n_{i-1,j-1} + \mu_y^2(1-\mu_x)^2u^n_{i,j-2} + \mu_x^2(1-\mu_y)^2u^n_{i-2,j}$$

$$+2\,\mu_x\mu_y^2(1-\mu_x)u^n_{i-1,j-2} + 2\mu_y\mu_x^2(1-\mu_y)u^n_{i-2,j-1} + \mu_x^2\,\mu_y^2\,u^n_{i-2,j-2}$$

$$S^{(3)}_{\Delta t} = (1-\nu_x-\nu_y)u^n_{i,j} + \nu_x u^n_{i-1,j} + \nu_y u^n_{i,j-1}$$

where $$\nu_x = a\,\frac{\Delta t}{\Delta x} \tag{4.12a}$$

$$\nu_y = b\,\frac{\Delta t}{\Delta y} \tag{4.12b}$$

and $$\mu = \frac{\nu}{2} \quad . \tag{4.13}$$

4.4 Consistency and Accuracy

To show consistency for the above schemes we note that they can be written in the form

$$u_{i,j}^{n+1} = \sum_{l,m=o}^{L,M} C_{l,m}\, u_{i-l,j-m}^{n} \tag{4.14}$$

and therefore that the difference operator $L(u_{i,j}^{n})$ can be written

$$L(u_{i,j}^{n}) = u_{i,j}^{n+1} - \sum_{l,m=o}^{L,M} C_{l,m}\, u_{i-l,j-m}^{n} = 0 \tag{4.15}$$

so that we can define the truncation error as

$$\Delta t\, \tau_{i,j} = L(v(x,y,t)) \tag{4.16}$$

where v is a smooth function that is sufficiently differentiable to allow a Taylor series expansion. The definition of consistency is that the numerical scheme converges to the partial differential equations we are solving as $\Delta t$ , $\Delta x$ , $\Delta y \to 0$ with $\frac{\Delta t}{\Delta x}$ , $\frac{\Delta t}{\Delta y}$ held constant. Expanding (4.15) in a Taylor series about the point $(i\Delta x\ ,\ j\Delta y\ ,\ n\Delta t)$ yields

$$\Delta t\, \tau_{i,j} = \left[u - \sum_{l,m=o}^{L,M} C_{l,m}\, u\right] + \left[\Delta t\, u_t - \sum_{l,m=o}^{L,M} C_{l,m}(-\, l\Delta x u_x - m\Delta y\, u_y)\right]$$

$$+ \left[\frac{(\Delta t)^2}{2} u_{tt} - \sum_{l,m=o}^{L,M} C_{l,m}\left[\frac{(l\Delta x)^2}{2} u_{xx} + ml\Delta x\Delta y u_{xy} + \frac{(m\Delta y)^2}{2} u_{yy}\right]\right]$$

$$+ \text{ higher order terms} . \qquad (4.17)$$

Hence, the definition of consistency shows that the given scheme is consistent if

$$\sum_{l,m=o}^{L,M} C_{l,m} = 1 \qquad (4.18)$$

We now apply the definition of consistency (4.17) to the three schemes:

For $S^{(1)}$ : $\sum_{l,m=o}^{1,1} C_{l,m} = (1-v_x)(1-v_y) + (1-v_x)v_y + (1-v_y)v_x$

$$+ v_x v_y$$

$$= (1-v_x)(1-v_y + v_y) + v_x(1-v_y + v_y)$$

$$= 1$$

For $S^{(2)}$ : $\sum_{l,m=o}^{2,2} C_{l,m} = (1-\mu_x)^2 (1-\mu_y)^2 + 2(1-\mu_x)(1-\mu_y)^2 \mu_x$

$$+ 2(1-\mu_y)(1-\mu_x)^2 \mu_y + 4\mu_x \mu_y(1-\mu_y)(1-\mu_x)$$

$$+ \mu_y^2(1-\mu_x)^2 + \mu_x^2(1-\mu_y)^2 + 2\mu_x\mu_y^2(1-\mu_x)$$

$$+ 2\mu_y\mu_x^2(1-\mu_y) + \mu_x^2\mu_y^2$$

$$= (1-\mu_x)^2 \{(1-\mu_y)^2 + 2\mu_y(1-\mu_y) + \mu_y^2\}$$

$$+ \mu_x(1-\mu_x)\ \{4\mu_y(1-\mu_y) + 2(1-\mu_y)^2 + 2\mu_y^2\}$$

$$+ \mu_x^2\ \{(1-\mu_y)^2 + 2\mu_y(1-\mu_y) + \mu_y^2\}$$

$$= (1-\mu_x)^2 + 2\mu_x(1-\mu_x) + \mu_x^2$$

$$= 1$$

For $S^{(3)}$ : $\sum_{l,m=o}^{1,1} C_{l,m} = 1 - \nu_x - \nu_y + \nu_x + \nu_y$

$$= 1 \ .$$

It is therefore clear that all three schemes are consistent.

Since the underlying one-dimensional solution operators are first order accurate, it is hoped, and will indeed be shown, that the splitting strategies are used also first order accurate.

From (4.17) we can write

$$\tau_{i,j} = \frac{1}{\Delta t}\, u \left[1 - \sum_{l,m=o}^{L,M} C_{l,m}\right] + u_t + \left[\sum_{l,m=o}^{L,M} l\, \frac{\Delta x}{\Delta t}\, C_{l,m}\right] u_x$$

$$+ \left[\sum_{l,m=o}^{L,M} m\, \frac{\Delta y}{\Delta t}\, C_{l,m}\right] u_y$$

$$+ \text{higher order terms} \qquad (4.19)$$

and thus we can see that for first order accuracy we require that

$$\sum_{l,m=o}^{L,M} l \frac{\Delta x}{\Delta t} C_{l,m} = a \qquad (4.20a)$$

$$\sum_{l,m=o}^{L,M} m \frac{\Delta y}{\Delta t} C_{l,m} = b \qquad (4.20b)$$

i.e.

$$\sum_{l,m=o}^{L,M} l\, C_{l,m} = v_x \qquad (4.21a)$$

$$\sum_{l,m=o}^{L,M} m\, C_{l,m} = v_y \qquad (4.21b)$$

Applying (4.21) to the schemes we have

$$S^{(1)}: \sum_{l,m=o}^{1,1} lC_{l,m} = (1-v_y)v_x + v_x v_y$$

$$= v_x$$

$$\sum_{l,m=o}^{1,1} mC_{l,m} = (1-v_x)v_y + v_x v_y$$

$$= v_y$$

$$S^{(2)}: \quad \sum_{l,m=o}^{2,2} {}^{l}C_{l,m} = 2\mu_x(1-\mu_x)(1-\mu_y)^2 + 4\mu_x\mu_y(1-\mu_x)(1-\mu_y)$$

$$+ 2\mu_x^2(1-\mu_y)^2 + 2\mu_x^2\mu_y^2(1-\mu_x) + 4\mu_y\mu_x^2(1-\mu_y)^2$$

$$+ 2\mu_x\mu_y^2$$

$$= \mu_x\{(1-\mu_x)(1-\mu_y)^2 + \mu_x(1-\mu_x)(1-\mu_y)$$

$$+ \mu_x(1-\mu_y)^2 + \mu_y^2(1-\mu_x)$$

$$+ 2\mu_x\mu_y(1-\mu_y) + 2\mu_x\mu_y^2\}$$

$$= 2\mu_x\{(1-\mu_x)\left[(1-\mu_y)^2 + 2\mu_y^2(1-\mu_y) + \mu_y^2\right]$$

$$+ \mu_x\left[\mu_y^2 + 2\mu_y(1-\mu_y) + (1-\mu_y)^2\right]\}$$

$$= v_x\{(1-\mu_x) + \mu_x\}$$

$$= v_x .$$

Similarly (or by symmetry)

$$\sum_{l,m=o}^{2,2} m\, C_{l,m} = v_y$$

$$S^{(3)}: \quad \sum_{l,m=o}^{1,1} mC_{l,m} = v_x$$

$$\sum_{l,m=o}^{1,1} lC_{l,m} = v_y \ .$$

Hence we have shown that the three schemes are first order accurate.

Before showing linear stability, it is of interest to use (4.17) to give some idea of the truncation error involved in applying each scheme. Since the schemes are consistent and first order accurate, then we can rewrite (4.17) as

$$\tau_{i,j} = \frac{\Delta t}{2} u_{tt} - \frac{1}{\Delta t} \sum_{l,m=o}^{L,M} C_{l,m} \left[ \frac{(l\Delta x)^2}{2} u_{xx} + ml\Delta x\Delta y u_{xy} + \frac{(m\Delta y)^2}{2} u_{yy} \right)$$

$$+ \text{higher order terms.} \qquad (4.22)$$

Now let us assume that the Taylor series expansion is written in the form with the second derivative term $u_{xx}$ in (4.22) replaced by

$$U_{xx} = u_{xx}(x_i + \theta_1 \Delta x, y, t) \qquad (4.23)$$

$$0 \leq \theta_1 \leq 1 \qquad (4.24)$$

and similarly $u_{yy}$ and $u_{xy}$ are replaced by similar expressions. Also, we note that, via equation (4.9), we can replace $u_{tt}$ as follows:

$$u_{tt} = a^2 u_{xx} + 2abu_{xy} + b^2 u_{yy} \tag{4.25}$$

and hence

$$\tau_{i,j} = \left[\frac{a^2\Delta t}{2} - \frac{1}{\Delta t} \sum_{l,m=o}^{L,M} C_{l,m} \frac{(l\Delta x)^2}{2}\right] U_{xx}$$

$$+ \left[ab\Delta t - \frac{1}{\Delta t} \sum_{l,m=o}^{L,M} C_{l,m}\, ml\Delta x\Delta y\right] U_{xx}$$

$$+ \left[\frac{b^2\Delta t}{2} - \frac{1}{\Delta t} \sum_{l,m=o}^{L,M} C_{l,m} \frac{(m\Delta y)^2}{2}\right] U_{yy} \; . \tag{4.26}$$

Thus

$$|\tau_{i,j}| \leq (|A| + |B| + |C|)M \tag{4.27}$$

where

$$M = \underset{\forall\theta}{\text{Max}} \left(|U_{xx}| \; , \; |U_{xy}| \; , \; |U_{yy}|\right) \tag{4.28}$$

and

$$A = a^2 \frac{\Delta t}{2} + \frac{1}{2\Delta t} \sum_{l,m=o}^{L,M} C_{l,m}(l\Delta x)^2 \tag{4.29a}$$

$$B = ab\Delta t + \frac{1}{\Delta t} \sum_{l,m=o}^{L,M} C_{l,m}\, lm\, \Delta x\, \Delta y \tag{4.29b}$$

$$C = b^2 \frac{\Delta t}{2} + \frac{1}{2\Delta t} \sum_{l,m=o}^{L,M} C_{l,m}\, (m\Delta y)^2 \ . \tag{4.29c}$$

In defining A,B,C we have assumed that the schemes are monotonicity preserving (see Roe [28]), that is

$$C_{l,m} \geq 0 \qquad \forall_{l,m} \tag{4.30}$$

we therefore need

$$0 \leq \nu_x \ , \ \nu_y \leq 1 \tag{4.31}$$

for $S^{(1)}$ ,

$$0 \leq \mu_x \ , \ \mu_y \leq 1 \tag{4.32}$$

for $S^{(2)}$ and

$$0 \leq v_x + v_y \leq 1 \tag{4.33}$$

for $S^{(3)}$ .

Manipulation of (4.29) leads to

$$A = \frac{(\Delta x)^2}{2\Delta t}\left\{v_x^{\,2} + \sum_{l,m=o}^{L,M} l^2 C_{l,m}\right\} \tag{4.34a}$$

$$B = \frac{\Delta x \Delta y}{\Delta t}\left\{v_x\, v_y + \sum_{l,m=o}^{L,M} ml\; C_{l,m}\right\} \tag{4.34b}$$

$$C = \frac{(\Delta y)^2}{2\Delta t}\left\{v_y^2 + \sum_{m,l=o}^{L,M} m^2\; C_{l,m}\right\} . \tag{4.34c}$$

Substituting the $C_{l,m}$ for each scheme yields

$S^{(1)}$ $$A = \frac{(\Delta x)^2}{2\Delta t} v_x(1+v_x) \tag{4.35a}$$

$$B = \frac{\Delta x \Delta y}{\Delta t} 2v_x\, v_y \tag{4.35b}$$

$$C = \frac{(\Delta y)^2}{2\Delta t} v_y(1+v_y) \tag{4.35c}$$

$S^{(2)}$ $$A = \frac{(\Delta x)^2}{2\Delta t} v_x(1+\frac{3}{2}v_x) \tag{4.36a}$$

$$B = \frac{\Delta x \Delta y}{\Delta t} 2v_x\, v_y \tag{4.36b}$$

$$C = \frac{(\Delta y)^2}{2\Delta t} v_y(1+\frac{3}{2}v_y) \tag{4.36c}$$

$S^{(3)}$ $$A = \frac{(\Delta x)^2}{2\Delta t} v_x(1+v_x) \tag{4.37a}$$

$$B = \frac{\Delta x \Delta y}{\Delta t} v_x\, v_y \tag{4.37b}$$

$$C = \frac{(\Delta y)^2}{2\Delta t} v_y(1+v_y) \quad . \tag{4.37c}$$

If we now make the further assumption that we are using square cells throughout the computational mesh, then we can write

$$\frac{\Delta t}{\Delta x} = \frac{\Delta t}{\Delta y} = \lambda \tag{4.38}$$

and therefore

$$v_x = a\lambda \tag{4.39a}$$

$$v_y = b\lambda \tag{4.39b}$$

Hence, in this simplified case, the truncation error for each scheme is

$$S^{(1)} : \quad |\tau_{i,j}^{(1)}| \leq \frac{\lambda^3}{2(\Delta t)^3} \left\{ a+b + \lambda((a+b)^2 + 2ab) \right\} M \tag{4.40a}$$

$$S^{(2)} : \quad |\tau_{i,j}^{(2)}| \leq \frac{\lambda^3}{2(\Delta t)^3} \left\{ a+b + \lambda(\tfrac{3}{2}(a+b)^2 + ab) \right\} M \tag{4.40b}$$

$$S^{(3)} : \quad |\tau_{i,j}^{(3)}| \leq \frac{\lambda^3}{2(\Delta t)^3} \left\{ a+b + \lambda(a+b)^2 \right\} M \, . \tag{4.40c}$$

This implies that

$$|\tau_{i,j}^{(3)}| \leq |\tau_{i,j}^{(1)}| \leq |\tau_{i,j}^{(2)}| \, . \tag{4.41}$$

## 4.5 Linear Stability

Although it was originally intended by the author to show Fourier stability of the three schemes, the complexity of the scheme $S^{(2)}$ made the algebra of such stability analysis impractical. Instead we shall look at stability in the $L_\infty$ norm.

Again we consider the schemes being used to solve the linear advection equation with positive advection coefficients. Once again we write the schemes in the form

$$u_{i,j}^{n+1} = \sum_{l,m=o}^{L,M} C_{l,m} \, U_{i-l,j-m}^{n} \, . \tag{4.14}$$

so that

$$||u_{i,j}^{n+1}|| \leq \sum_{l,m=o}^{L,M} |C_{l,m}| \; ||u_{i-1,j-m}^{n}|| \tag{4.42}$$

$$\leq \sum_{l,m=o}^{L,M} |C_{l,m}| \max_{i,j} ||u_{i-1,j-m}^{n}|| \tag{4.43}$$

$$\leq \max_{i,j} ||u_{i-1,j-m}^{n}||$$

iff $$\sum_{l,m=o}^{L,M} |C_{l,m}| \leq 1 \; . \tag{4.44}$$

Thus, for $S^{(1)}$ , we require

$$|1-\upsilon_x||1-\upsilon_y| + |\upsilon_x||1-\upsilon_y| + |\upsilon_y||1-\upsilon_x| + |\upsilon_x||\upsilon_y| \leq 1 \tag{4.45}$$

i.e. $$(|1-\upsilon_x| + |\upsilon_x|)(|1-\upsilon_y| + |\upsilon_y|) \leq 1 \; . \tag{4.46}$$

Now $$|1-\upsilon| + |\upsilon| = 1 \quad \text{iff} \quad 0 < \upsilon < 1 \tag{4.47}$$

since e.g. if $\upsilon > 1$ then

$$|1-\upsilon| + |\upsilon| > 1 \; . \tag{4.48}$$

Hence $v_x$ , $v_y$ cannot be greater than one

i.e. for $S^{(1)}$ to be stable

$$\underline{0 \leq v_x \leq 1 \quad \text{and} \quad 0 \leq v_y \leq 1} \ . \tag{4.49}$$

For $S^{(2)}$ (4.44) gives

$$|1-\mu_x|^2|1-\mu_y{}^2| + 2|\mu_x||1-\mu_x||1-\mu_y|^2 + 2|\mu_y||1-\mu_y||1-\mu_x|^2$$

$$+ 4|\mu_x||\mu_y|\ |1-\mu_x||1-\mu_y| + |\mu_y|^2|1-\mu_x|^2 + |\mu_x|^2|1-\mu_y|^2$$

$$+ 2|\mu_x||\mu_y|^2|1-\mu_x| + 2|\mu_y||\mu_x|^2|1-\mu_y| + |\mu_y|^2|\mu_x|^2 \leq 1$$

i.e.

$$(|1-\mu_x| + |\mu_x|)^2\ (|1-\mu_y| + \mu_y|)^2 \ \leq 1 \ .$$

hence

$$(|1-\mu_x| + |\mu_x|)\ (|1-\mu_y| + |\mu_y|) \ \leq 1$$

and by similar arguments for $S^{(1)}$ we have that

$$\underline{0 \leq \mu_x \leq 1 \qquad\qquad 0 \leq \mu_y \leq 1} \ .$$

We now turn our attention to $S^{(3)}$ ; for this scheme the stability criterion is

$$0 \leq |1-v_x-v_y| + |v_x| + |v_y| \leq 1$$

or

$$|1-v_x-v_y| \leq 1-|v_x| - |v_y|$$

which is satisfied for

$$\underline{v_x + v_y \leq 1} .$$

In the following section we will show how the three different strategies compare in numerical tests via various different test problems.

## §5 Numerical Tests

The previous chapters have concentrated on various aspects of operator splitting and we have now come to the point where we compare and complement the analytic results with numerical tests. However, before describing the test problems we will study how, in two-dimensions, the resolution of each of the three schemes is affected by information propagating in directions that are not aligned with the grid.

### 5.1 Propagation of a shock

Since shocks are a common occurence in nonlinear gas dynamics, we investigate how well each split scheme resolves the propagation of a simple scalar discontinuity travelling obliquely to the grid lines.

We consider solving the Burgers'-like equation

$$u_t + (\tfrac{1}{2} \cos\theta\, u^2)_x + (\tfrac{1}{2} \sin\theta\, u^2)_y = 0 \qquad (5.1)$$

with initial data $u(x,y,0) = u_o$ as shown in the diagram

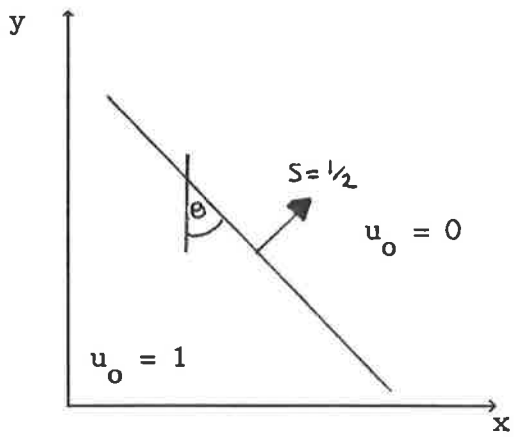


figure D

Initial data of shock propagation problem

The analytic solution of this problem is that the discontinuity line propagates at a speed $s = \frac{1}{2}$ normal to itself. To test the accuracy of the three schemes we consider advancing the solution through one time-step and compare the results with the analytic solution in one cell for various values of $\theta$ .

We discretise the computational domain such that the mesh points occur at the centre of each computational cell. Since we are only considering the solution in one cell after one time step, we need at most nine computational cells to accommodate the three first order schemes described previously. Thus the (square) mesh and the initial data are taken as follows

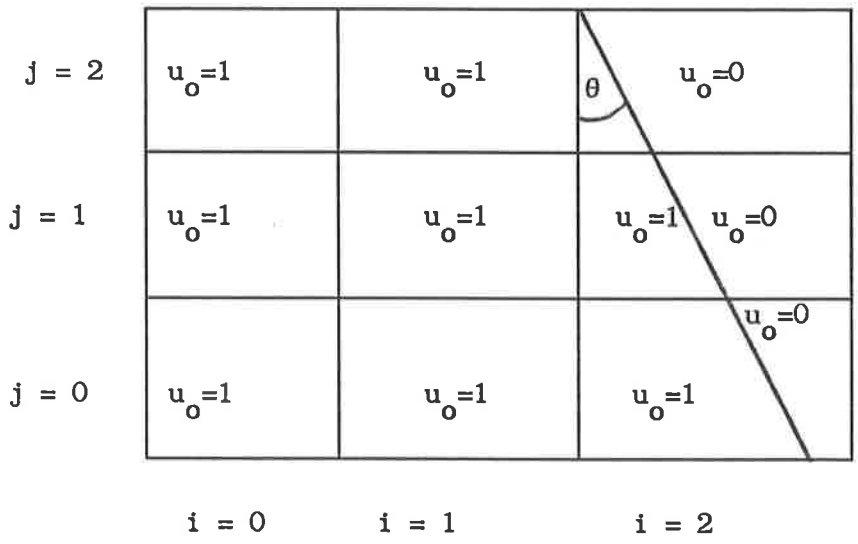


figure E

We now project the values of the intial data onto the mesh points in the manner

$$u_{ij} = \frac{1}{\Delta x\ \Delta y} \int_{y_{j-\frac{1}{2}}}^{y_{j+\frac{1}{2}}} \int_{x_{i-\frac{1}{2}}}^{x_{i+\frac{1}{2}}} u\ dx\ dy \qquad (5.2)$$

which yields the following values for $u_{ij}$

$$u_{0j} = u_{1j} = 1 \qquad \forall_j$$

$$u_{20} = \begin{cases} \frac{5t}{2} & 0 \le \theta \le \tan^{-1}(\frac{1}{3}) \\ 1 - \frac{(1-2t)^2}{2t} & \tan^{-1}(\frac{1}{3}) \le \theta \le \tan^{-1}(\frac{1}{2}) \\ 1 & \tan^{-1}(\frac{1}{2}) \le \theta \le \tan^{-1}(1) \end{cases}$$

$$u_{21} = \begin{cases} \frac{3t}{2} & 0 \le \theta \le \tan^{-1}(\frac{1}{2}) \\ 1 - \frac{(1-t)^2}{2t} & \tan^{-1}(\frac{1}{2}) \le \theta \le \tan^{-1}(1) \end{cases}$$

$$u_{22} = \frac{t}{2}$$

where

$$t = \tan \theta \ .$$

The exact solution for $u_{22}$ after a time $\Delta t$ is given by the projected value

$$u_{22} = \begin{cases} \frac{1}{2}\left[t + \frac{\Delta t}{\Delta x}\ \frac{1}{c}\right] & t + \frac{\Delta t}{\Delta x}\ \frac{1}{2c} \le 1 \\ 1 - \frac{1}{2}\left[1 - \frac{\Delta t}{\Delta x}\ \frac{1}{2c}\right]^2 \frac{1}{t} & \frac{\Delta t}{\Delta x}\ \frac{1}{2c} \le 1 \le t + \frac{\Delta t}{\Delta x}\ \frac{1}{2c} \\ 1 & \frac{\Delta t}{\Delta x}\ \frac{1}{2c} > 1 \end{cases}$$

where $c = \cos\theta$ .

The three schemes were tested against the exact solution, the underlying one-dimensional operator in each case being the first order upwind scheme of Cole-Murman (see §4).

Figures 12 through 15 show the approximate solutions for $u_{22}$ using the three operator split schemes for various different values of $\frac{\Delta t}{\Delta x}$ with $\theta$ varying between $0^o$ and $45^o$.

Figures 16 through 19 show the absolute errors incurred by the three schemes and figures 20 through 23 show the relative error for the three schemes.

We see from these figures that the angle of the shock affects the error greatly and that for angles $\theta > 20^o$ the error in one time-step is considerable. It is observable in these results that the scheme $S^{(2)}$ always does worse than either of the other two schemes. More interestingly, though, is the way in which $S^{(1)}$ behaves in comparison to $S^{(3)}$ : for an angle of less than $22^o$ (approximately) $S^{(1)}$ performs marginally better than $S^{(3)}$ but for larger angles $S^{(3)}$ performs better. We note that for $\frac{\Delta t}{\Delta x} = 1.0$ the C.F.L. condition for $S^{(3)}$ is violated.

We now describe the full test problems.

## 5.2 Two Advection problems

Consider solving the advection equation

$$u_t + u_x + u_y = 0 \qquad (5.3)$$

using two sets of initial data. The first set consists of a smooth function defined on [0,1] x [0,1] of the following form

$$u_o(x,y) = \begin{cases} 4 \cos^2 \left[\frac{5\pi R}{2}\right] & R \leq 0.2 \\ 0 & R > 0.2 \end{cases}$$

where $R^2 = (x - 0.25)^2 + (y - 0.25)^2$ .

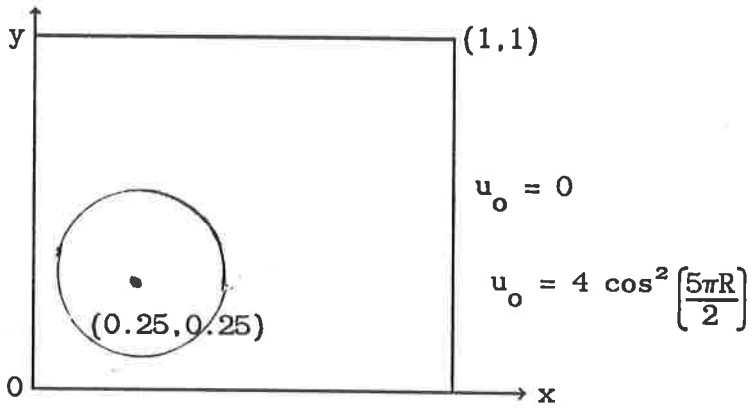


figure F

The second set of intial data is a discontinuous 'box' function on [0,1] x [0,1] defined as follows

$$u_o(x,y) = \begin{cases} 4 & 0.004 \leq x,y \leq 0.46 \\ 0 & \text{elsewhere} \end{cases}$$

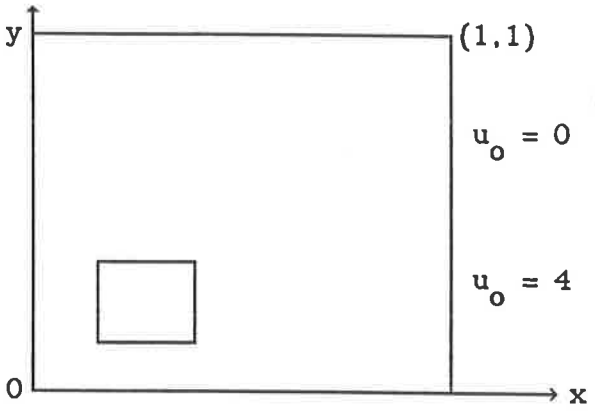


figure G

## 5.3 Two Riemann Problems

Recent work has been directed towards obtaining analytic solutions of simple scalar two-dimensional Riemann problems (see for example Klingenberg [22], Lindquist [23]). In the sense used here, a two-dimensional Riemann problem is a scalar non-linear problem of the form

$$u_t + f(u)_x + g(u)_y = 0 \qquad (5.4)$$

with initial data

$$u_o(x,y) = \begin{cases} a & x > 0,\ y > 0 \\ b & x > 0,\ y < 0 \\ c & x < 0,\ y > 0 \\ d & x < 0,\ y < 0 \end{cases}$$

where a,b,c,d are constants.

Analytic entropy satisfying solutions are now available for certain special cases, e.g. when $f = g$ and a,b,c,d satisfy certain criteria [22],[23]. It is from this set of solved two-dimensional Riemann problems that we draw the next two test problems, i.e. we consider

$$u_t + (\tfrac{1}{2}u^2)_x + (\tfrac{1}{2}u^2)_y = 0$$

with the two sets of inital data:

$$u_o(x,) = \begin{cases} -1 & x,y > 0 \\ \frac{1}{2} & y > 0,\ x < 0 \\ 0 & y < 0,\ x > 0 \\ 1 & x,y < 0 \end{cases}$$

(ii)

$$u_o(x,y) = \begin{cases} -\frac{1}{2} & x,y > 0 \\ \frac{1}{2} & y > 0\ ,\ x < 0 \\ 0 & y < 0,\ x > 0 \\ 1 & x,y < 0 \end{cases}$$

These two problems are solved on the region $[-\frac{1}{2},\frac{1}{2}] \times [-\frac{1}{2},\frac{1}{2}]$. Having described the test problems we now reveal the analytic solution.

## 5.4 Analytic Solutions

The four preceding test problems have been chosen for their relative simplicity and also because analytic solutions exist for comparison with the numerical tests. The analytic solution to the advection problems at time T is given by

$$u(x,y,T) = u_o(x-T,\ y-T) \tag{5.5}$$

i.e. the initial data is advected without deformation, rotation or diffusion along a line parallel to the curve $x = y$ .

Analytic solutions of the Riemann problems are more complex than the advection problems. We can apply the Rankine-Hugoniot jump condition along the shock interfaces to yield part of the solution, although it is obvious that this does not yield the full solution. The full solutions to the two Riemann problems may best be shown pictorially. For the first Riemann problem the exact solution is as in the diagram

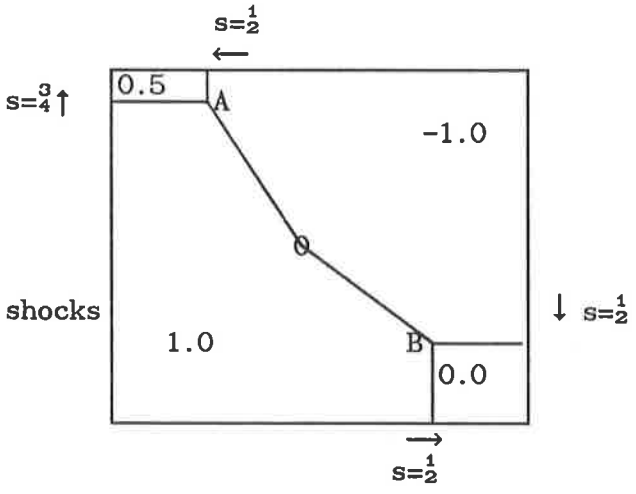


Analytic solution of first Riemann problem

figure H

where s is the shock speed

In the above figure H, let A and B denote the intersection points of the three shock interfaces (initially the points A and B are at the origin). Then at time T

$$A = \left[ -\frac{T}{2} , \frac{3T}{4} \right]$$

$$B = \left[ \frac{T}{2} , -\frac{T}{2} \right]$$

and the secondary shock (not present in the initial data) is along the curve joining AO and OB where O is the origin.

For the second Riemann problem, the exact solution is as in Figure I.

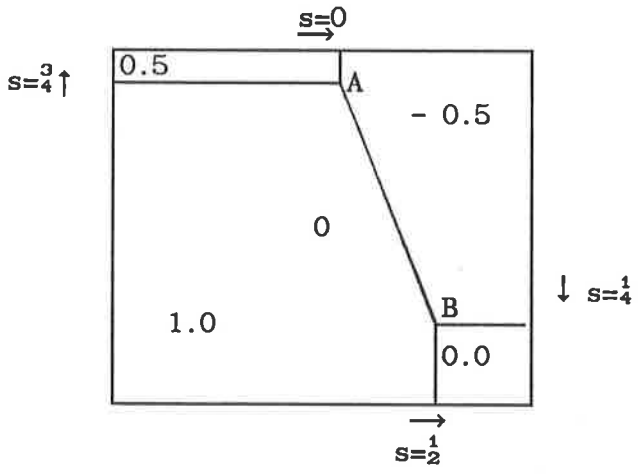


Analytic solution of second Riemann problem

figure I

Again, in figure I, we let A and B be the points of the corners of the shocks. Then, at time T

$$A = \left[0 \ , \ \frac{3T}{4}\right]$$

$$B = \left[\frac{T}{2} \ , \ \frac{-T}{4}\right]$$

and the secondary shock lies along the line joining A and B .

## 6.5 Boundaries, Errors and other Numerical Considerations

The boundary conditions used were made as simple as possible so as not to detract from the purpose of the analysis. For the advection equation 'periodic' boundary conditions were used, i.e. the actual computational domain is considered as the central part of a much bigger domain that is divided into equal sized sub-domains. Exactly the same process is assumed to be occuring in each sub-domain so that if data moves out of the central sub-domain, then exactly the same data moves into the central sub-domain from an adjacent sub-domain (see figure J below).

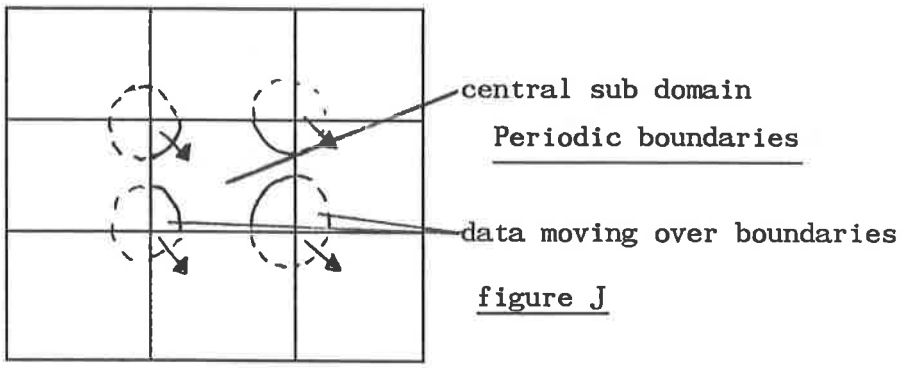


figure J

For the two Riemann problems we assume tranparent boundary conditions normal to the boundaries. Their effect on the interior solution may be monitored by assuming that any resulting disturbances propagate into the interior at a finite known speed.

Turning our attention now to calculation of errors, we look at five simple types of error estimate. The three simplest are defined as follows

(i) error in the $l_\infty$ norm defined as

$$e_\infty = \underset{\forall i,j}{\text{Max}} \{(u^n_{i,j})\} \tag{5.6}$$

(ii) error in the $l_1$ norm

$$e_1 = \sum_{\forall i,j} |u_T(i\Delta x, j\Delta y) - u^N_{i,j}| \, \Delta x \, \Delta y \tag{5.7}$$

(iii) error in the $l_2$ norm

$$e_2 = \sqrt{\sum_{\forall i,j} (u_T(i\Delta x, j\Delta y) - u^N_{i,j})^2} \, \Delta x \, \Delta y \tag{5.8}$$

where $u_T(i\Delta x, j\Delta y)$ is the exact solution at time $T = N\Delta t$ and grid position $(x,y) = (i\Delta x, j\Delta y)$ .

We note that the first error estimate is only useful for the advection problems where the maximum height of exact solution is 4.

We also have two other methods of monitoring the numerical

solution, namely the energy error and a two dimensional TV (q.v. section 3).

We can look at the loss of "energy" within the system (5.4): i.e. multiplying

$$u_t + f(u)_x + g(u)_y = 0 \tag{5.9}$$

by $u$ leads to

$$uu_t = \frac{\partial(\frac{1}{2}u^2)}{\partial t} = - u[f(u)_x + g(u)_y] \ .$$

Integrating over the domain, we find that

$$\frac{\partial}{\partial t} \int \tfrac{1}{2}u^2 \, dx \, dy \Big|_0^t + \int_0^t \int u[f(u)_x + g(u)_y] dx \, dy$$

is constant in time. Thus we define the "energy" error to be

$$e_E(u) = \Big| \int \tfrac{1}{2} u^2 \, dx \, dy \Big|_0^t + \Delta t \sum_{n=1}^{N} \int u^n [f_x + g_y] \, dx \, dy \tag{5.10}$$

which should not grow with $t$ . A discrete approximation $e_E^n(u^n)$ to (5.10) can be constructed in which $f_x, g_y, u^n$, approximations to $f(u)_x$, $g(u)_y$ and $u(x,y,t)$ are given by the approximate solution and the integration in (5.10) is carried out numerically. The initial energy in the error $u-u^n$ being zero, a measure of the error is

obtained by calculating the growth of $e_E^n\ (u^n - u)$.

As well as looking at the loss of energy within the numerical computation, we can also look at the two-dimensional 'total variation' (TV) in the sense of Goodman and Leveque [24]. In this paper the TV is defined as the direct extension from one dimension into two dimensions:

$$TV(u) = \int |u_x| + |u_y| \, dx \, dy \tag{5.11}$$

(c.f. section 3) with discrete analogue being

$$TV(u^n) = \sum_{\forall j,n} \{\Delta y |u_{j+1,k} - u_{j,k}| + \Delta x |u_{j,k+1} - u_{j,k}|\} \ . \tag{5.12}$$

It is worth noting that, in studying the first of the two Riemann problems presented earlier, the exact solution is not TV bounded in the above sense and therefore the above TV norm is misleading when applied to certain test problems for example, the first of the two Riemann problems has an initial TV of 1.99 and at time $t = 0.5$ the TV is about 3 . However, for the advection problems (5.12) proves to be a useful monitor.

All the schemes applied to the test problems described above were carried out on a 101 x 101 grid with

$$\Delta x = \Delta y = 0.01$$

and

$$\Delta t = 0.0025 \ .$$

## 5.6 A Further Test Problem

The motivation behind the work of this report is to investigate genuinely two-dimensional algorithms for non-linear gas dynamics and for this reason we include the following additional test problem.

This test problem is a cylindrically symmetric extension to the shocktube problem of Sod [25] and involves solving a non-linear system of hyperbolic p.d.e's. The problem represents a fairly mild shock problem in the field of computational fluid dynamics.

Here we are dealing with a two-dimensional gas lying, initially at rest, in a square region. The region is divided by a circular membrane of radius $R$ . There are finite jumps in density and pressure across the membrane. At time $t = 0$ , the membrane is removed (or burst). A shockwave and contact form and move away from the origin whilst an expansion moves towards the origin.

Reflection boundary conditions were implemented along the four boundaries. However, the solution is not allowed to progress too far, so that the boundaries have no effect on the solution.

The equations of motion governing the flow are the two-dimensional Euler equations (see §3). The underlying one-dimensional solution operator is the linearised approximate Riemann solver of Roe [4] (see also Roe and Pike [16], Barley [20]) with an entropy fix. The second order scheme is as above, but with the

'superbee' limiter added into the scheme. [13].

The initial data is

$$\left.\begin{array}{l} \rho = 1.0 \\ u = v = 0 \\ p = 1.0 \end{array}\right\} r < R$$

$$\left.\begin{array}{l} \rho = 0.125 \\ u = v = 0 \\ p = 0.1 \end{array}\right\} r > R$$

where $r = \sqrt{x^2 + y^2}$ and $R = 0.5$ . The solution domain is $[-1,1] \times [-1,1]$ with

$$\Delta y = \Delta x = 0.02$$

$$\Delta t = 0.003 \ .$$

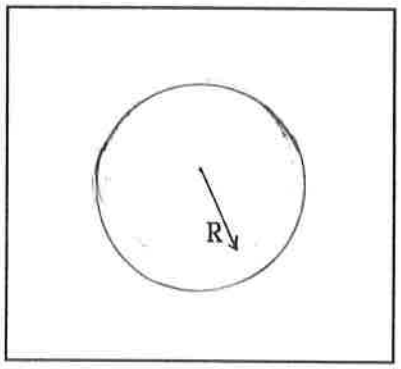


high pressure and density

membrane

low pressure and density

figure K

Initial data for gas dynamic test problem.

Results of the tests described here are given in the following section.

## §6 Results

The three splitting strategies $S^{(1)}, S^{(2)}, S^{(3)}$, described in Section 4 were applied to the five test problems described in the previous section. The underlying one-dimensional operator for the three splitting strategies in the scalar case is the Enquist-Osher scheme [15] which has been extended to a high resolution scheme by the employment of the 'superbee' limiter (see Sweby [13]). For the gas dynamic problem the underlying one-dimensional operator is Roe's scheme, again being extended to second order by use of the 'superbee' limiter.

For all the scalar test problems the following ratio's were used

$$\frac{\Delta t}{\Delta x} = \frac{\Delta t}{\Delta y} = 0.25 \qquad \text{where} \quad \Delta t = 0.0025$$

so that the maximum value of the CFL number is less than $0.5$ .

Each solution was advanced to a final time of $T = 0.5$ (200 time steps) and graphical and diagnostic output was produced at this time.

Table 1 shows the values of the various errors incurred by the three schemes applied to the scalar test problems and first and second order results can be compared. Table 2 shows the initial and final TV of the exact solutions to the test problems. More enlightening are the graphs (figures 24 through 47) which give more of an idea about how the schemes compare with each other in relation to various test problems.

Table 1: Errors Incurred During Computation of the Solution of the Scalar Test Problems

| PROBLEM | ORDER | FIRST | | | SECOND | | |
|---|---|---|---|---|---|---|---|
| | SCHEME | $S^{(1)}$ | $S^{(2)}$ | $S^{(3)}$ | $S^{(1)}$ | $S^{(2)}$ | $S^{(3)}$ |
| | Error Estimate | | | | | | |
| Advection of a cosine-Blip | $e_\infty$ | 2.62612 | 2.47159 | 2.64336 | 3.92507 | 3.92877 | 3.92767 |
| | $e_1$ | 0.06384 | 0.07159 | 0.06378 | 0.00508 | 0.00531 | 0.02358 |
| | $e_2$ | 0.18589 | 0.20624 | 0.18624 | 0.01806 | 0.01895 | 0.08852 |
| | $e_E$ | 0.07078 | 0.07744 | 0.06081 | 0.00230 | 0.00243 | 0.00711 |
| | TV | 2.53306 | 2.45347 | 2.55452 | 3.16336 | 3.16496 | 3.28374 |
| Advection of a box | $e_\infty$ | 3.99671 | 3.99131 | 3.99998 | 4.00000 | 4.00000 | 4.00000 |
| | $e_1$ | 0.32414 | 0.34774 | 1.18850 | 0.06964 | 0.07132 | 0.07624 |
| | $e_2$ | 0.62718 | 0.65064 | 2.01847 | 0.33532 | 0.33974 | 0.38381 |
| | $e_E$ | 0.43680 | 0.46850 | 0.33989 | 0.08302 | 0.08492 | 0.07788 |
| | TV | 6.87715 | 6.87243 | 6.87998 | 6.88000 | 6.88000 | 7.85398 |
| 1st Riemann Problem | $e_\infty$ | 1.00000 | 1.00000 | 1.00000 | 1.00000 | 1.00000 | 1.00000 |
| | $e_1$ | 0.08565 | 0.08613 | 0.08556 | 0.08251 | 0.08261 | 0.08241 |
| | $e_2$ | 0.37778 | 0.37800 | 0.37767 | 0.37865 | 0.37888 | 0.37853 |
| | $e_E$ | 0.37778 | 0.37731 | 0.37986 | 0.43100 | 0.43349 | 0.43286 |
| | TV | 2.86500 | 2.86500 | 2.86500 | 2.86500 | 2.86500 | 2.86502 |
| 2nd Riemann Problem | $e_\infty$ | 1.00000 | 1.00000 | 1.00000 | 1.00000 | 1.00000 | 1.00000 |
| | $e_1$ | 0.01265 | 0.01321 | 0.01233 | 0.00853 | 0.00858 | 0.00821 |
| | $e_2$ | 0.07831 | 0.07805 | 0.07608 | 0.08148 | 0.08156 | 0.07962 |
| | $e_E$ | 0.13526 | 0.13457 | 0.13711 | 0.16224 | 0.16332 | 0.16441 |
| | TV | 2.00000 | 2.00000 | 2.00000 | 2.00000 | 2.00000 | 2.00000 |

Before discussing the results, it is worthwhile pointing out that the label on each graph ('S1CBA1' on figure 24 for example) is an indication to the problem being solved. The first two characters, S followed by a digit, refer to the splitting strategy being applied i.e.

$$S1 \equiv S^{(1)}, \qquad S2 \equiv S^{(2)}, \qquad S3 \equiv S^{(3)}$$

The final character (always a digit) refers to the order of the underlying one-dimensional solution operator i.e.

1 ≡ first order

2 ≡ second order

The characters appearing before the order reference and after the splitting reference refer to the test problem, the key for this being

CBA ≡ advection of a cosine blip

BA ≡ advection of a box

RP1 ≡ first Riemann problem

RP2 ≡ second Riemann problem

We conclude this section with a discussion of the results.

The two most noticeable features present in the solution of the

advection problems are the 'squaring' of data in the second order results and the stretching of data perpendicular to the direction of motion. This second feature is present in all the solutions but more obvious in the results for $S^{(3)}$ and is due to the data being allowed to travel in two directions only, i.e. the data naturally tries to allign with the grid. The reason for $S^{(3)}$ suffering from this affliction more than $S^{(1)}$ or $S^{(2)}$ is that $S^{(3)}$ fails to compensate for the cross-terms $(u_{xy})$ in the Taylor-expansion for the scheme.

The squaring of the data in the second order results is due to grid alignment i.e. since the schemes are applied on a square grid, the data only travel in the direction that the underlying one-dimensional scheme is being applied in and since the scheme is only applied in two directions, data will tend to align with these two prefered directions. This is more apparent in the second order results since the stencil of the underlying one-dimensional operator lies over more grid points for the second order scheme than for the first order scheme and so the split scheme will produce more one-dimensional effects.

The results for the scalar Riemann problems are very good for all of the schemes although this is probably due to the discontinuities being initially aligned with the grid.

Despite the abovementioned grid effects, we can see that for the advection problems $S^{(1)}$ produces marginally better results than $S^{(2)}$ and $S^{(3)}$, however, $S^{(3)}$ produces the best results for the Riemann problems.

The results for the gas dynamic problem show the same effects as

in the scalar test problem, i.e. there is slight squaring of data due to the grid effects although they are not as noticeable, especially in the results for $S^{(3)}$ which are comparable to the results for $S^{(1)}$ in both the first order and second order tests.

Table 2 : Initial and final TV for the Scalar Test Problems

(Exact Solutions)

| Problem | Blip Advection | Box Advection | Riemann 1 | Riemann 2 |
|---|---|---|---|---|
| Initial TV | 3.2 | 6.88 | 1.99 | 1.5 |
| Final TV | 3.2 | 6.88 | 3.065 | 2.000 |

## §7 Conclusion

Although the failure of $S^{(3)}$ to perform as well as hoped would at first seem to suggest that we cannot consider $S^{(3)}$ if we are going to apply operator splitting, we can take heart in the fact that is easy to take $S^{(3)}$ out of the splitting framework and use it as a basis for a genuinely two-dimensional scheme. It can be seen that the computational time used by $S^{(3)}$ is far less than that used by the other two methods, and so it is hoped that, if one is going to consider solving hyperbolic conservation laws in two-dimensions, then one may consider using $S^{(3)}$ with additional terms to handle the cross derivative terms in the Taylor expansion for the scheme.

By considering the stencils for $S^{(1)}$ and $S^{(3)}$ we can see that both of these schemes could be taken out of the operator splitting framework and considered as bases for genuinely two-dimensional schemes (see Priestley [26]).

We sum up by stating the obvious need for genuinely two-dimensional schemes (based on $S^{(3)}$, perhaps) and hopefully the next few years may see the development of two-dimensional schemes that have all the necessary features (such as entropy satisfaction and TVD) that are the hallmark of high resolution schemes in one-dimension.

Aknowledgements

I would like to thank my supervisor, Dr. M.J. Baines and Dr. P.K. Sweby for many useful discussions. I would also like to thank P.Glaister and Dr A. Priestley for useful interjections and inspiration. Thanks are due also to Sue Davis for her patience in the preparation of this report.

I aknowledge the financial support of SERC and AWE Aldermaston.

References

[1] Strang, G. "On the Construction and Comparison of Finite Difference Schemes", SIAM J. Numer. Anal., Vol 5, No 3 (1968).

[2] Yanenko, N.N. "The Method of Fractional Steps", Springer-Verlag, New York (1971).

[3] Sod, G.A. "Numerical Methods in Fluid Dynamics. Initial and Initial Boundary Value Problems". Cambridge University Press (1985).

[4] Roe, P.L. "Approximate Riemann Solvers, Parameter Vectors, and Difference Schemes". J. Comput. Phys. 43, p.357 (1981).

[5] Oleinik, O.A. "On Discontinuous Solutions of Non-linear Differential Equations". Uspekhi Mat. Nauk., 12 (1957).

[6] Smoller, J. "Shock Waves and Diffusion-Reaction Equations". Springer-Verlag, New York (1983).

[7] Lax, P.D. "Hyperbolic Conservation Laws and the Mathematical Theory of Shockwaves". SIAM Regional Conference Series in "Lectures in Applied Mathematics" (1972).

[8] Lax, P.D. and Wendroff, B. "Systems of Conservation Laws". Comm. Pure and Applied Maths. Vol. XIII, p.217 (1960).

[9] Warming, R.F. and Beam R.M., "Upwind Second Order Difference Schemes and Applications in Aerodynamics". AIAA Journal Vol. 41, No. 9 (1976).

[10] Woodward, P.R. and Colella, P. "The Piecewise Parabolic Method (PPM) for Gas-Dynamical Simulations". J.C.P. 54, p.174 (1984).

[11] Boris, J.P. and Book, D.L. "Flux Corrected Transport. I. SHASTA, A Fluid Transport Algorithm that Works". J.C.P. 11, p. 38 (1973).

[12] Van Leer, B. "Towards the Ultimate Finite Difference Scheme I". Lecture Notes in Physics, 18, Springer, Berlin (1973).

[13] Sweby, P.K. "High Resolution Schemes Using Flux Limiters for Hyperbolic Conservation Laws". SIAM J. Numer. Anal. 21, p.995. (1984).

[14] Harten, A., Osher, S., Enquist, B. and Chakravarthy, S.R. "Some Results on Uniformly High Order Accurate Essentially Non-Oscillatory Schemes". J. App. Num. Math (to appear) (1986).

[15] Osher, S. "Riemann Solvers, the Entropy Condition, and Difference Approximations". SIAM J. Numer. Anal. 21, p.217 (1984).

[16] Roe, P.L. and Pike, J. "Efficient Construction and Utilisation of Approximate Riemann Solutions". Comp. Meth. in Appl. Science and Engin VI, 499 (1984).

[17] Sweby, P.K. and Baines, M.J. "On Convergence of Roe's Scheme for the General Non-Linear Scalar Wave Equation". J. Comput. Phys. Vol. 56, No 1.

[18] Glaister, P. "Flux Difference Splitting Techniques for the Euler Equations in Non-Cartesian Geometry". Numer. Anal. Report 8/85 Department of Math., University of Reading. (1985).

[19] Glaister, P. "An Approximate Linearised Riemann Solver in One-Dimension with a General Equation of State". Numer. Anal. Report 7/86, Dept. of Math., Reading University (1986).

[20] Barley, J.J. "A Two-Dimensional Algorithm for the Non-linear Equations of Gas Dynamics Employing Operator Splitting". Numer. Anal. Report, 4/87, Dept. of Math., University of Reading.

[21] Roe, P.L. "Discontinuous Solutions to Hyperbolic Systems Under Operator Splitting". ICASE Report no. 87-64, NASA Langley (1987).

[22] Klingenberg, C. "Hyperbolic Conservation Laws in Two-Dimensions : Some Numerical and Theoretical Results". Institute Mittag-Leffler, Heidelberg, Report No. 2 (1986).

[23] Lindquist, W.B. "Construction of Solutions for Two-Dimensional Riemann Problems". Comp. and Maths with Appl., Vol 12a, (preprint) (1986).

[24] Goodman, J.B. and Le Veque, R.J. "On the Accuracy of Stable Schemes for 2-D Scalar Conservation Laws". Courant Institute, New York (preprint) (1985).

[25] Sod, G.A. "A Survey of Several Finite Difference Methods for Systems of Non-linear Hyperbolic Conservation Laws". J. Comput. Phys. 27 p.1 (1978).

[26] Priestley, A. "Roe Type Schemes for the 2-D Shallow Water Equations". Numer. Anal. Report 8/87, Dept. of Math., University of Reading (1987).

[27] Murman, E.M. and Cole, J.D. "Calculations of Plane Steady Transonic Flows". AIAA Journal, Vol. 9, p.114 (1971).

[28] Roe, P.L. "Numerical Algorithms for the Linear Wave Equation". R.A.E. Technical Report (1981).

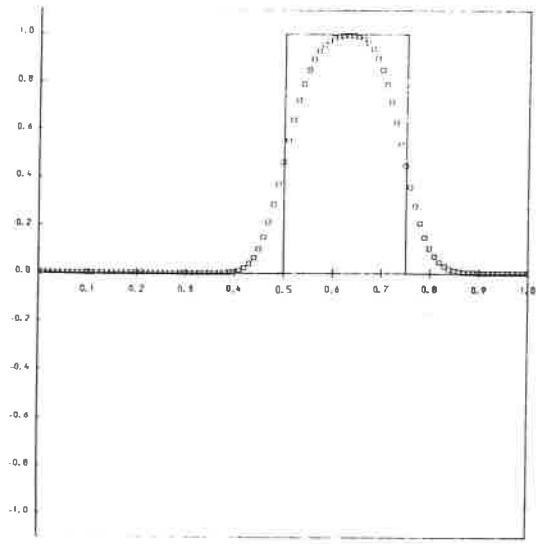

LINEAR ADVECTION EQUATION
HOMOGENEOUS
SQUARE WAVE DATA
PERIODIC BOUNDARY CONDITIONS
$\Delta x$ = 0.0100
MESH RATIO= 0.25
T= 0.25 ( 100 STEPS)

- , - EXACT SOLUTION

COLE-MURMAN (ROE) SCHEME ,
NO LIMITER, 1ST ORDER

figure #1

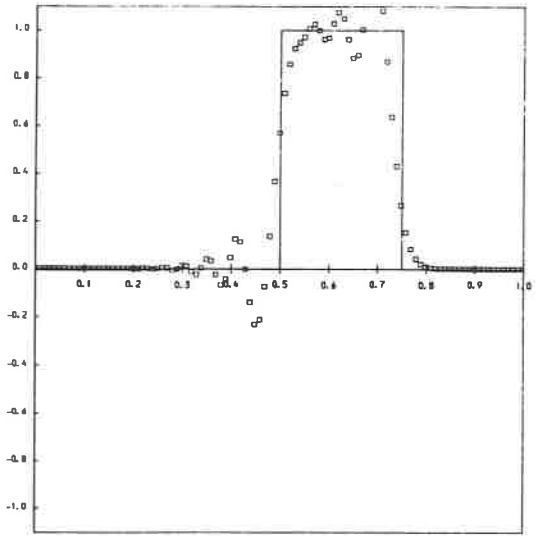

LINEAR ADVECTION EQUATION
HOMOGENEOUS
SQUARE WAVE DATA
PERIODIC BOUNDARY CONDITIONS
$\Delta x$ = 0.0100
MESH RATIO= 0.25
T= 0.25 ( 100 STEPS)

- , - EXACT SOLUTION

LAX-WENDROFF SCHEME ,

figure #2

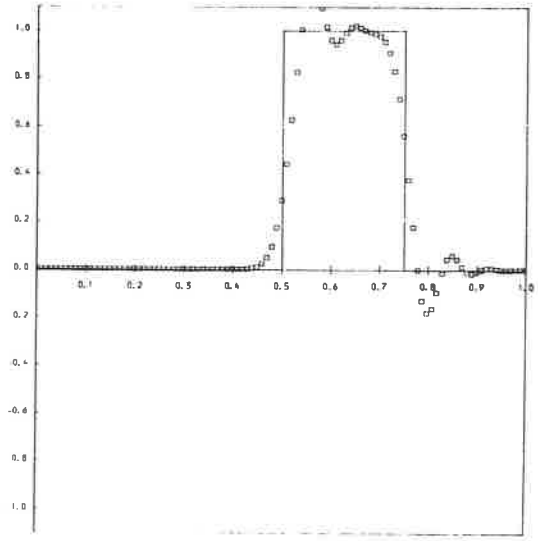

LINEAR ADVECTION EQUATION
HOMOGENEOUS
SQUARE WAVE DATA
PERIODIC BOUNDARY CONDITIONS
$\Delta x$ = 0.0100
MESH RATIO= 0.25
T= 0.25 ( 100 STEPS)

- , - EXACT SOLUTION

WARMING AND BEAM SCHEME ,

figure #3

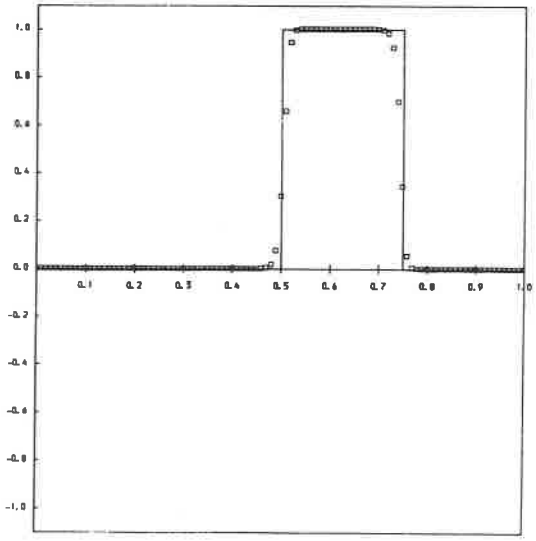

LINEAR ADVECTION EQUATION
HOMOGENEOUS
SQUARE WAVE DATA
PERIODIC BOUNDARY CONDITIONS
$\Delta x$ = 0.0100
MESH RATIO= 0.25
T= 0.25 ( 100 STEPS)

- , - EXACT SOLUTION

COLE-MURMAN (ROE) SCHEME ,
SUPERBEE LIMITER

figure #4

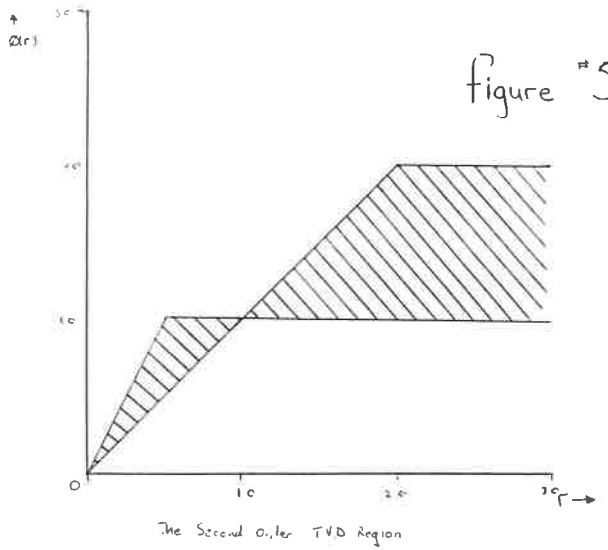


The Second Order TVD Region

figure #5

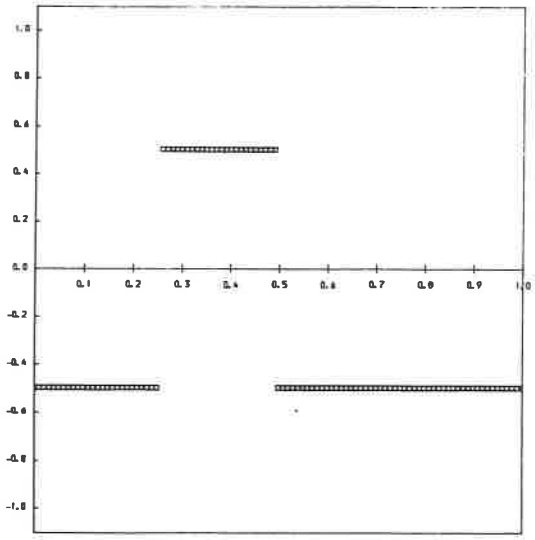

INVISCID BURGERS EQUATION
HOMOGENEOUS
SQUARE WAVE DATA
PERIODIC BOUNDARY CONDITIONS
Δx = 0.0100
MESH RATIO= 0.25
T= 0.03 & 0.24 ( 14 & 98 STEPS)

- , - EXACT SOLUTION (MFE)

COLE-MURMAN (ROE) SCHEME ,
NO LIMITER, 1ST ORDER

figure #6

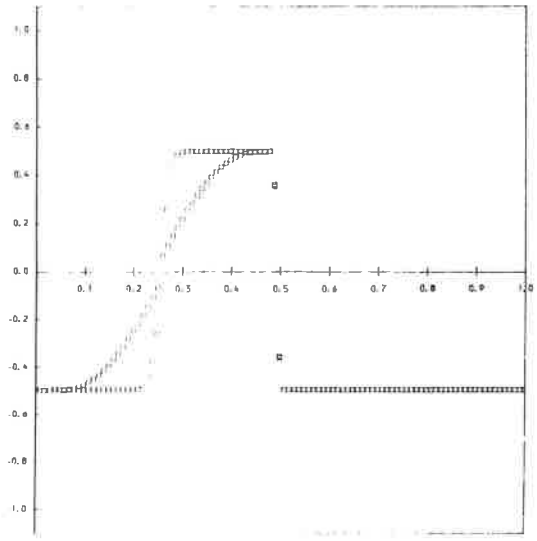

INVISCID BURGERS EQUATION
HOMOGENEOUS
SQUARE WAVE DATA
PERIODIC BOUNDARY CONDITIONS
Δx = 0.0100
MESH RATIO= 0.25
T= 0.03 & 0.24 ( 14 & 98 STEPS)

- , - EXACT SOLUTION (MFE)

ENGQUIST-OSHER SCHEME ,
NO LIMITER, 1ST ORDER

figure #7

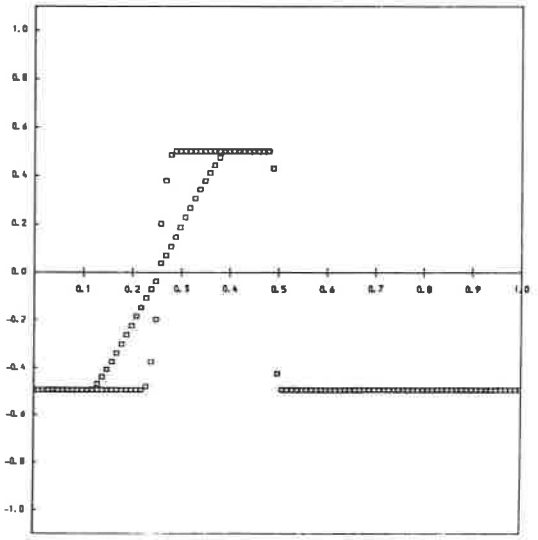

INVISCID BURGERS EQUATION
HOMOGENEOUS
SQUARE WAVE DATA
PERIODIC BOUNDARY CONDITIONS
Δx = 0.0100
MESH RATIO= 0.25
T= 0.03 & 0.24 ( 14 & 98 STEPS)

- , - EXACT SOLUTION (MFE)

ENGQUIST OSHER SCHEME ,
SUPERBEE LIMITER

figure #8

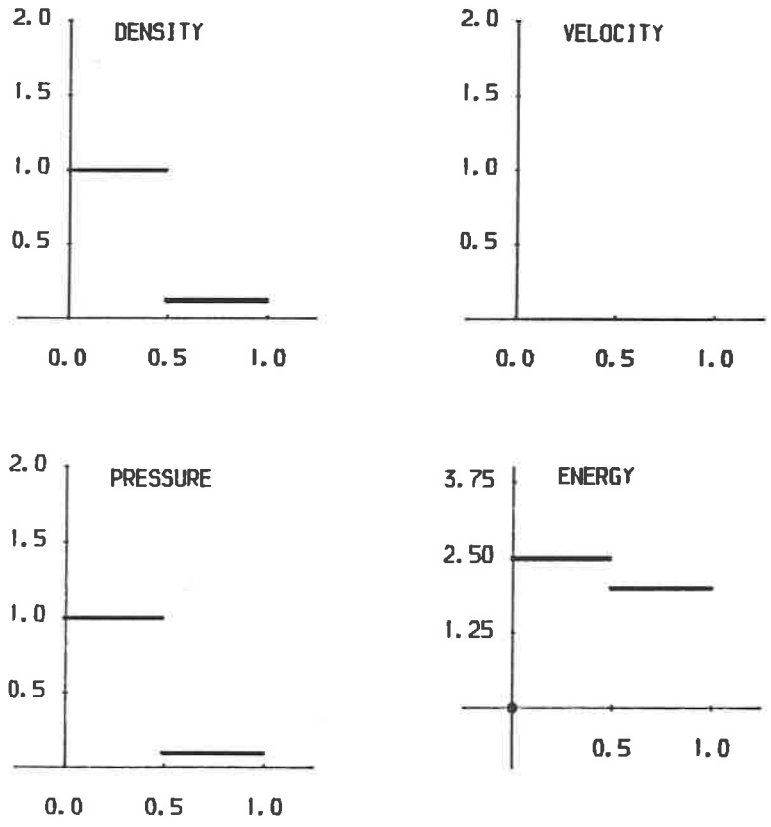
2.0
DENSITY
1.5
1.0
0.5
0.0
0.5
1.0
2.0
VELOCITY
1.5
1.0
0.5
0.0
0.5
1.0
2.0
PRESSURE
1.5
1.0
0.5
0.0
0.5
1.0
3.75
ENERGY
2.50
1.25
0.5
1.0
T= 0.000 , 0 STEPS
SODS PROBLEM
MESH RATIO = 0.150 , 101 POINTS
U-A FIELD :- NO LIMITER
U FIELD :- NO LIMITER
U+A FIELD :- NO LIMITER

figure #9

Figure #10

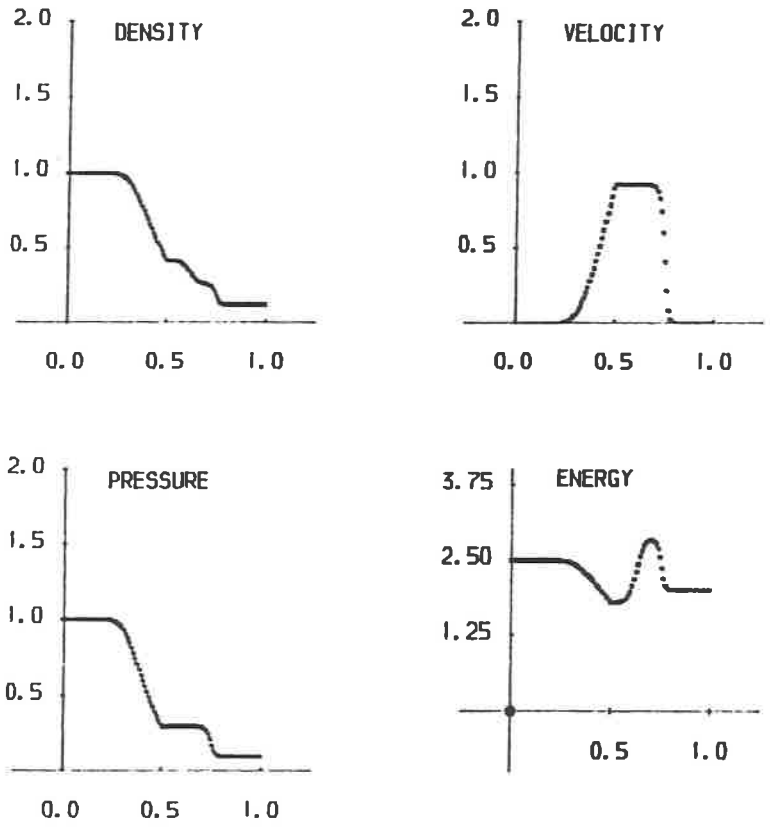


T= 0.144 , 96 STEPS
SODS PROBLEM
MESH RATIO = 0.150 , 101 POINTS

U-A FIELD :- NO LIMITER
U FIELD :- NO LIMITER
U+A FIELD :- NO LIMITER

Figure #11

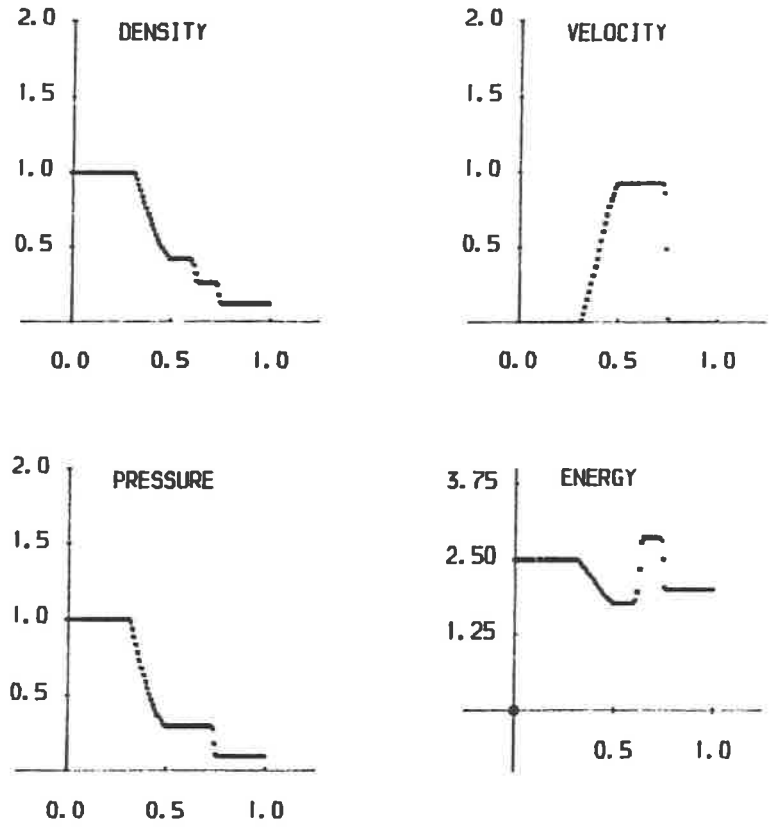


T= 0.144 , 96 STEPS
SODS PROBLEM
MESH RATIO = 0.150 , 101 POINTS

U-A FIELD :- SUPERBEE LIMITER
U FIELD :- SUPERBEE LIMITER
U+A FIELD :- SUPERBEE LIMITER

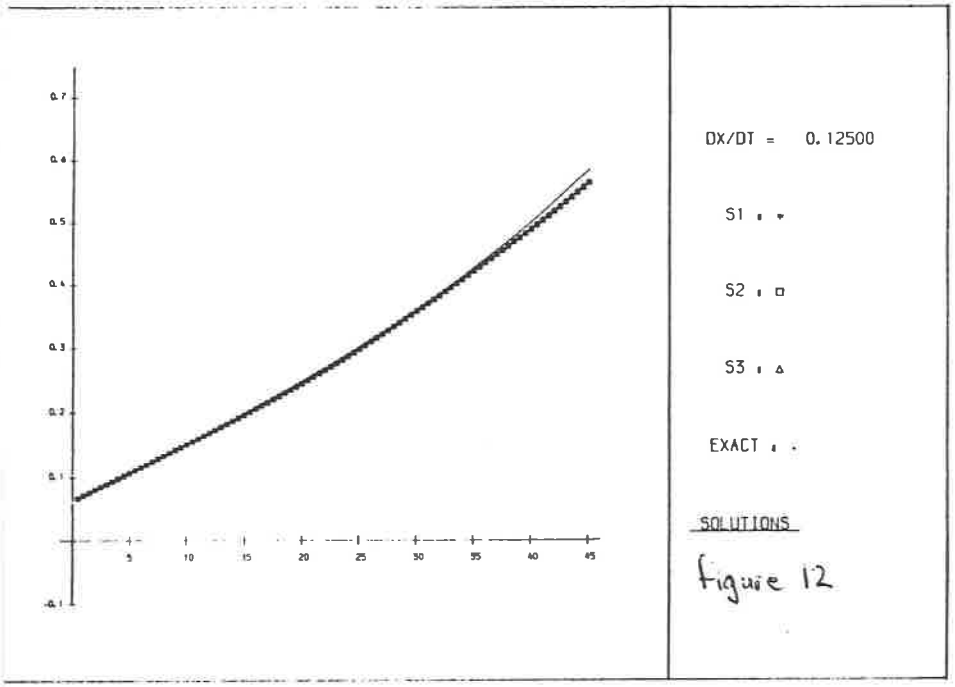


Figure 12

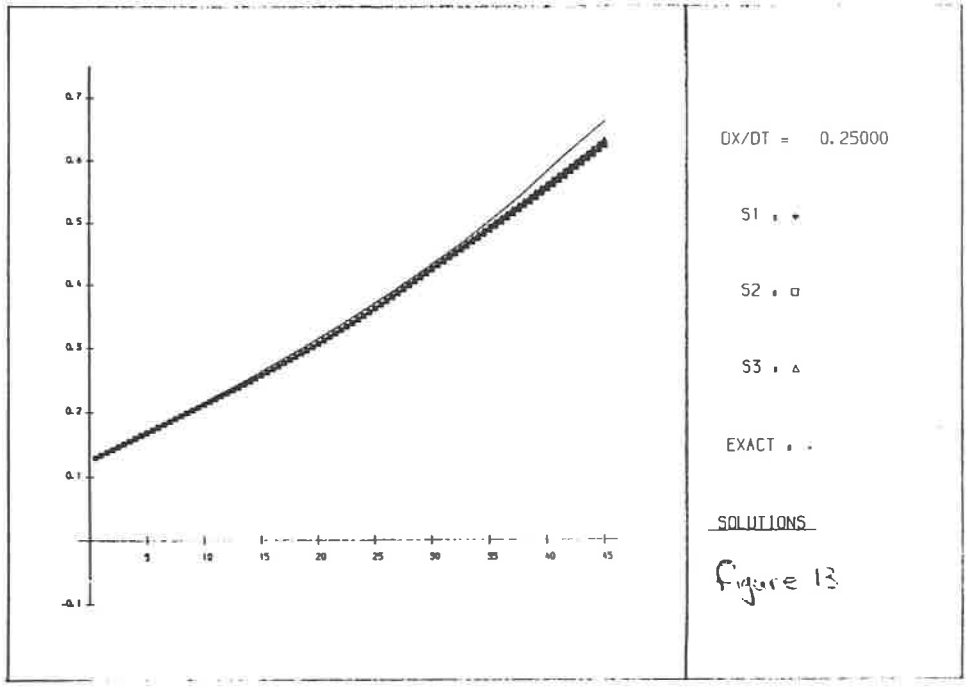


Figure 13

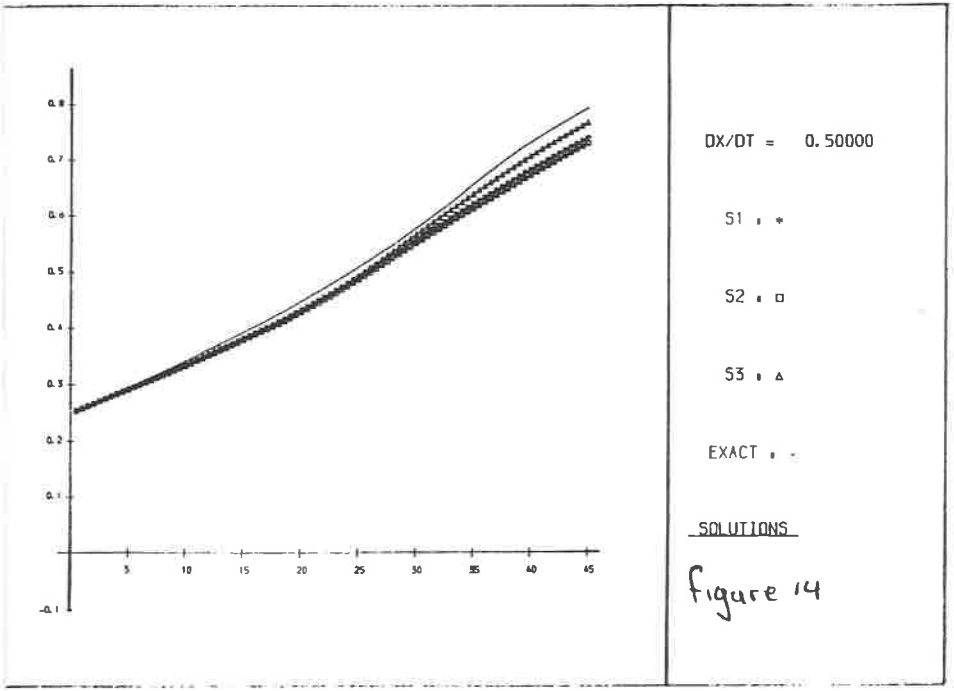


Figure 14

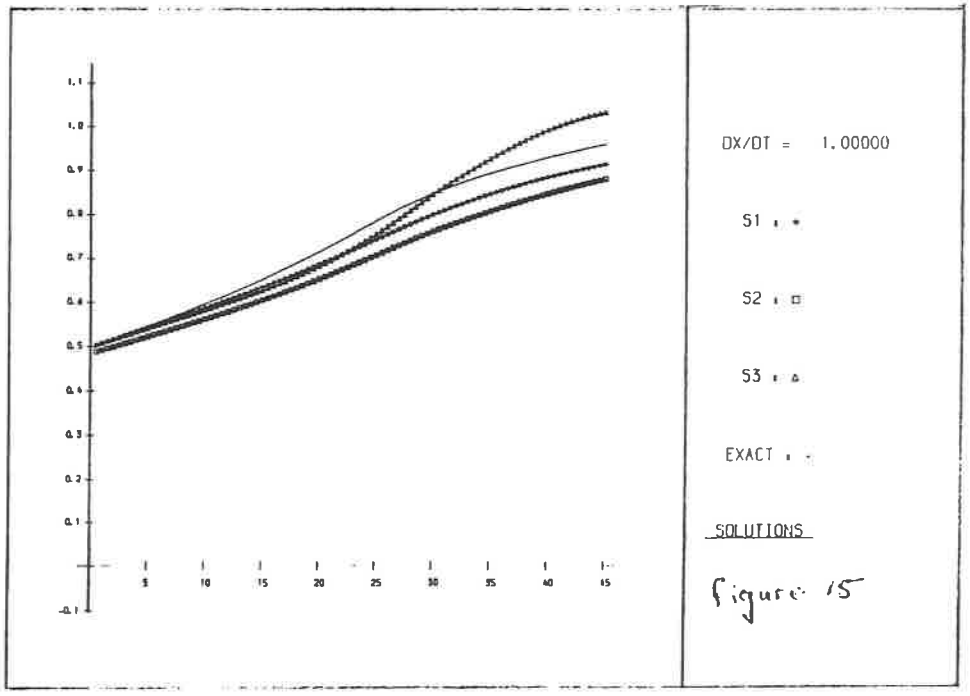


Figure 15

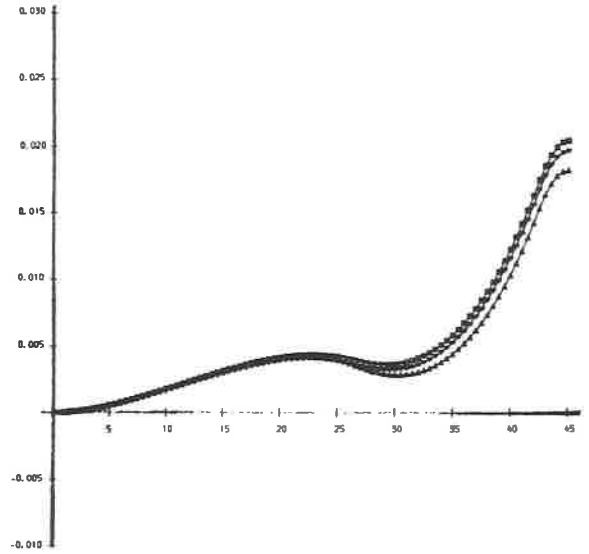


DX/DT = 0.12500

S1 : *

S2 : □

S3 : △

ERRORS

figure 16

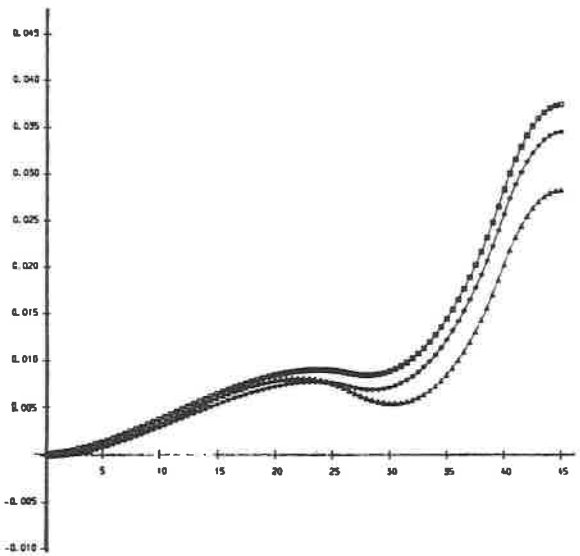


DX/DT = 0.25000

S1 : *

S2 : □

S3 : △

ERRORS

figure 17

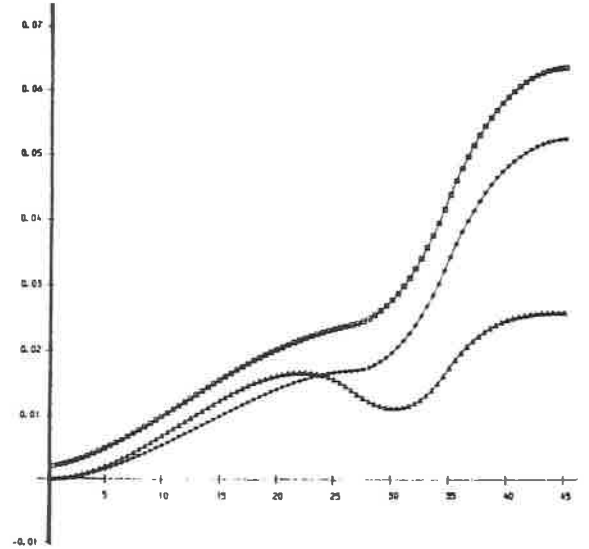


DX/DT = 0.50000

S1 : *

S2 : □

S3 : △

ERRORS

figure 18

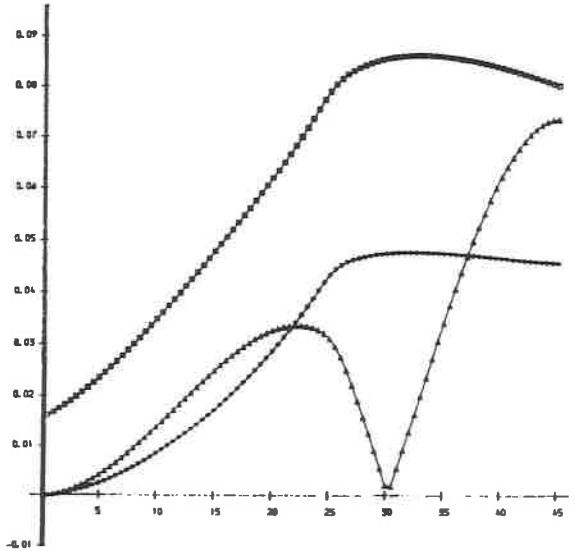


DX/DT = 1.00000

S1 : *

S2 : □

S3 : △

ERRORS

figure 19

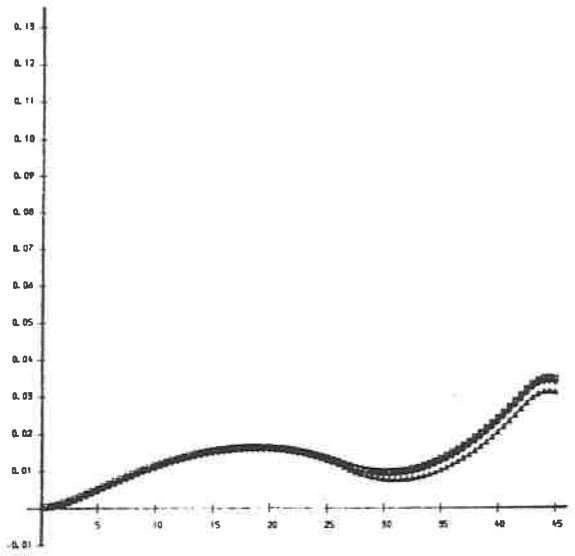

DX/DT = 0.12500

S1 : *

S2 : □

S3 : △

RELATIVE ERRORS

figure 20

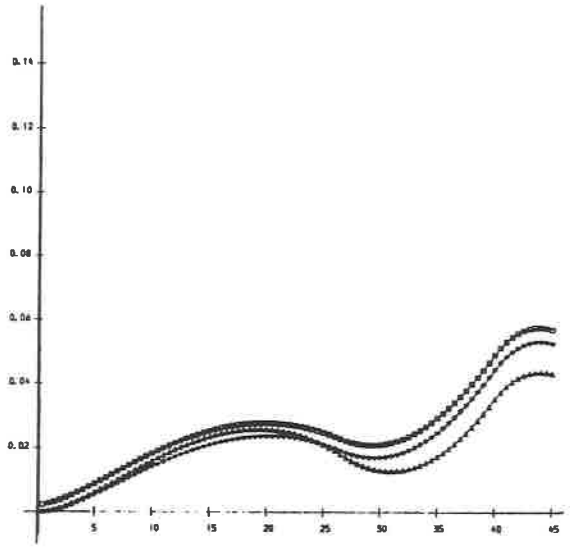

DX/DT = 0.25000

S1 : *

S2 : □

S3 : △

RELATIVE ERRORS

figure 21

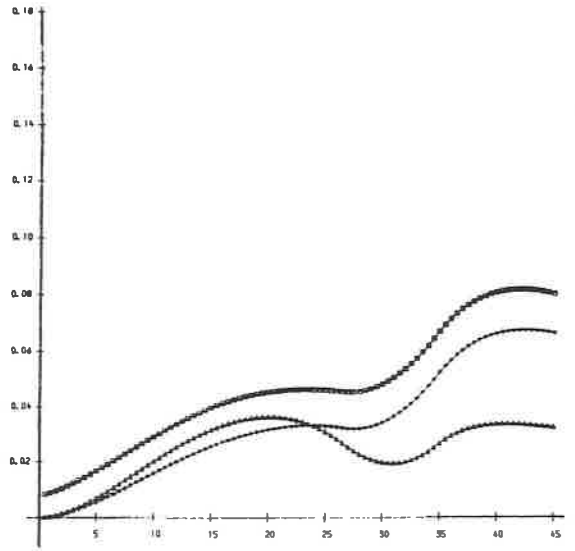

DX/DT = 0.50000

S1 : *

S2 : □

S3 : △

RELATIVE ERRORS

figure 22

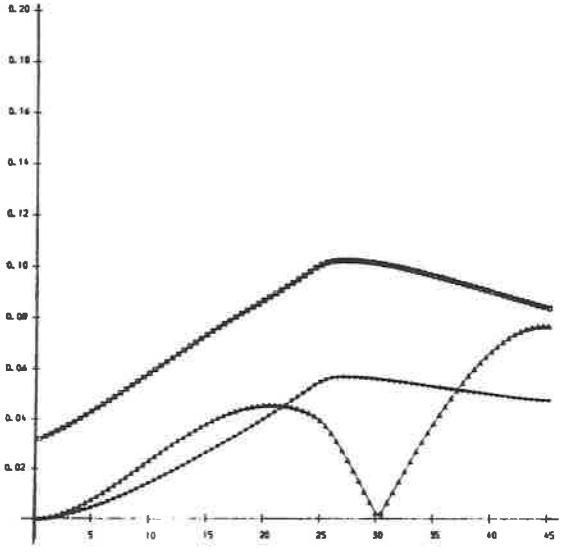

DX/DT = 1.00000

S1 : *

S2 : □

S3 : △

RELATIVE ERRORS

figure 23

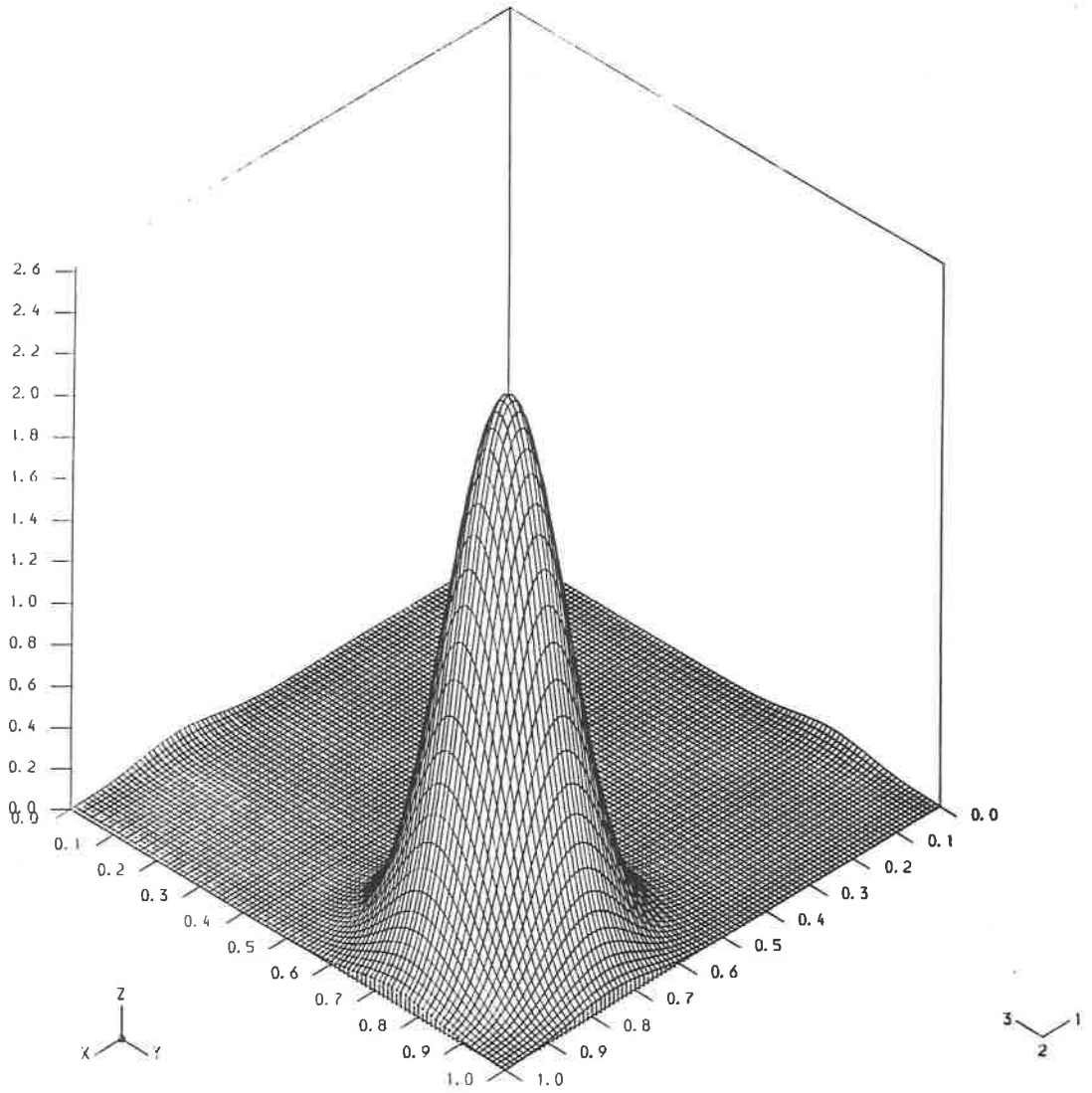


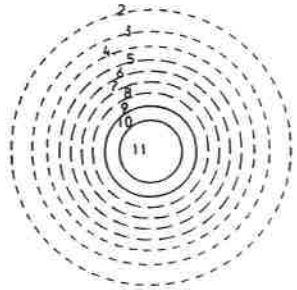


S1CBA1

CONTOUR HEIGHTS

| | | | |
|---|---|---|---|
| 1 | 0.0000 | 2 | 0.2626 |
| 3 | 0.5252 | 4 | 0.7878 |
| 5 | 1.0504 | 6 | 1.3131 |
| 7 | 1.5757 | 8 | 1.8383 |
| 9 | 2.1009 | 10 | 2.3635 |
| 11 | 2.6261 | | |

Figure 24

# LINEAR ADVECTION OF A BLIP

SOLN. AT TIME T = 0.50

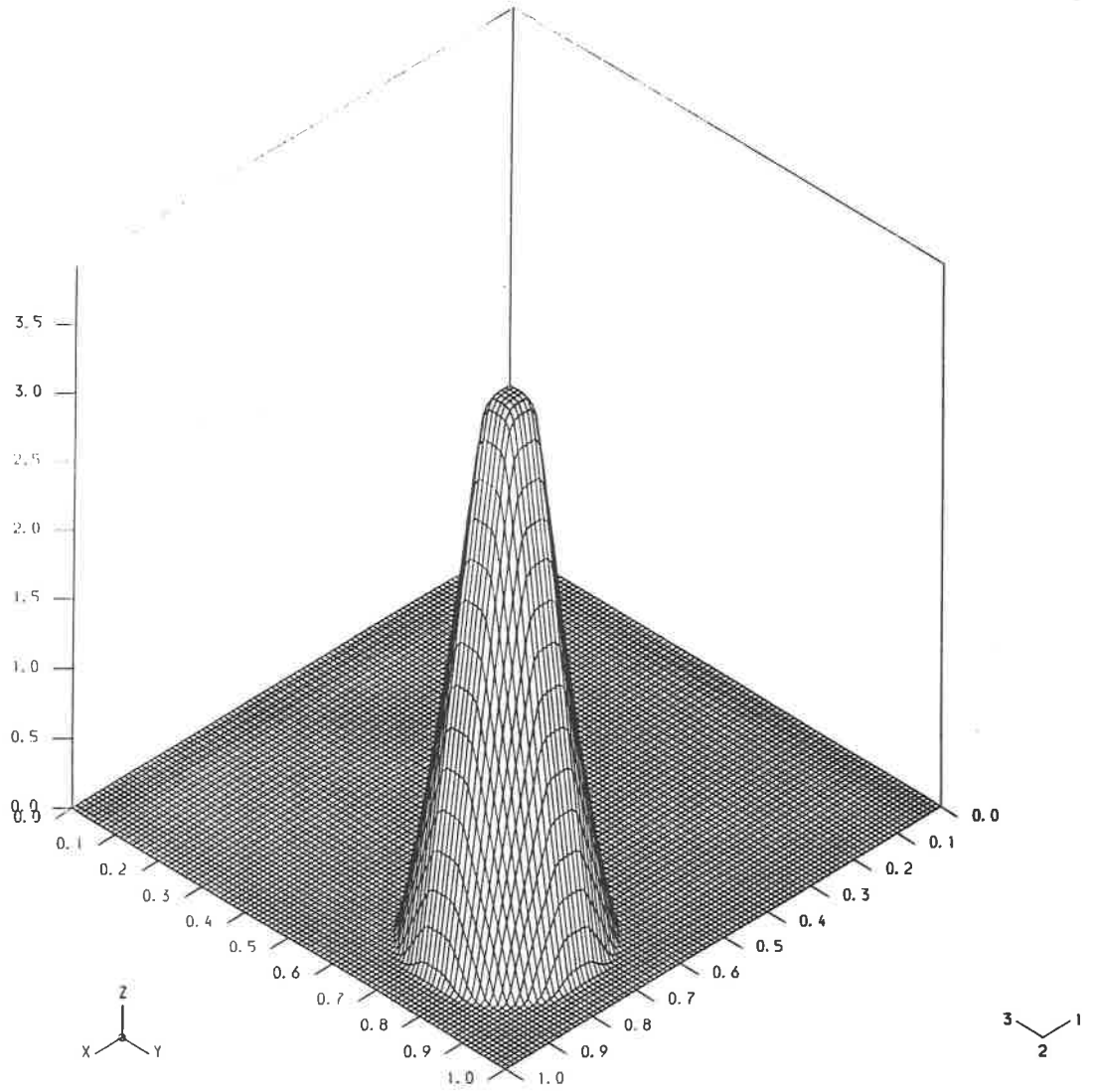


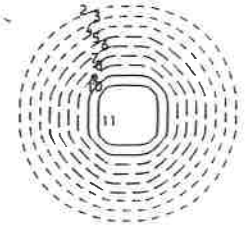

S1CBA2

CONTOUR HEIGHTS

| | | | |
|---|---|---|---|
| 1 | 0.0000 | 2 | 0.3925 |
| 3 | 0.7850 | 4 | 1.1775 |
| 5 | 1.5700 | 6 | 1.9625 |
| 7 | 2.3550 | 8 | 2.7475 |
| 9 | 3.1401 | 10 | 3.5326 |
| 11 | 3.9251 | | |

Figure 25

# LINEAR ADVECTION OF A BLIP

SOLN. AT TIME T = 0.50

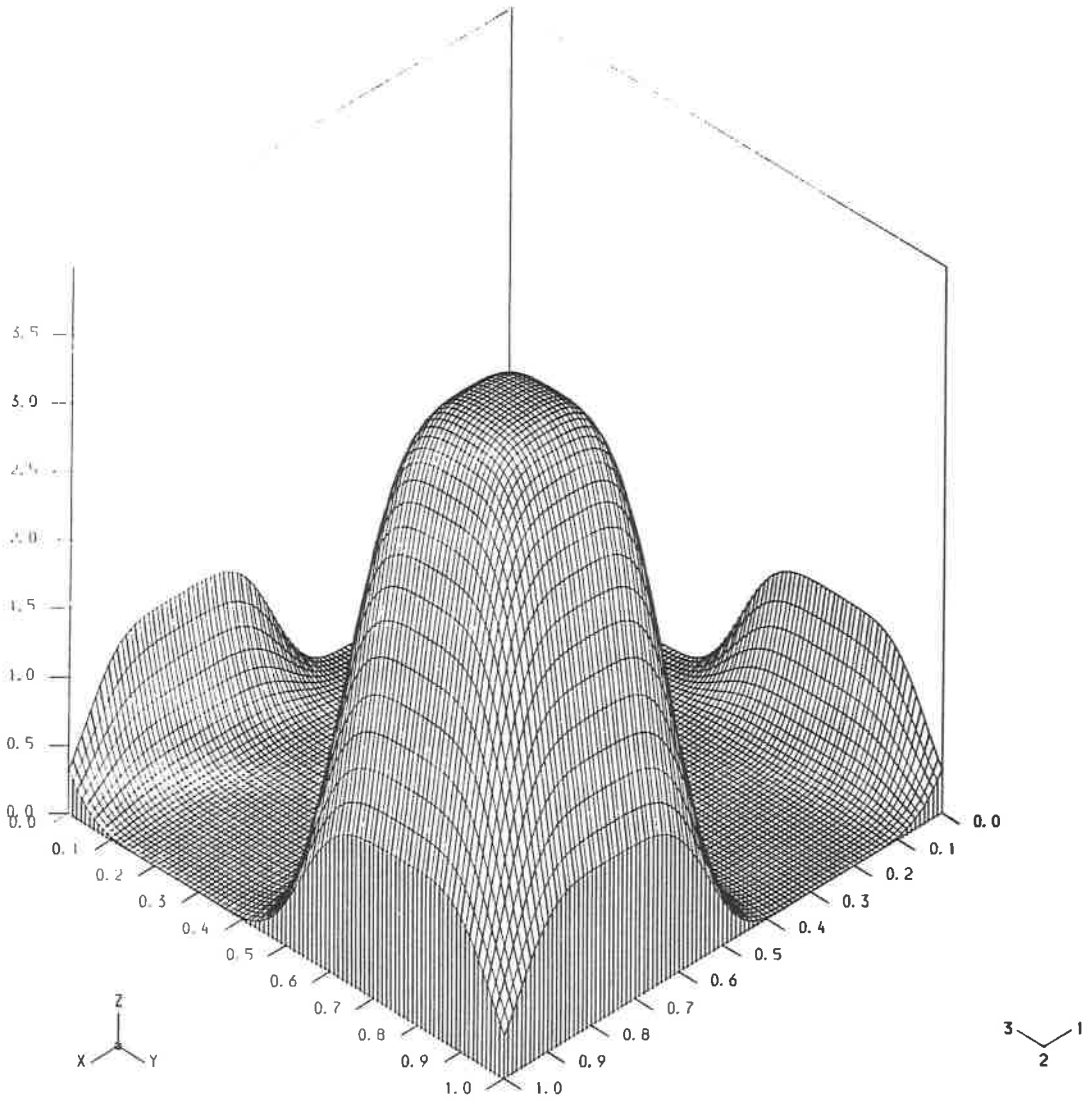


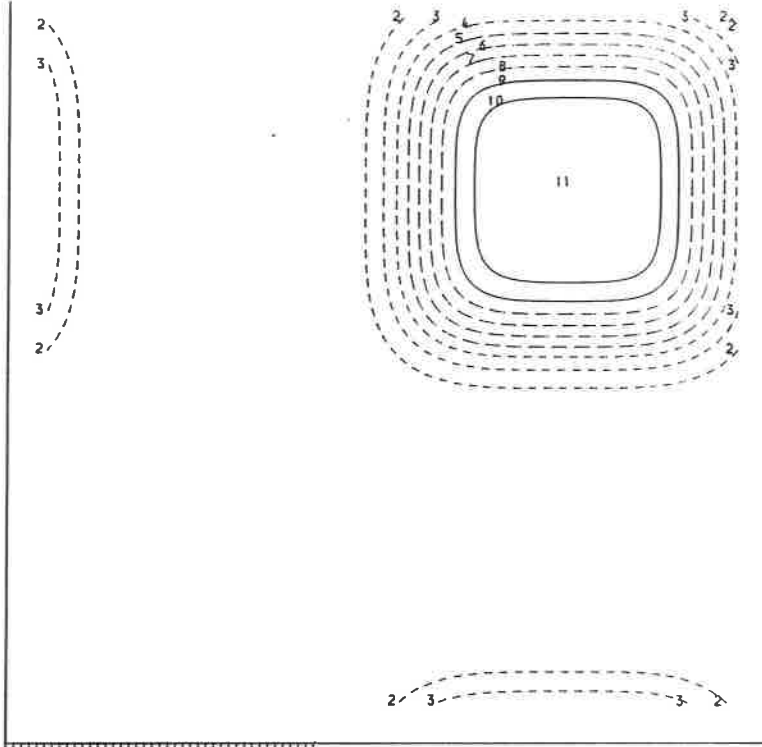


S 1 B A 1

CONTOUR HEIGHTS

| | | | |
|---|---|---|---|
| 1 | 0.0000 | 2 | 0.3997 |
| 3 | 0.7993 | 4 | 1.1990 |
| 5 | 1.5987 | 6 | 1.9984 |
| 7 | 2.3980 | 8 | 2.7977 |
| 9 | 3.1974 | 10 | 3.5970 |
| 11 | 3.9967 | | |

Figure 26

# LINEAR ADVECTION OF A BOX

SOLN. AT TIME T = 0.50

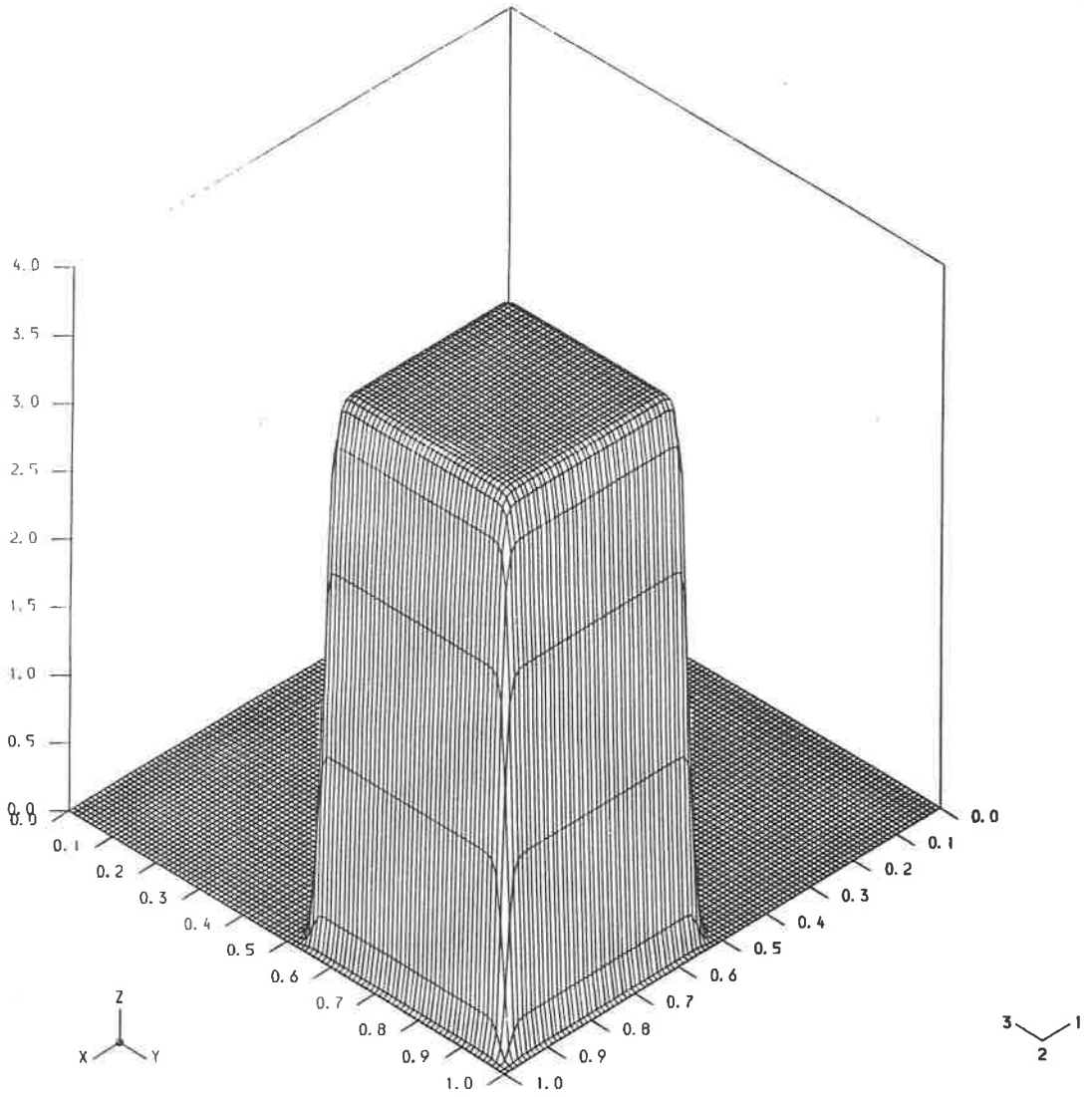


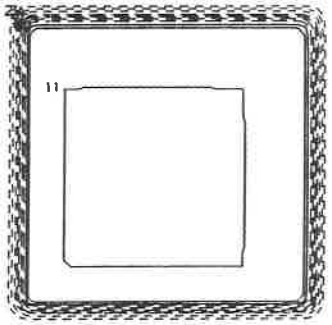


S 1 B A 2

CONTOUR HEIGHTS

| | | | |
|---|---|---|---|
| 1 | 0.0000 | 2 | 0.4000 |
| 3 | 0.8000 | 4 | 1.2000 |
| 5 | 1.6000 | 6 | 2.0000 |
| 7 | 2.4000 | 8 | 2.8000 |
| 9 | 3.2000 | 10 | 3.6000 |
| 11 | 4.0000 | | |

Figure 27

# LINEAR ADVECTION OF A BOX

SOLN. AT TIME T = 0.50

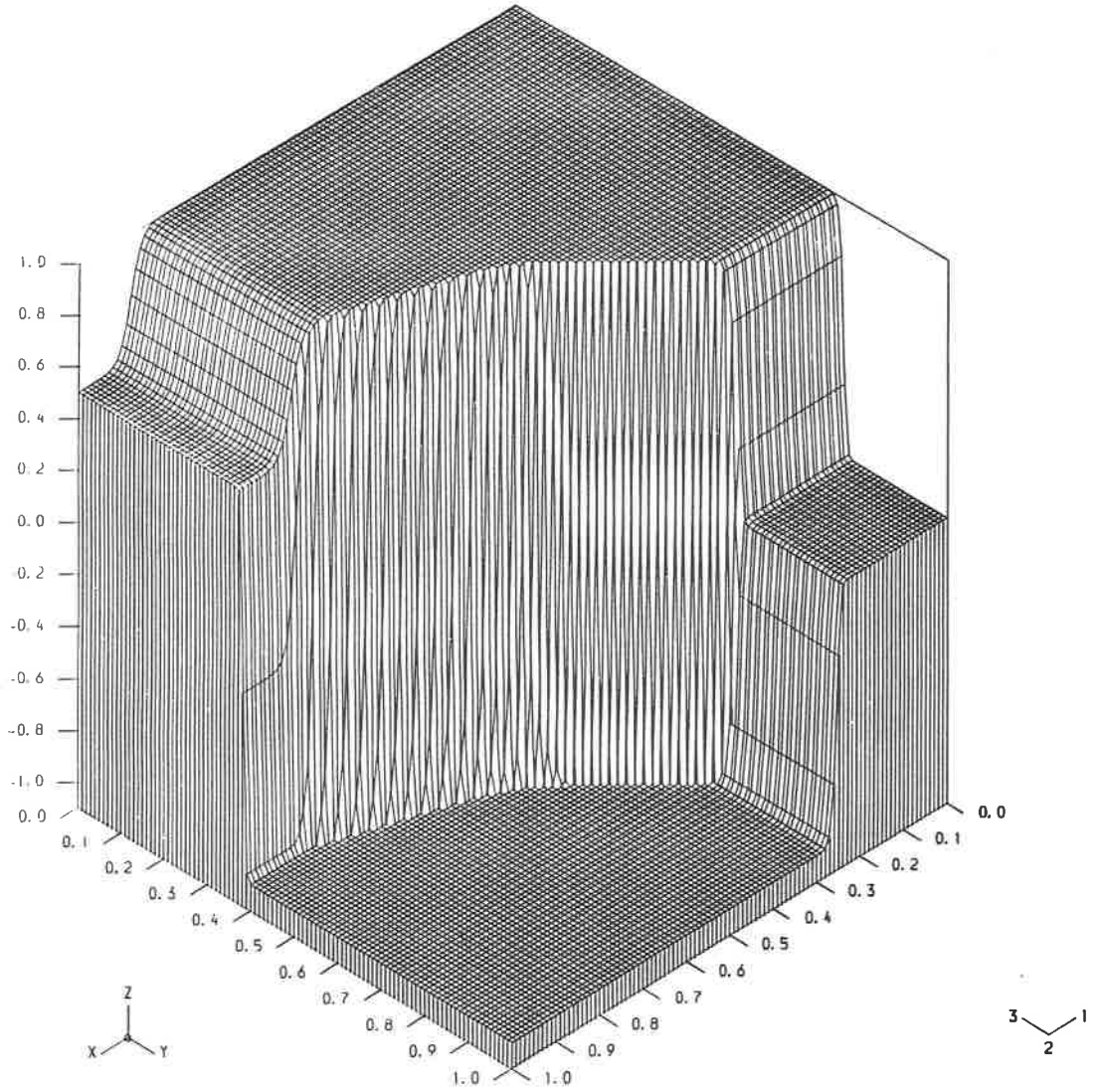


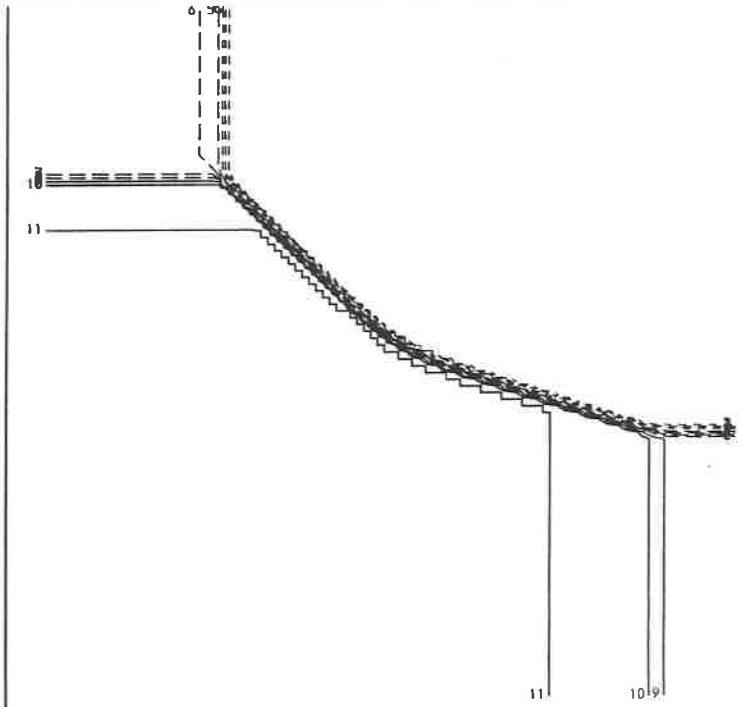


S 1 R P 1 1

CONTOUR HEIGHTS

| | | | |
|---|---|---|---|
| 1 | -1.0000 | 2 | -0.8000 |
| 3 | -0.6000 | 4 | -0.4000 |
| 5 | -0.2000 | 6 | 0.0000 |
| 7 | 0.2000 | 8 | 0.4000 |
| 9 | 0.6000 | 10 | 0.8000 |
| 11 | 1.0000 | | |

Figure 28

# TWO DIMENSIONAL RIEMANN PROBLEM

SOLN. AT TIME T = 0.50

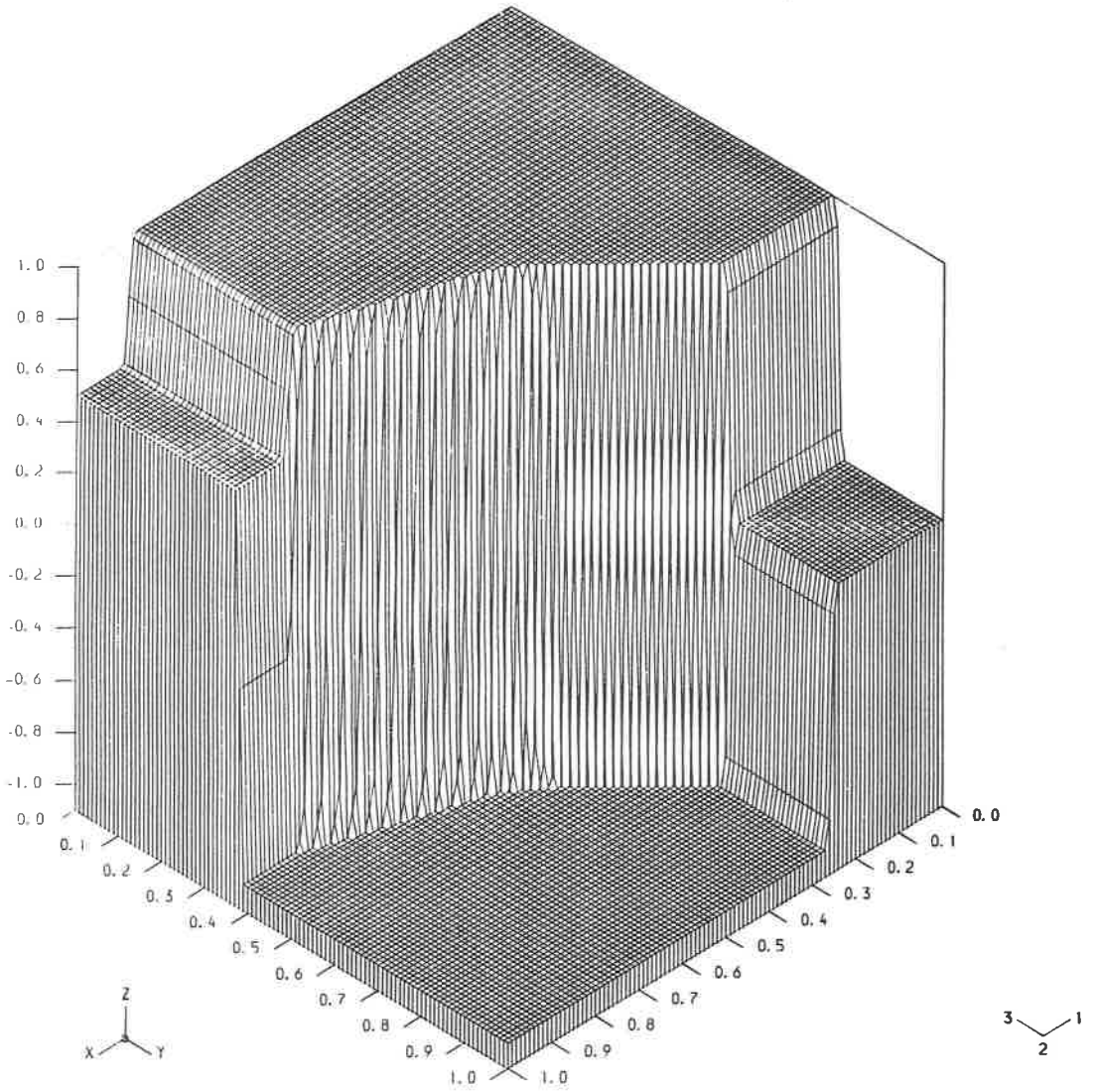


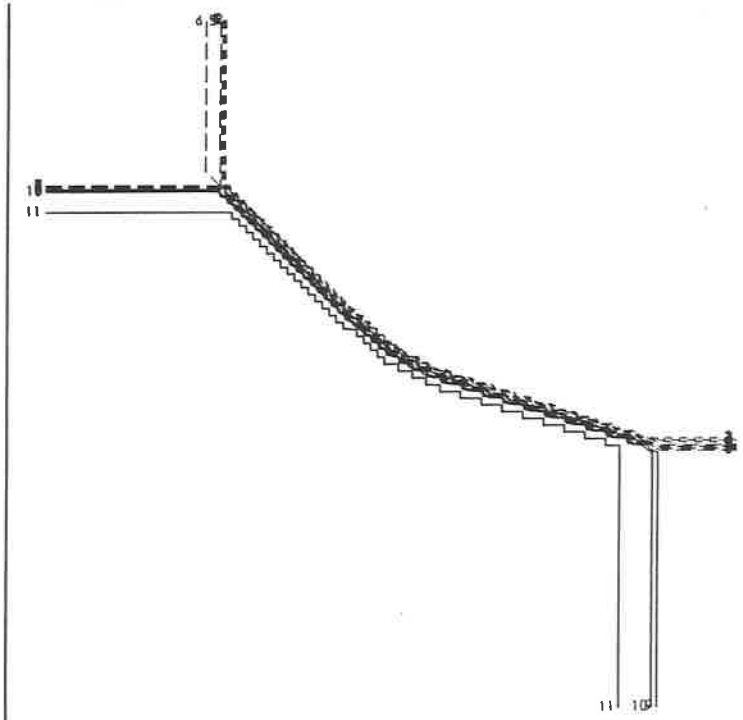


S 1 R P 1 2

CONTOUR HEIGHTS

| | | | |
|---|---|---|---|
| 1 | -1.0000 | 2 | -0.8000 |
| 3 | -0.6000 | 4 | -0.4000 |
| 5 | -0.2000 | 6 | 0.0000 |
| 7 | 0.2000 | 8 | 0.4000 |
| 9 | 0.6000 | 10 | 0.8000 |
| 11 | 1.0000 | | |

Figure 29

# TWO DIMENSIONAL RIEMANN PROBLEM

SOLN. AT TIME T = 0.50

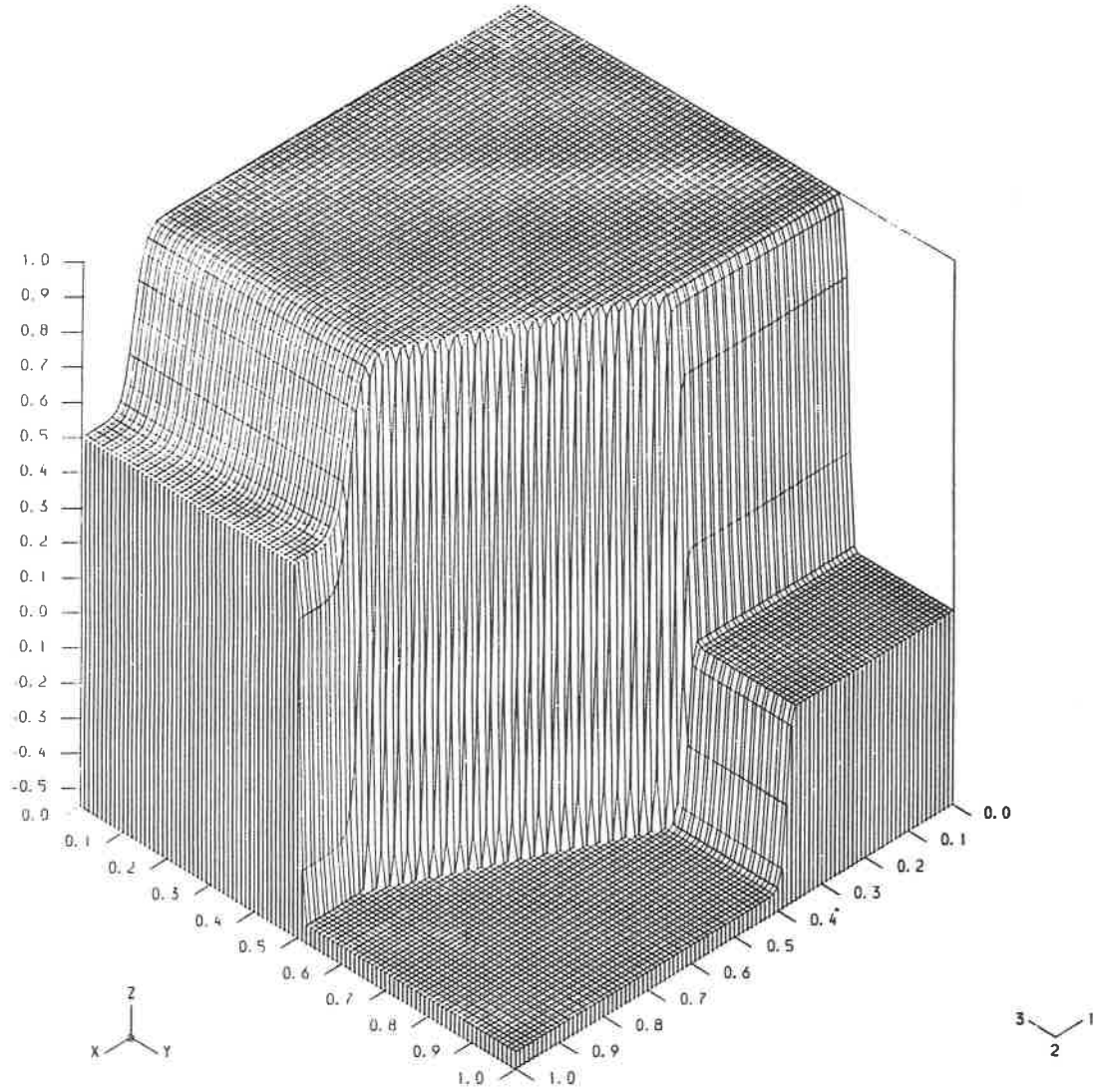


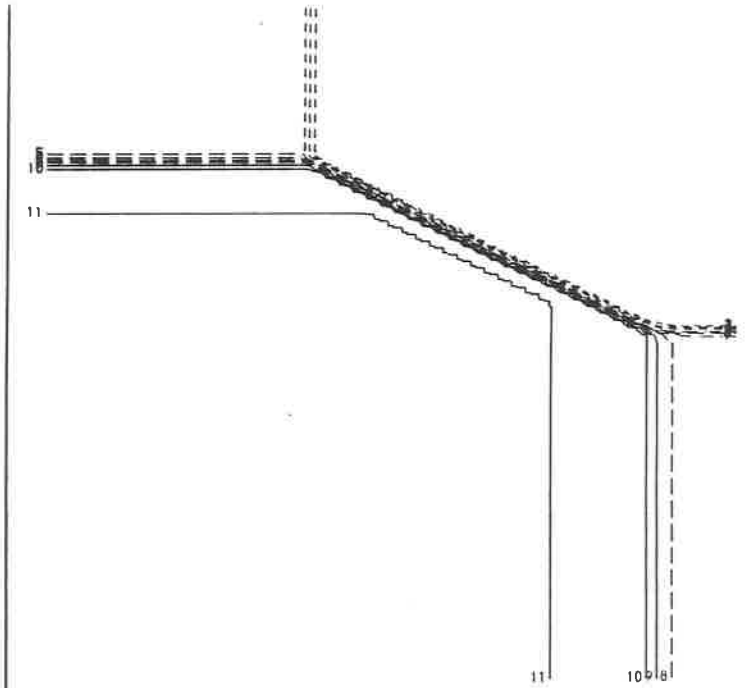


S 1 R P 2 1

CONTOUR HEIGHTS

| | | | |
|---|---|---|---|
| 1 | -0.5000 | 2 | -0.3500 |
| 3 | -0.2000 | 4 | -0.0500 |
| 5 | 0.1000 | 6 | 0.2500 |
| 7 | 0.4000 | 8 | 0.5500 |
| 9 | 0.7000 | 10 | 0.8500 |
| 11 | 1.0000 | | |

Figure 30

# TWO DIMENSIONAL RIEMANN PROBLEM

SOLN. AT TIME T = 0.50

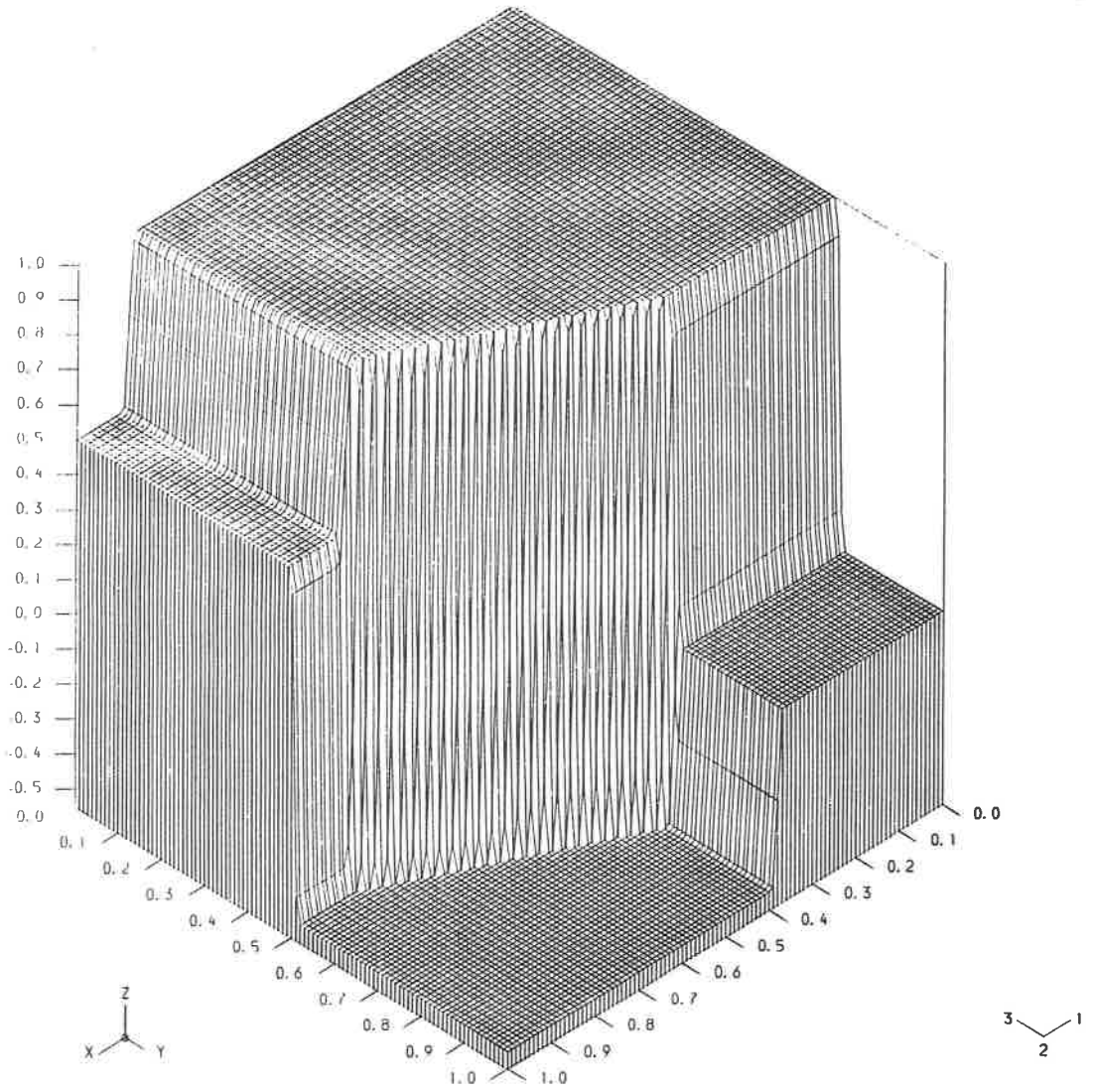


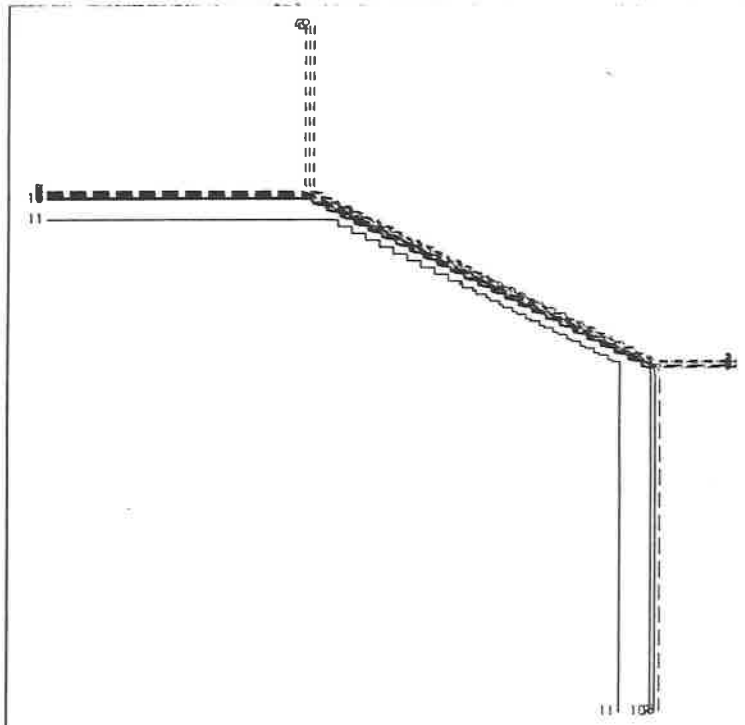

S 1 R P 2 2

CONTOUR HEIGHTS

| | | | |
|---|---|---|---|
| 1 | -0.5000 | 2 | -0.3500 |
| 3 | -0.2000 | 4 | -0.0500 |
| 5 | 0.1000 | 6 | 0.2500 |
| 7 | 0.4000 | 8 | 0.5500 |
| 9 | 0.7000 | 10 | 0.8500 |
| 11 | 1.0000 | | |

Figure 31

# TWO DIMENSIONAL RIEMANN PROBLEM

SOLN. AT TIME T = 0.50

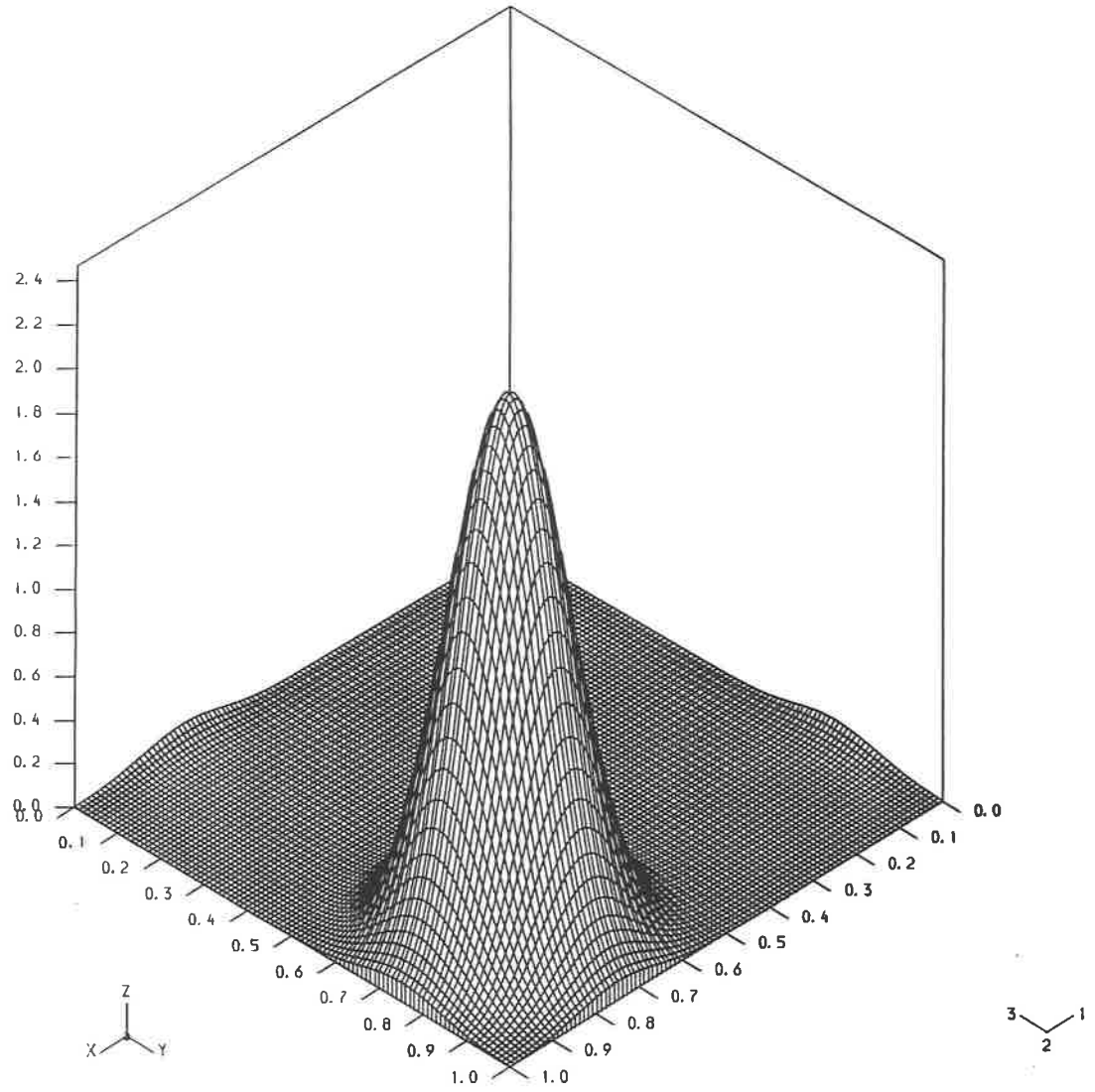


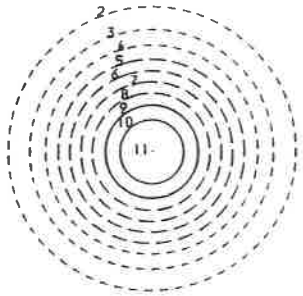


S 2 C B A 1

CONTOUR HEIGHTS

| | | | |
|---|---|---|---|
| 1 | 0.0000 | 2 | 0.2472 |
| 3 | 0.4943 | 4 | 0.7415 |
| 5 | 0.9886 | 6 | 1.2358 |
| 7 | 1.4830 | 8 | 1.7301 |
| 9 | 1.9773 | 10 | 2.2244 |
| 11 | 2.4716 | | |

Figure 32

# LINEAR ADVECTION OF A BLIP

SOLN. AT TIME T = 0.50

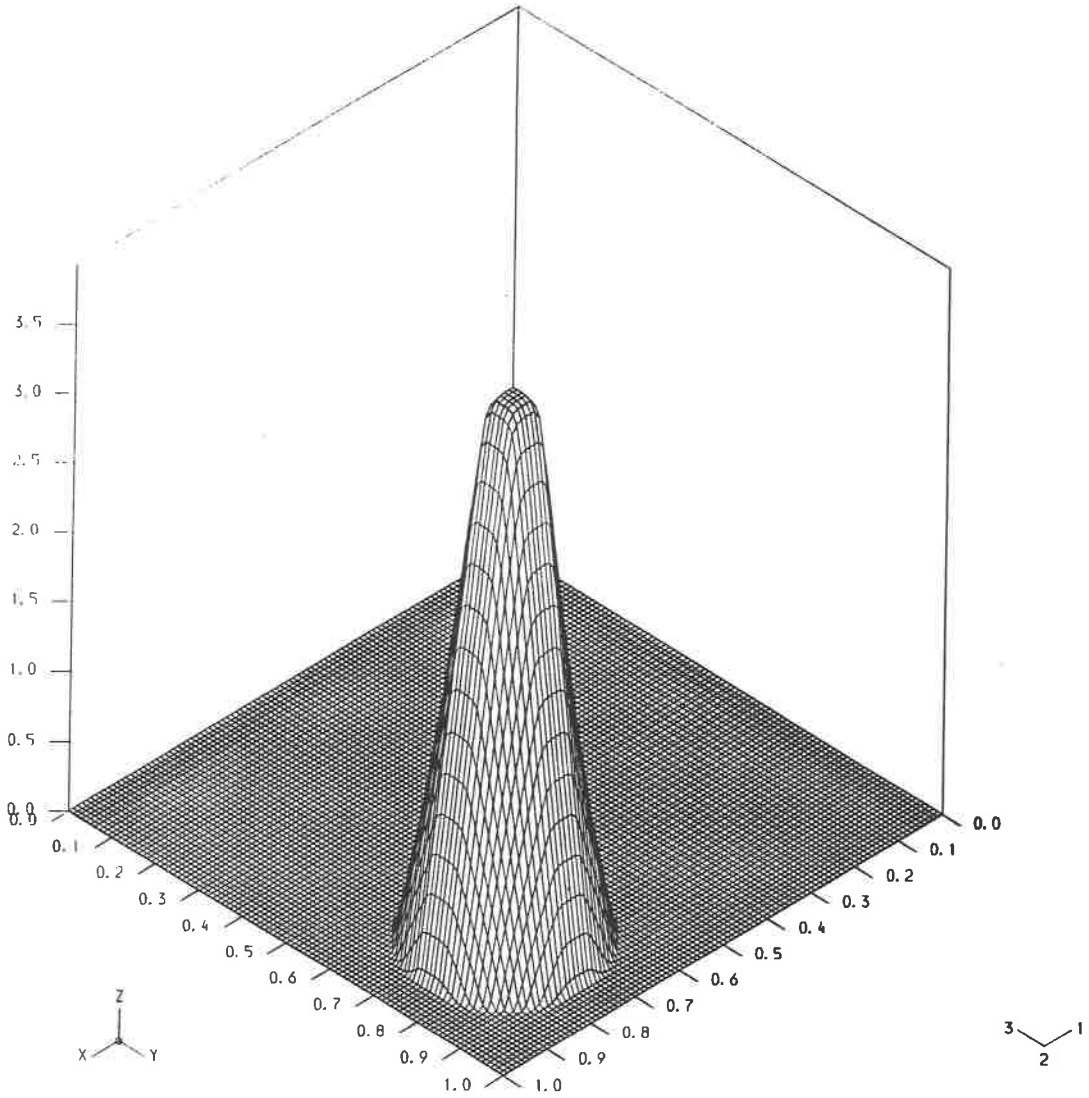


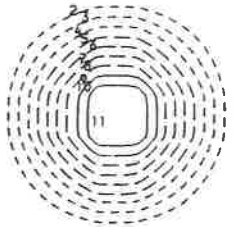

S 2 C B A 2

CONTOUR HEIGHTS

| | | | |
|---|---|---|---|
| 1 | 0.0000 | 2 | 0.3929 |
| 3 | 0.7858 | 4 | 1.1786 |
| 5 | 1.5715 | 6 | 1.9644 |
| 7 | 2.3573 | 8 | 2.7501 |
| 9 | 3.1430 | 10 | 3.5359 |
| 11 | 3.9288 | | |

Figure 33

# LINEAR ADVECTION OF A BLIP

SOLN. AT TIME T = 0.50

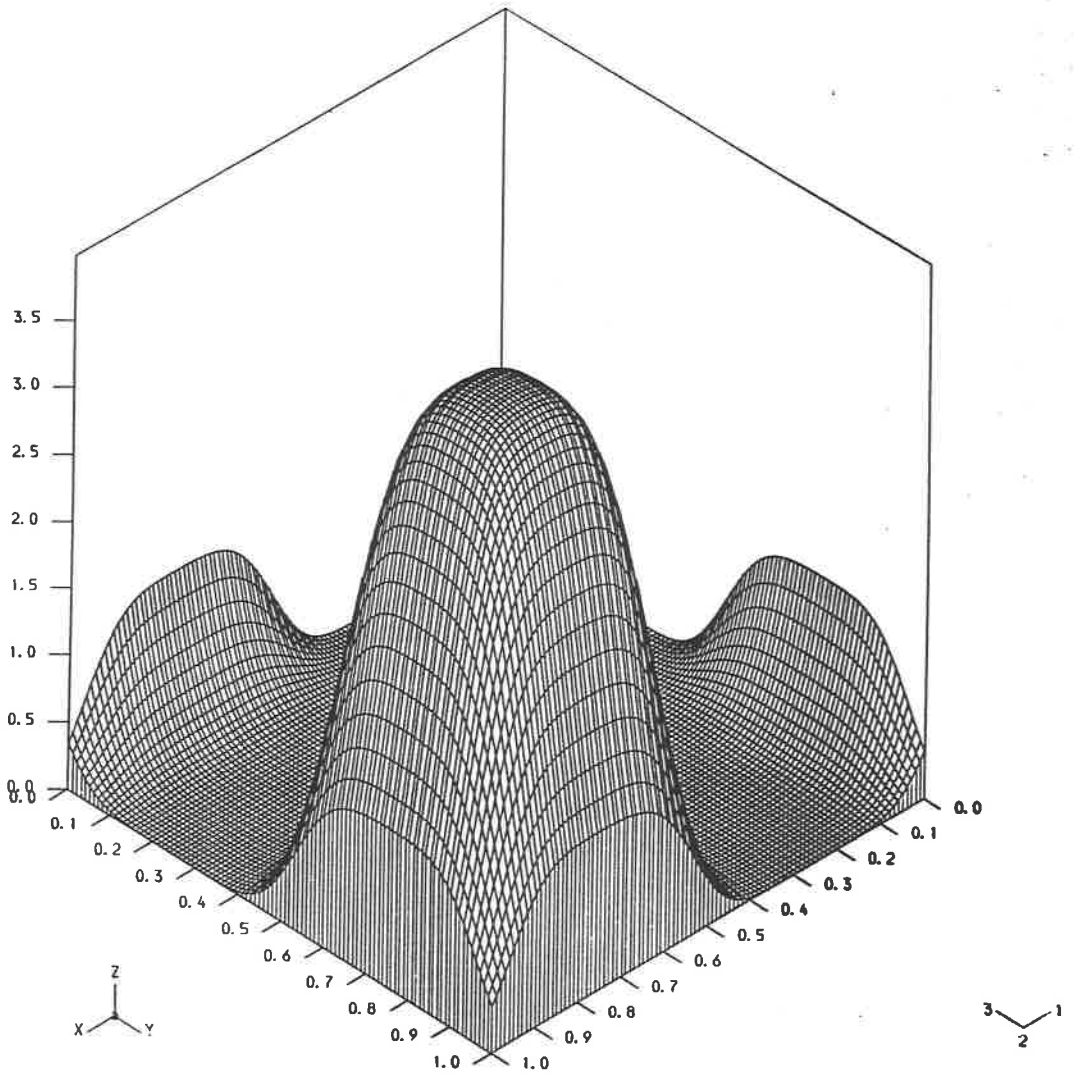


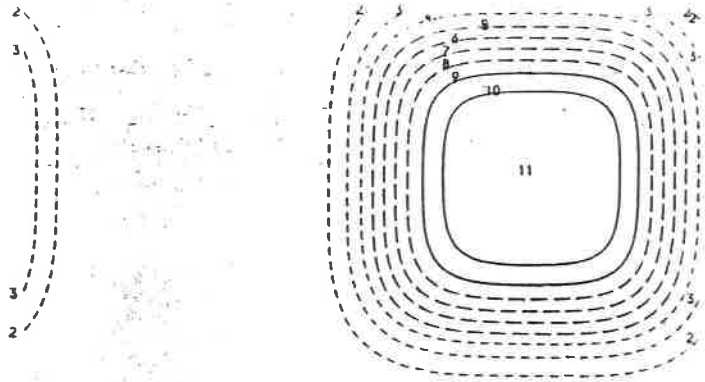



S 2 B A 1

CONTOUR HEIGHTS

| | | | |
|---|---|---|---|
| 1 | 0.0000 | 2 | 0.3991 |
| 3 | 0.7983 | 4 | 1.1974 |
| 5 | 1.5965 | 6 | 1.9957 |
| 7 | 2.3948 | 8 | 2.7939 |
| 9 | 3.1930 | 10 | 3.5922 |
| 11 | 3.9913 | | |

Figure 34

# LINEAR ADVECTION OF A BOX

SOLN. AT TIME T = 0.50

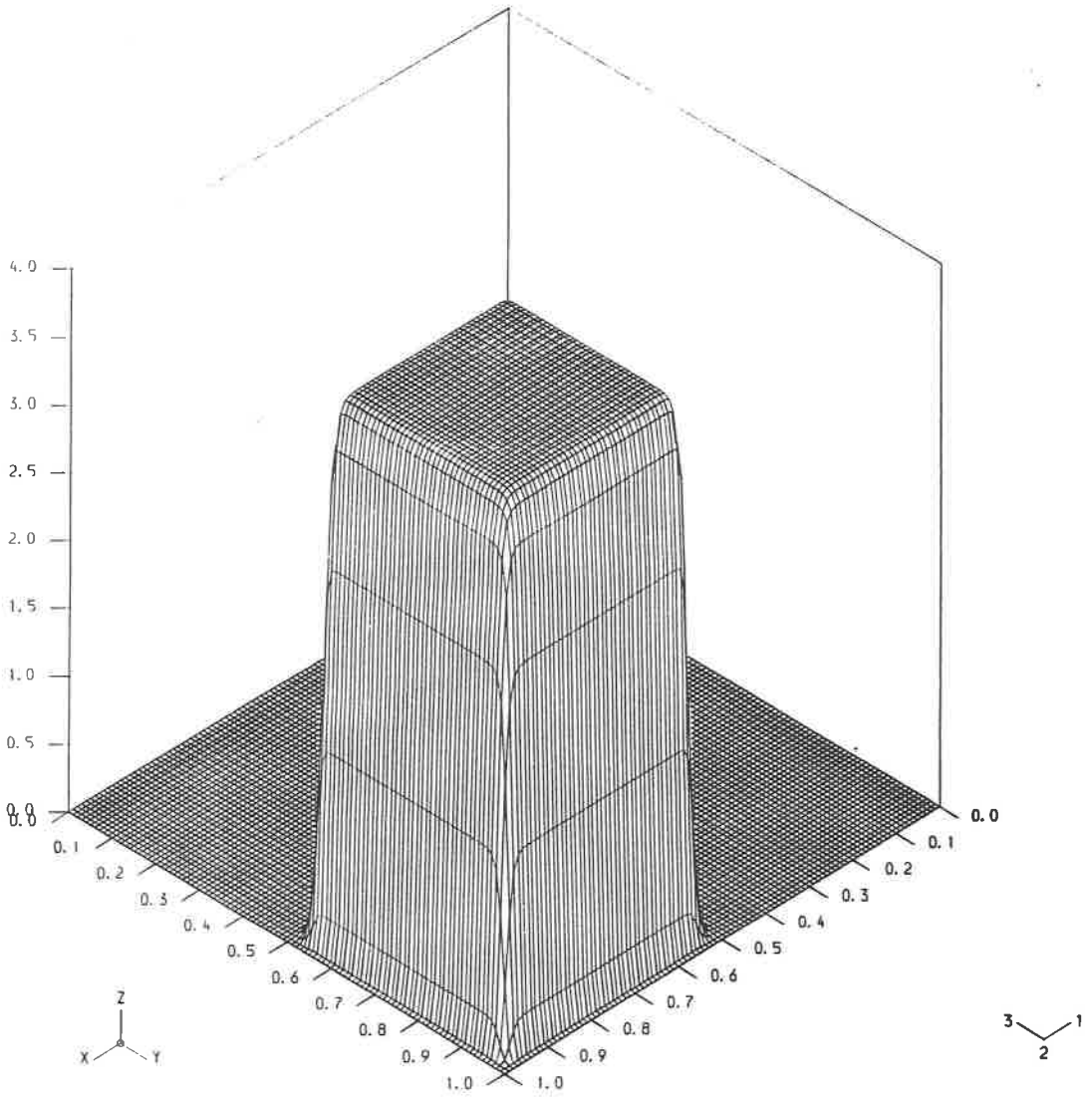


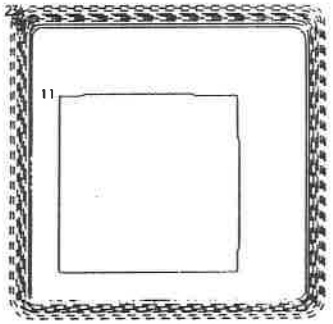


S 2 B A 2

CONTOUR HEIGHTS

| | | | |
|---|---|---|---|
| 1 | 0.0000 | 2 | 0.4000 |
| 3 | 0.8000 | 4 | 1.2000 |
| 5 | 1.6000 | 6 | 2.0000 |
| 7 | 2.4000 | 8 | 2.8000 |
| 9 | 3.2000 | 10 | 3.6000 |
| 11 | 4.0000 | | |

Figure 35

# LINEAR ADVECTION OF A BOX

SOLN. AT TIME T = 0.50

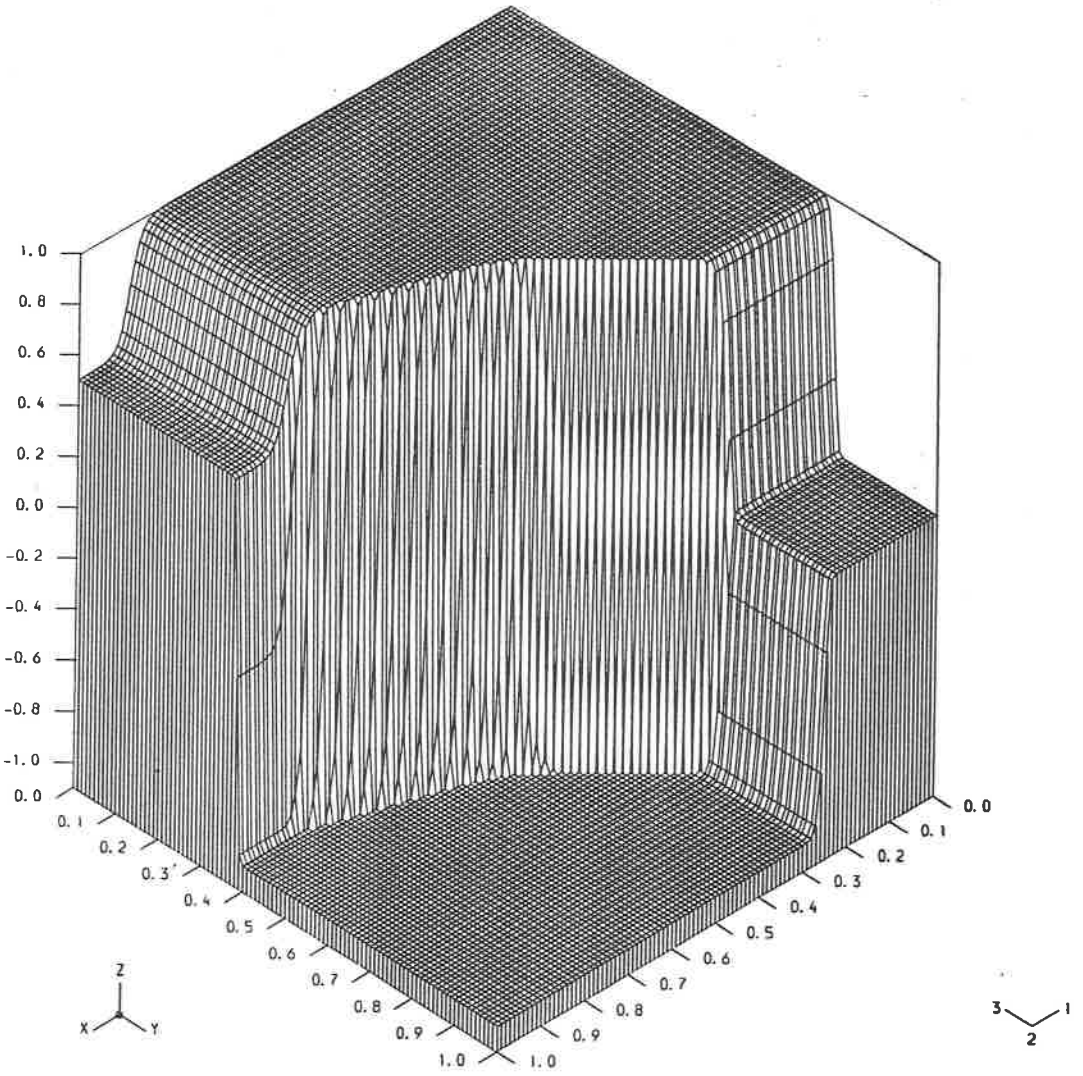


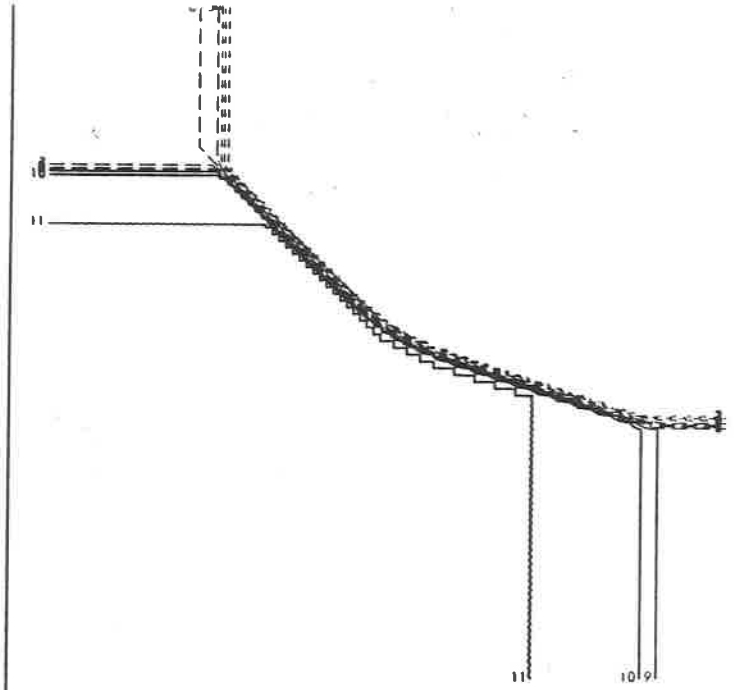


S 2 R P 1 1

CONTOUR HEIGHTS

| | | | |
|---|---|---|---|
| 1 | -1.0000 | 2 | -0.8000 |
| 3 | -0.6000 | 4 | -0.4000 |
| 5 | -0.2000 | 6 | 0.0000 |
| 7 | 0.2000 | 8 | 0.4000 |
| 9 | 0.6000 | 10 | 0.8000 |
| 11 | 1.0000 | | |

Figure 36

# TWO DIMENSIONAL RIEMANN PROBLEM

SOLN. AT TIME T = 0.50

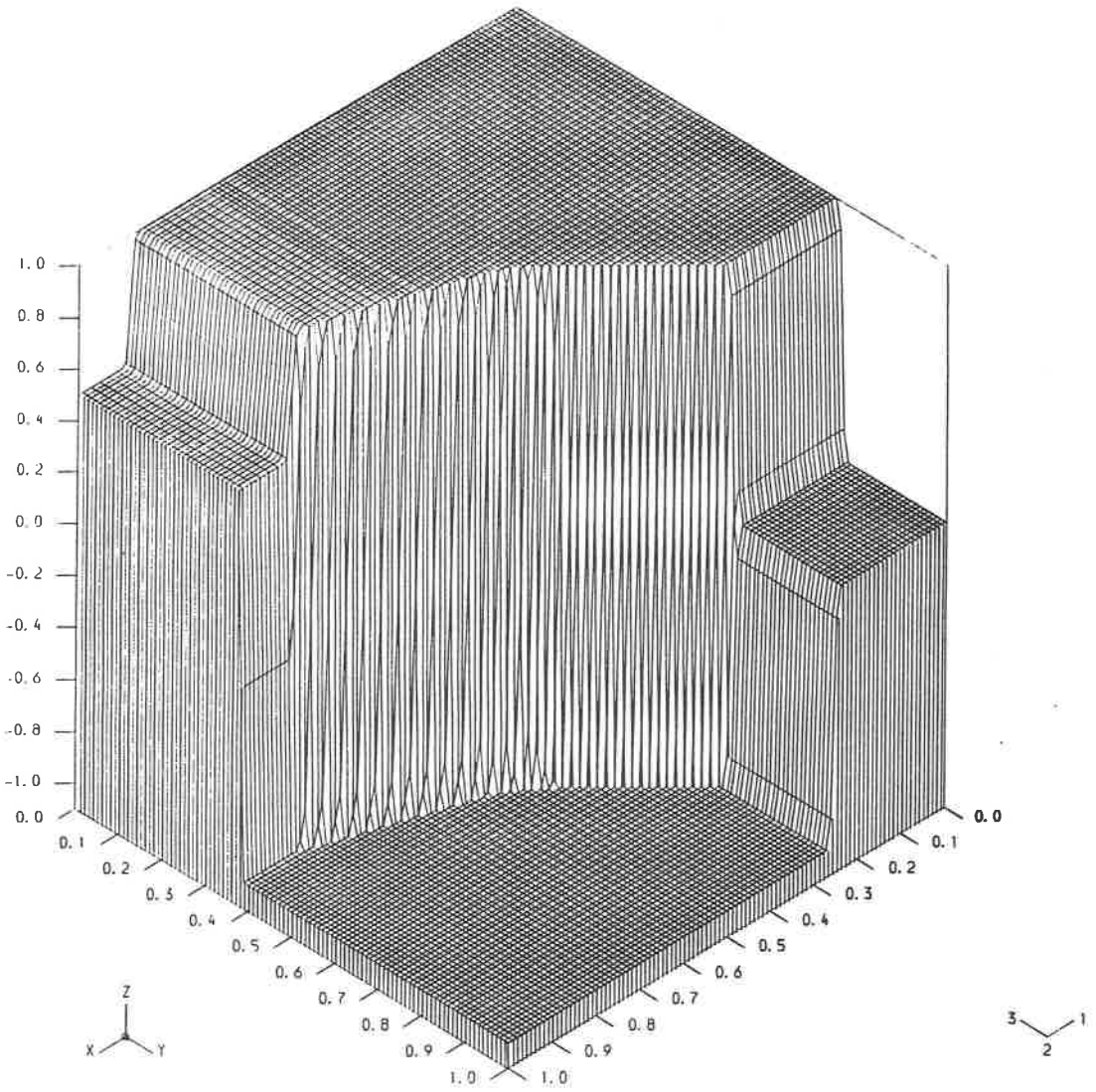


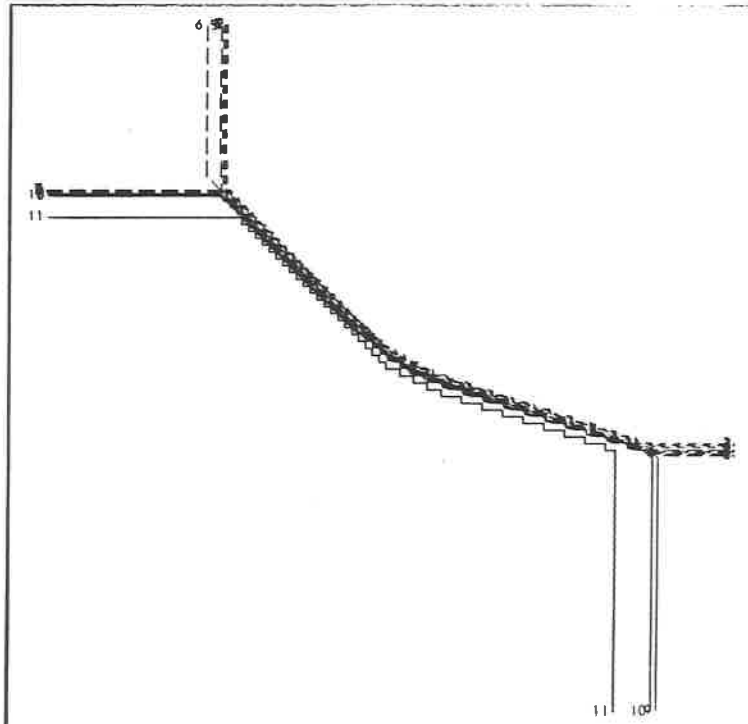


S 2 R P 1 2

CONTOUR HEIGHTS

| | | | |
|---|---|---|---|
| 1 | -1.0000 | 2 | -0.8000 |
| 3 | -0.6000 | 4 | -0.4000 |
| 5 | -0.2000 | 6 | 0.0000 |
| 7 | 0.2000 | 8 | 0.4000 |
| 9 | 0.6000 | 10 | 0.8000 |
| 11 | 1.0000 | | |

Figure 37

# TWO DIMENSIONAL RIEMANN PROBLEM

SOLN. AT TIME T = 0.50

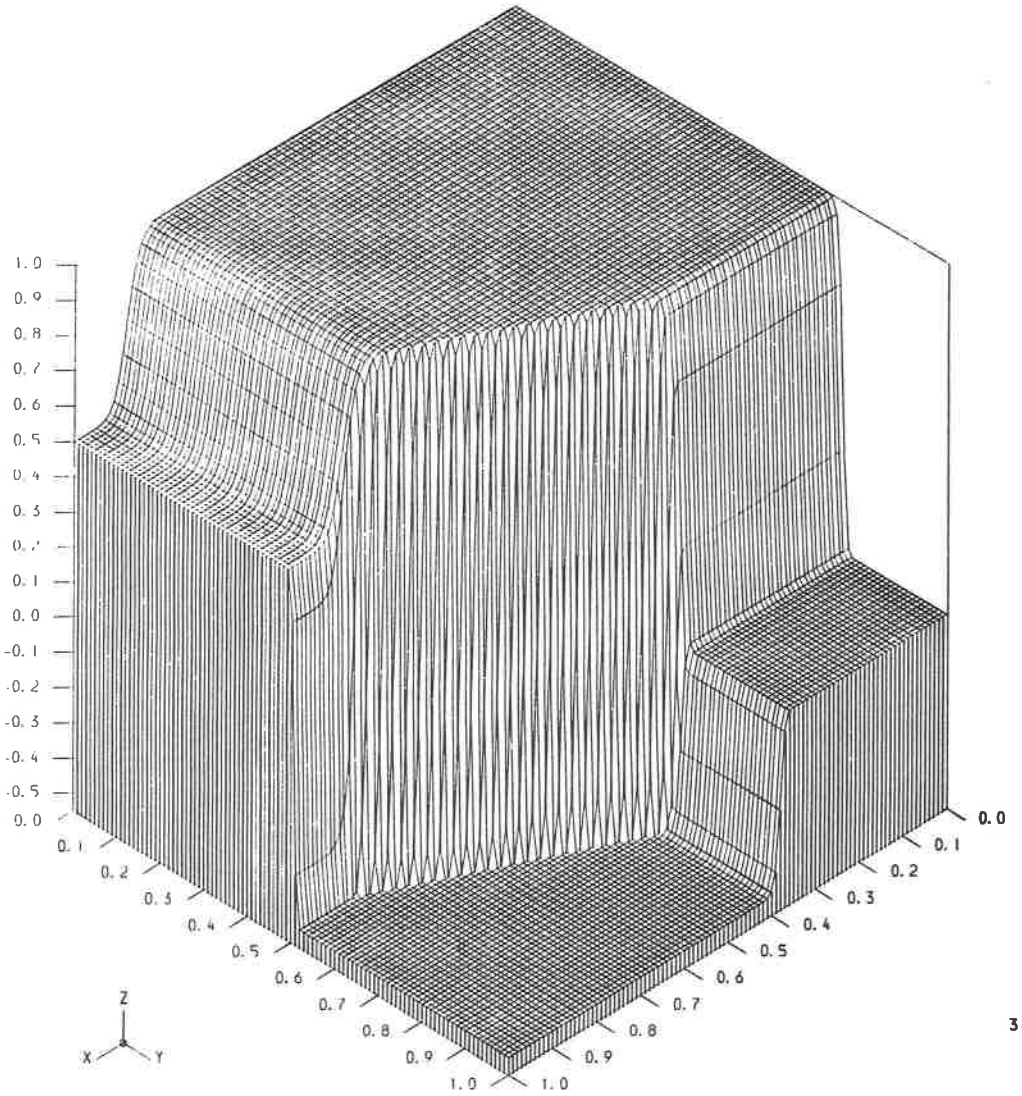


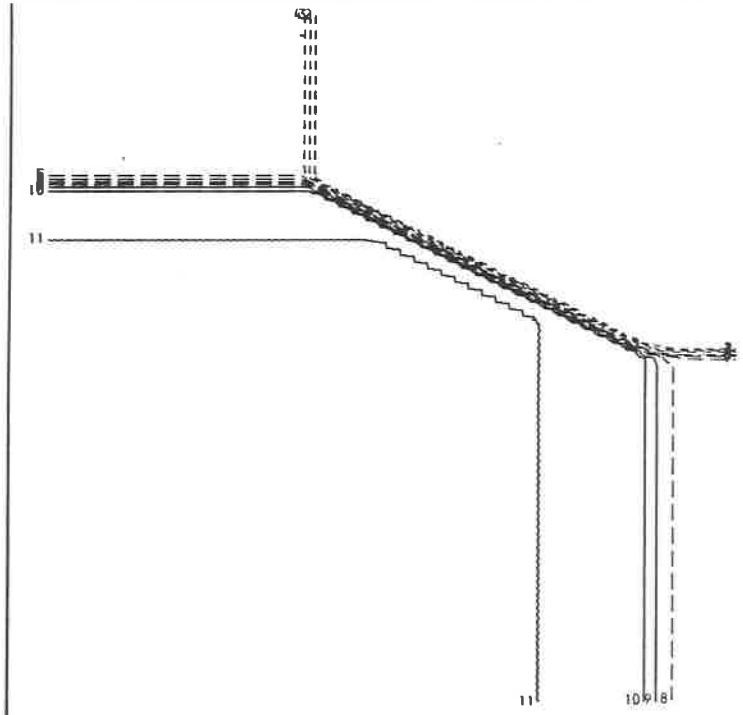


S 2 R P 2 1

CONTOUR HEIGHTS

| | | | |
|---|---|---|---|
| 1 | -0.5000 | 2 | -0.3500 |
| 3 | -0.2000 | 4 | -0.0500 |
| 5 | 0.1000 | 6 | 0.2500 |
| 7 | 0.4000 | 8 | 0.5500 |
| 9 | 0.7000 | 10 | 0.8500 |
| 11 | 1.0000 | | |

Figure 38

# TWO DIMENSIONAL RIEMANN PROBLEM

SOLN. AT TIME T = 0.50

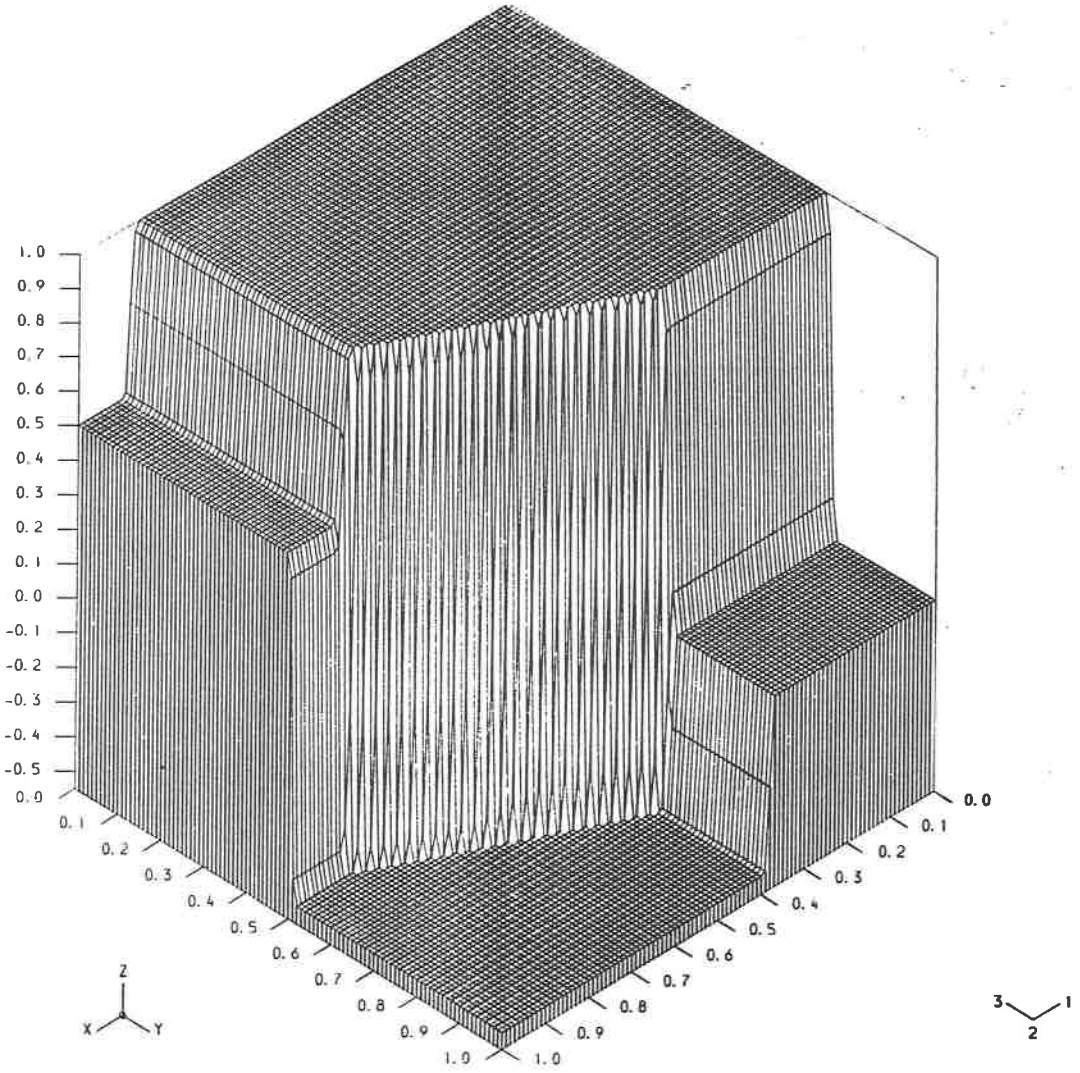


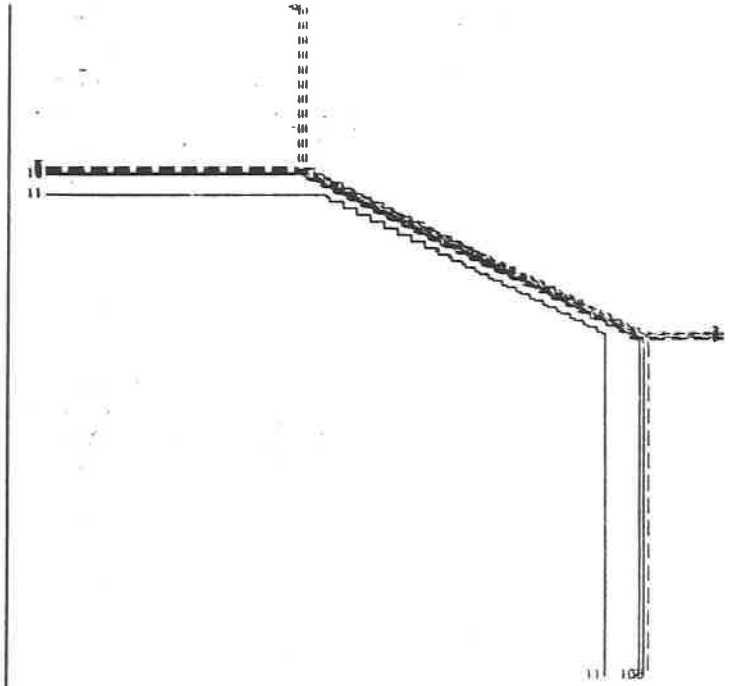

S 2 R P 2 2

CONTOUR HEIGHTS

| | | | |
|---|---|---|---|
| 1 | -0.5000 | 2 | -0.3500 |
| 3 | -0.2000 | 4 | -0.0500 |
| 5 | 0.1000 | 6 | 0.2500 |
| 7 | 0.4000 | 8 | 0.5500 |
| 9 | 0.7000 | 10 | 0.8500 |
| 11 | 1.0000 | | |

Figure 39

# TWO DIMENSIONAL RIEMANN PROBLEM

SOLN. AT TIME T = 0.50

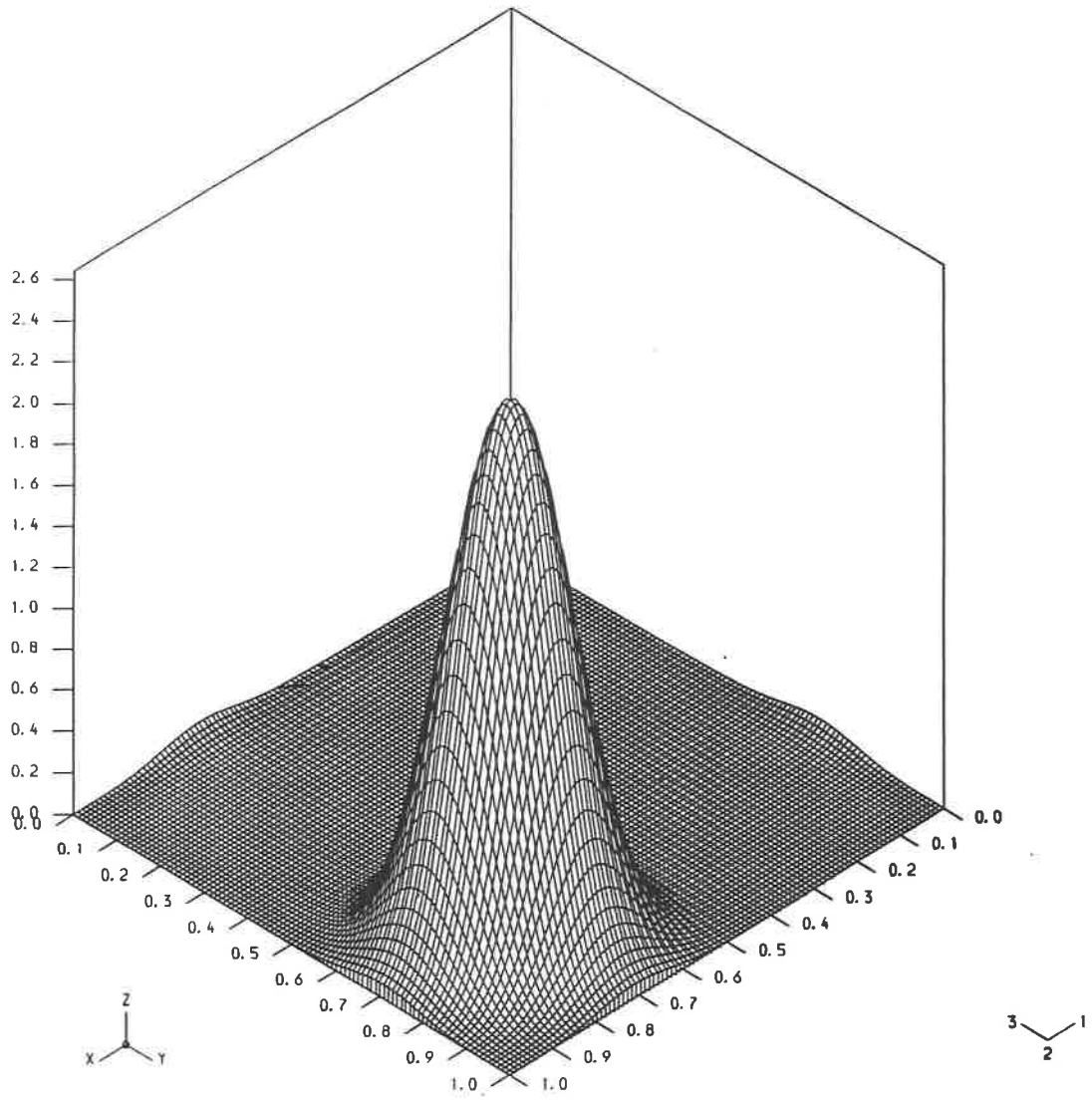


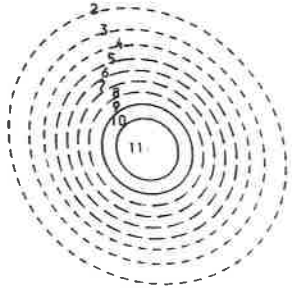


S 3 C B A 1

CONTOUR HEIGHTS

| | | | |
|---|---|---|---|
| 1 | 0.0000 | 2 | 0.2643 |
| 3 | 0.5287 | 4 | 0.7930 |
| 5 | 1.0573 | 6 | 1.3217 |
| 7 | 1.5860 | 8 | 1.8503 |
| 9 | 2.1147 | 10 | 2.3790 |
| 11 | 2.6434 | | |

Figure 40

# LINEAR ADVECTION OF A BLIP

SOLN. AT TIME T = 0.50

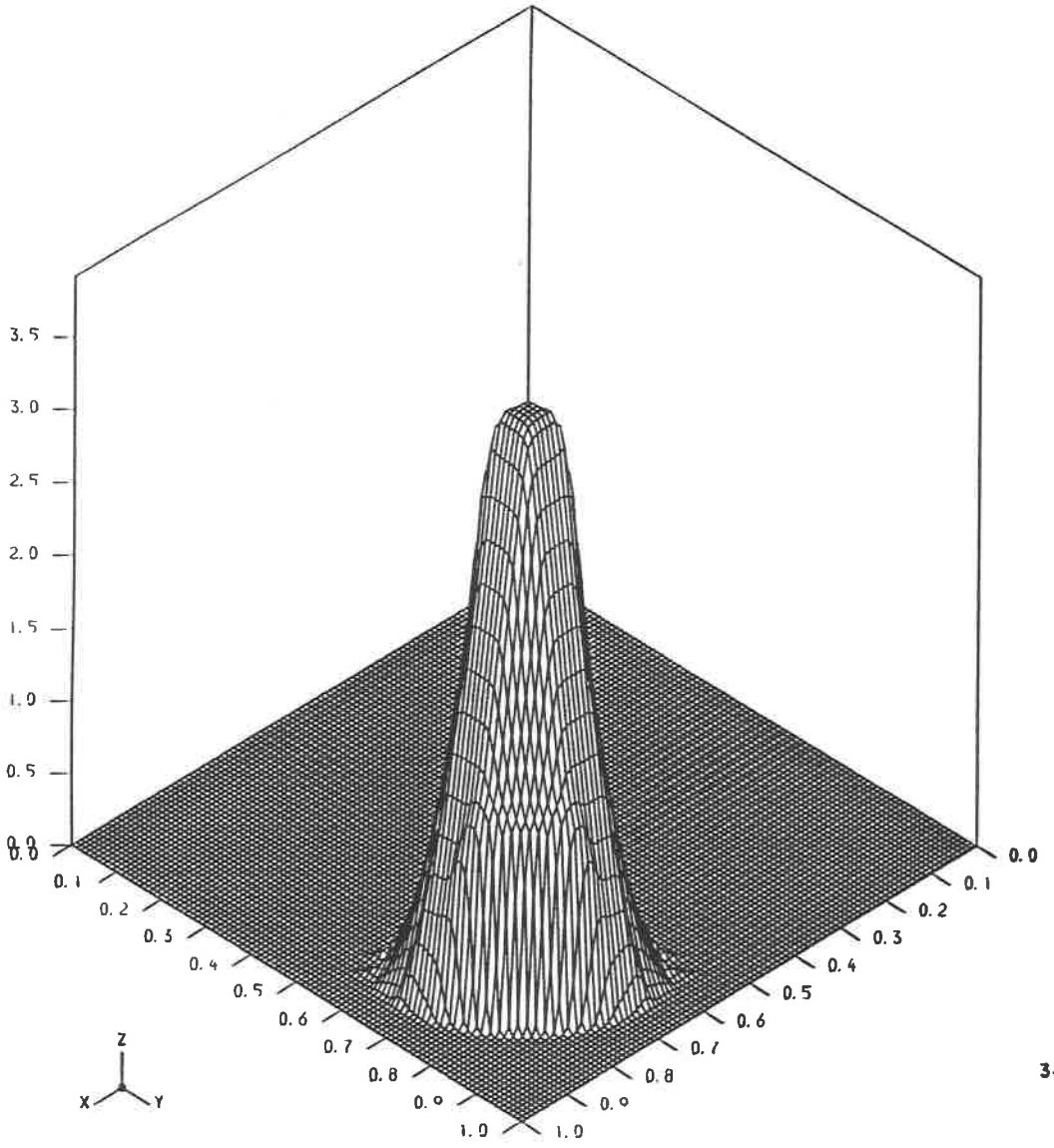


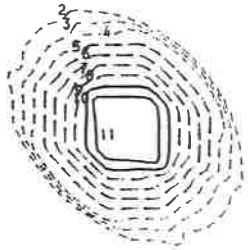


S 3 C B A 2

CONTOUR HEIGHTS

| | | | |
|---|---|---|---|
| 1 | 0.0000 | 2 | 0.3928 |
| 3 | 0.7855 | 4 | 1.1783 |
| 5 | 1.5711 | 6 | 1.9638 |
| 7 | 2.3566 | 8 | 2.7494 |
| 9 | 3.1421 | 10 | 3.5349 |
| 11 | 3.9277 | | |

Figure 41

# LINEAR ADVECTION OF A BLIP

SOLN. AT TIME T = 0.50

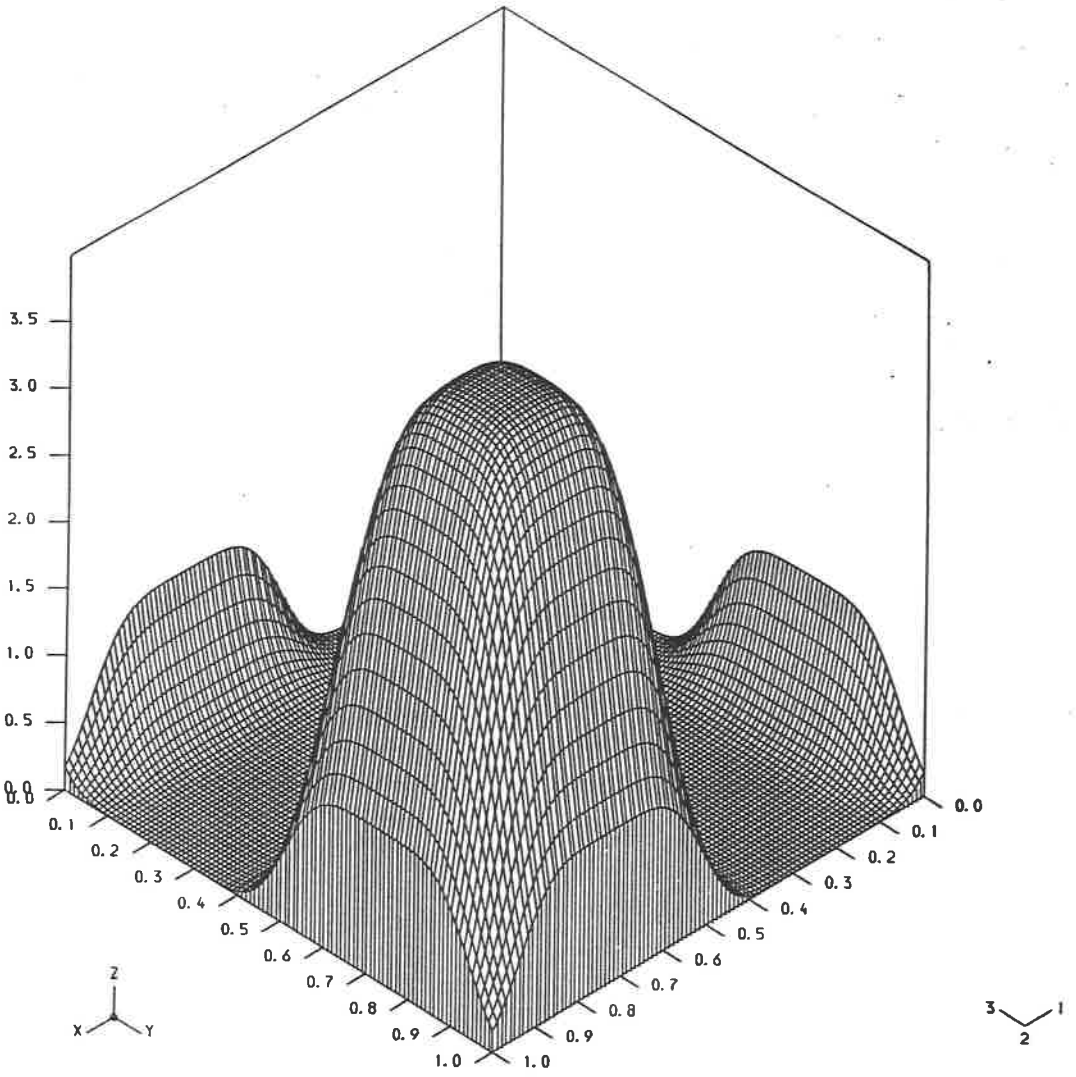


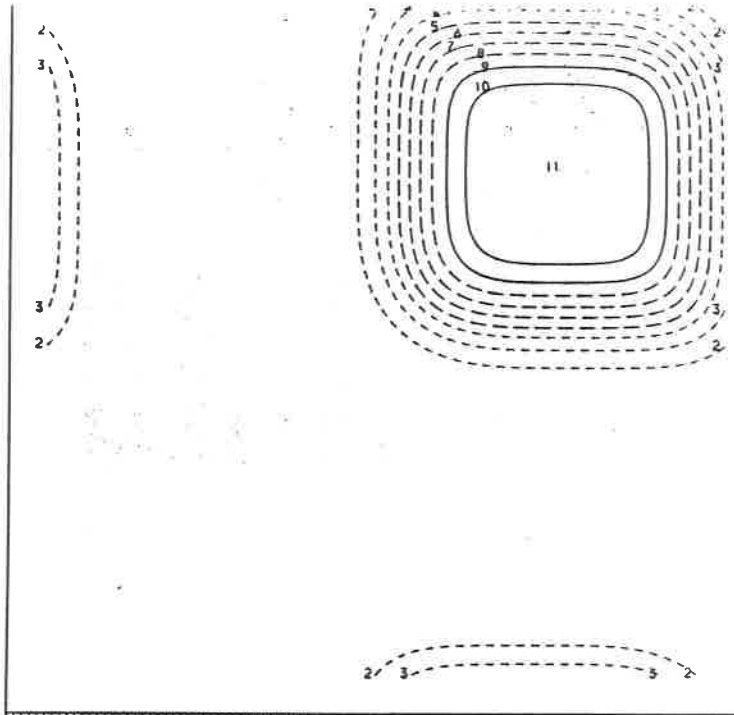


S 3 B A 1

CONTOUR HEIGHTS

| | | | |
|---|---|---|---|
| 1 | 0.0000 | 2 | 0.3997 |
| 3 | 0.7993 | 4 | 1.1990 |
| 5 | 1.5987 | 6 | 1.9984 |
| 7 | 2.3980 | 8 | 2.7977 |
| 9 | 3.1974 | 10 | 3.5970 |
| 11 | 3.9967 | | |

Figure 42

# LINEAR ADVECTION OF A BOX

SOLN. AT TIME T = 0.50

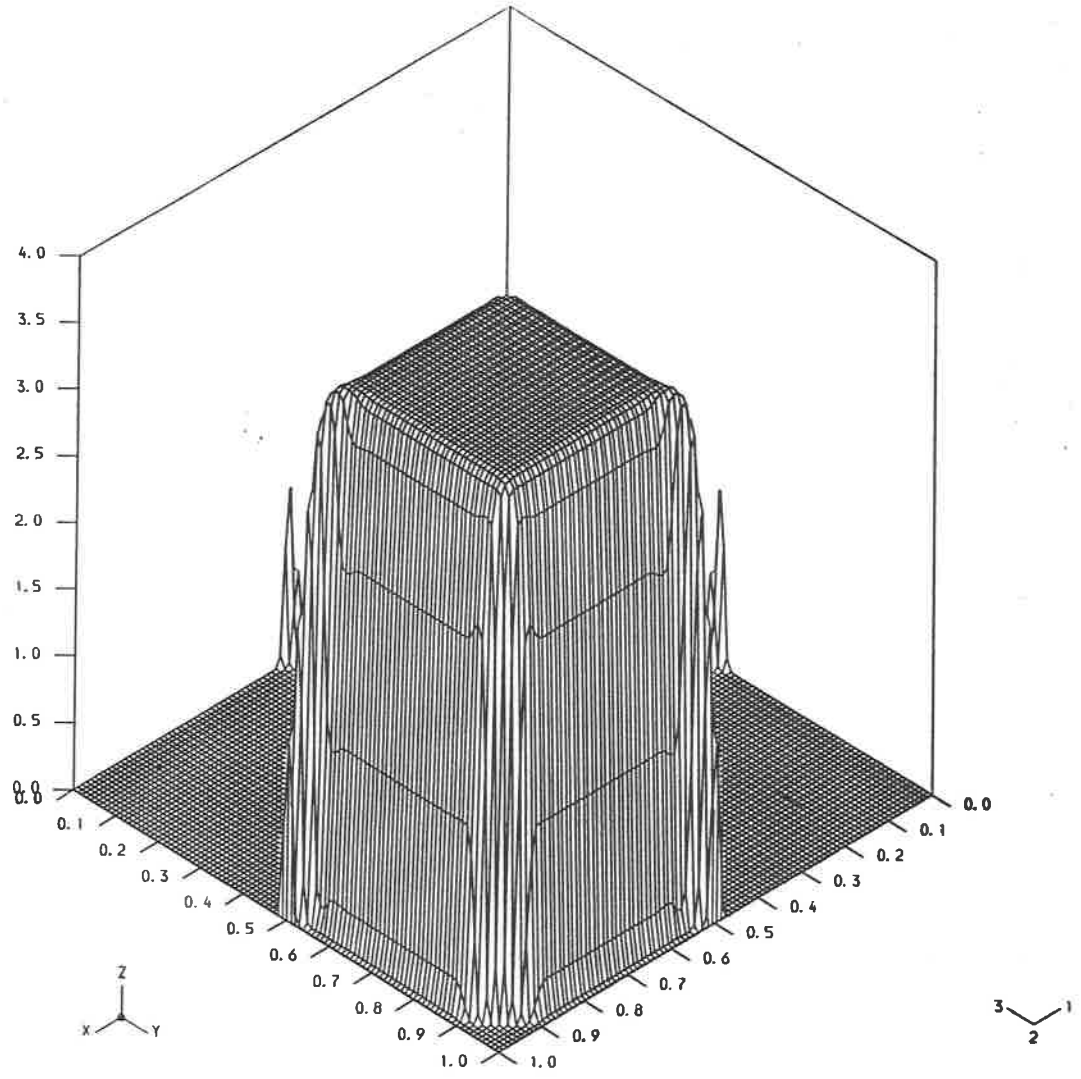


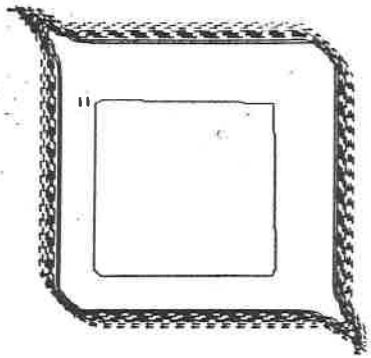

S 3 B A 2

CONTOUR HEIGHTS

| | | | |
|---|---|---|---|
| 1 | 0.0000 | 2 | 0.4000 |
| 3 | 0.8000 | 4 | 1.2000 |
| 5 | 1.6000 | 6 | 2.0000 |
| 7 | 2.4000 | 8 | 2.8000 |
| 9 | 3.2000 | 10 | 3.6000 |
| 11 | 4.0000 | | |

Figure 43

# LINEAR ADVECTION OF A BOX

SOLN. AT TIME T = 0.50

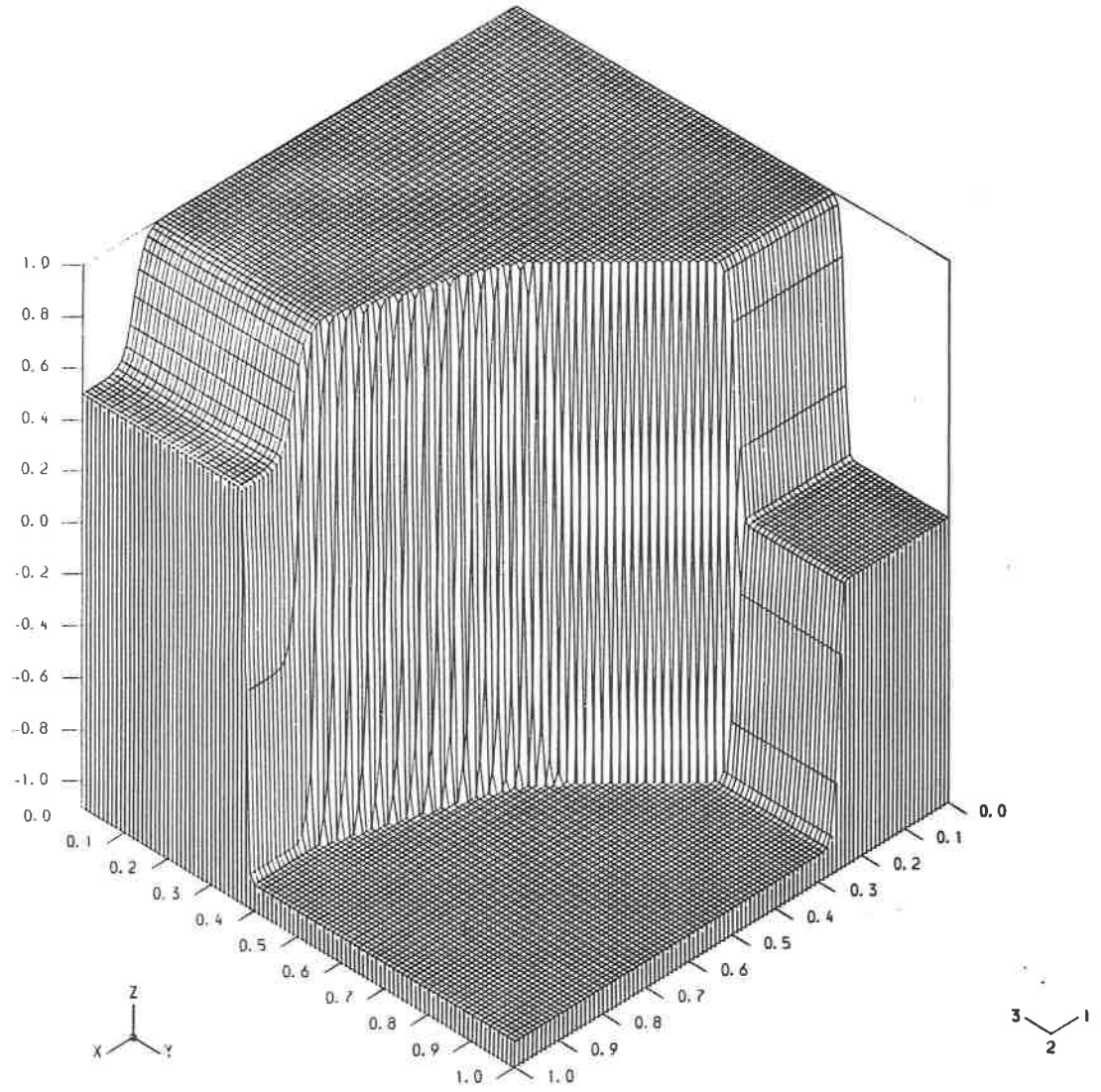


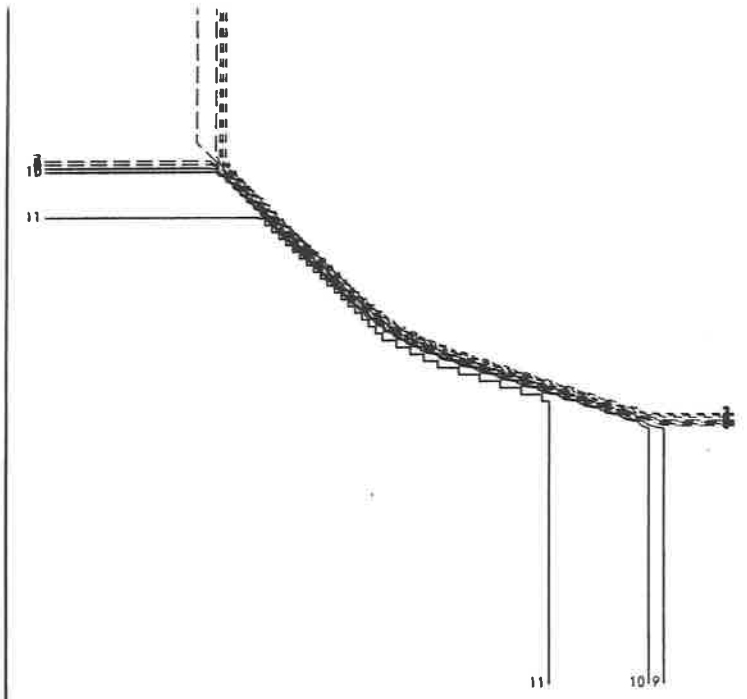


S 3 R P 1 1

CONTOUR HEIGHTS

| | | | |
|---|---|---|---|
| 1 | -1.0000 | 2 | -0.8000 |
| 3 | -0.6000 | 4 | -0.4000 |
| 5 | -0.2000 | 6 | 0.0000 |
| 7 | 0.2000 | 8 | 0.4000 |
| 9 | 0.6000 | 10 | 0.8000 |
| 11 | 1.0000 | | |

Figure 44

# TWO DIMENSIONAL RIEMANN PROBLEM

SOLN. AT TIME T = 0.50

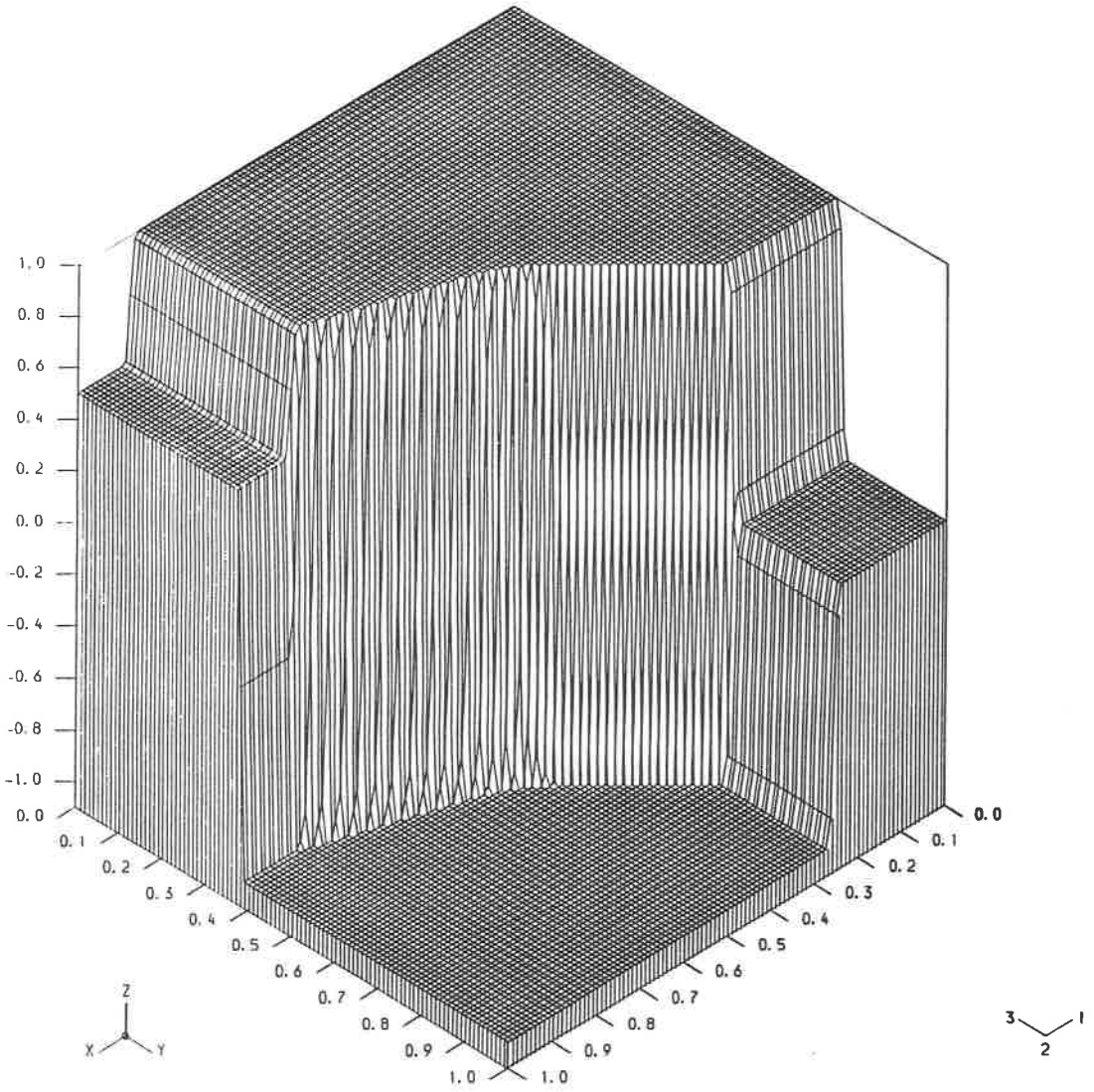


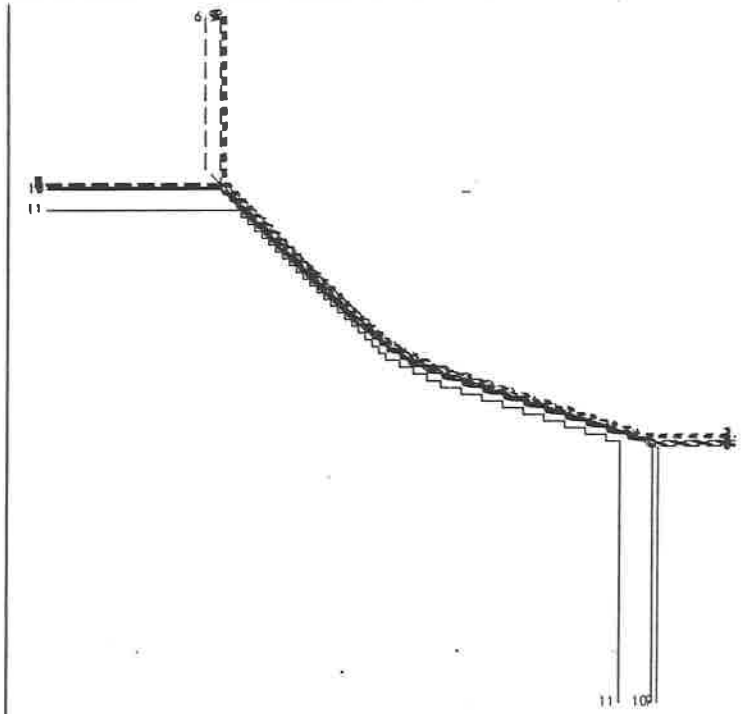


S 3 R P 1 2

CONTOUR HEIGHTS

| | | | |
|---|---|---|---|
| 1 | -1.0000 | 2 | -0.8000 |
| 3 | -0.6000 | 4 | -0.4000 |
| 5 | -0.2000 | 6 | 0.0000 |
| 7 | 0.2000 | 8 | 0.4000 |
| 9 | 0.6000 | 10 | 0.8000 |
| 11 | 1.0000 | | |

Figure 45

# TWO DIMENSIONAL RIEMANN PROBLEM

SOLN. AT TIME T = 0.50

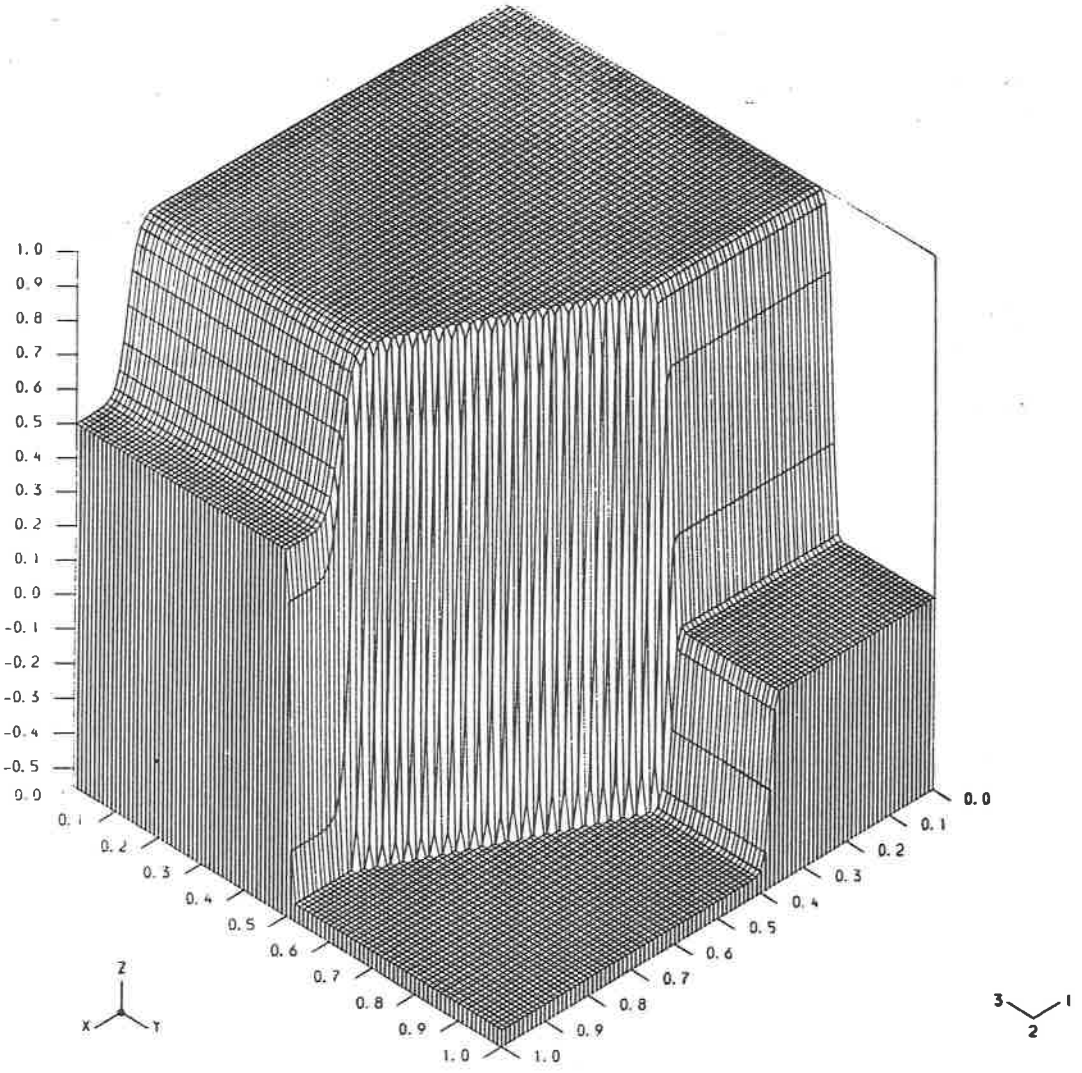


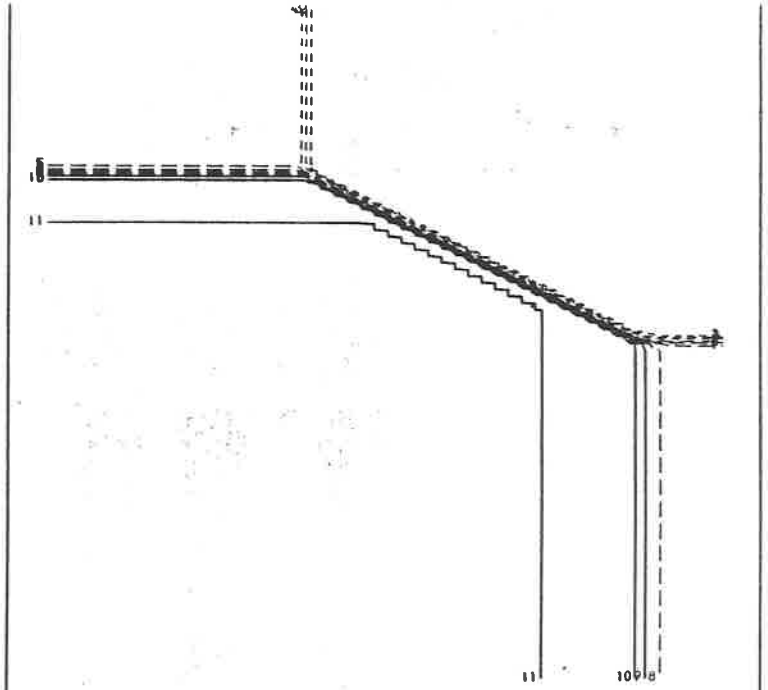

S 3 R P 2 1

CONTOUR HEIGHTS

| | | | |
|---|---|---|---|
| 1 | -0.5000 | 2 | -0.3500 |
| 3 | -0.2000 | 4 | -0.0500 |
| 5 | 0.1000 | 6 | 0.2500 |
| 7 | 0.4000 | 8 | 0.5500 |
| 9 | 0.7000 | 10 | 0.8500 |
| 11 | 1.0000 | | |

Figure 46

# TWO DIMENSIONAL RIEMANN PROBLEM

SOLN. AT TIME T = 0.50

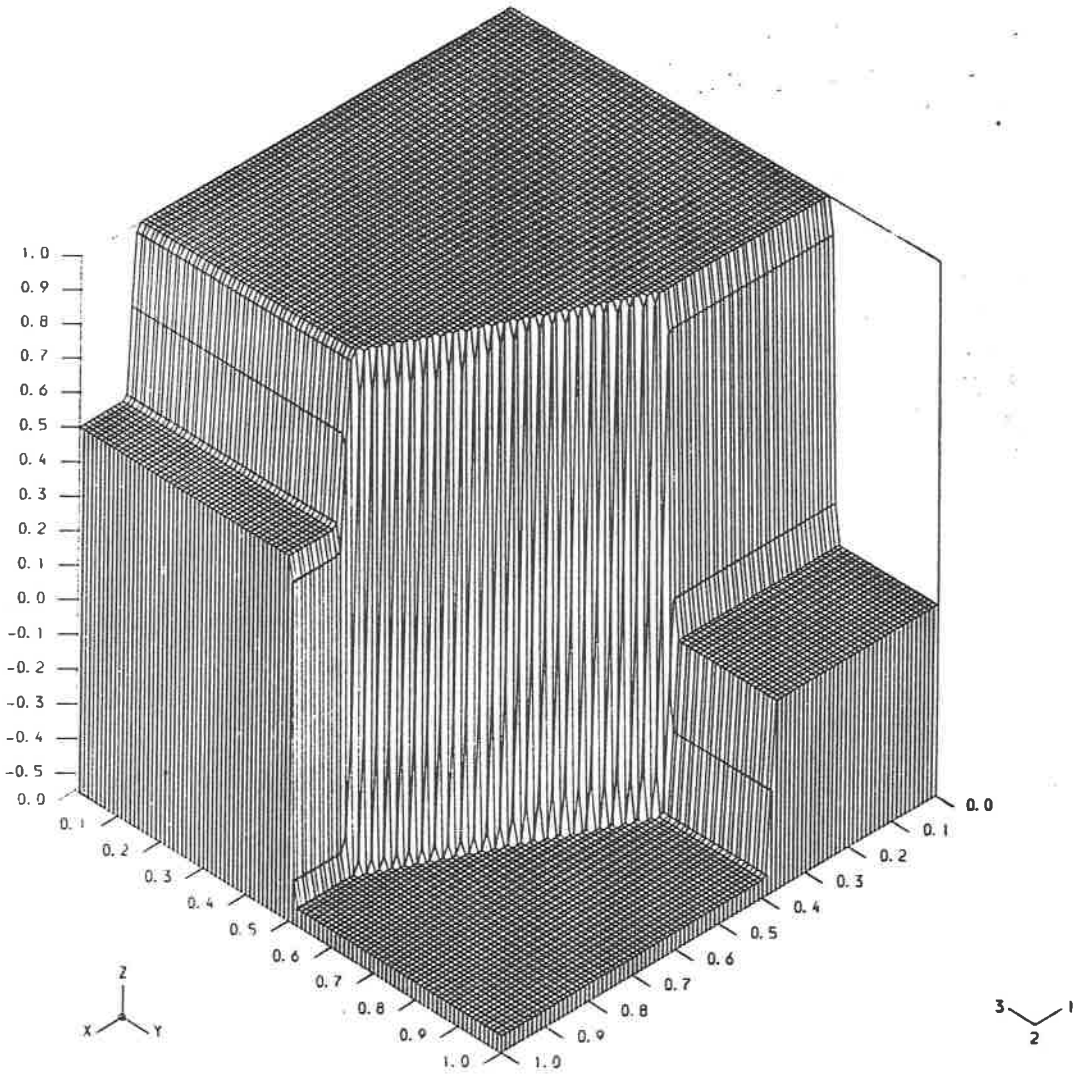


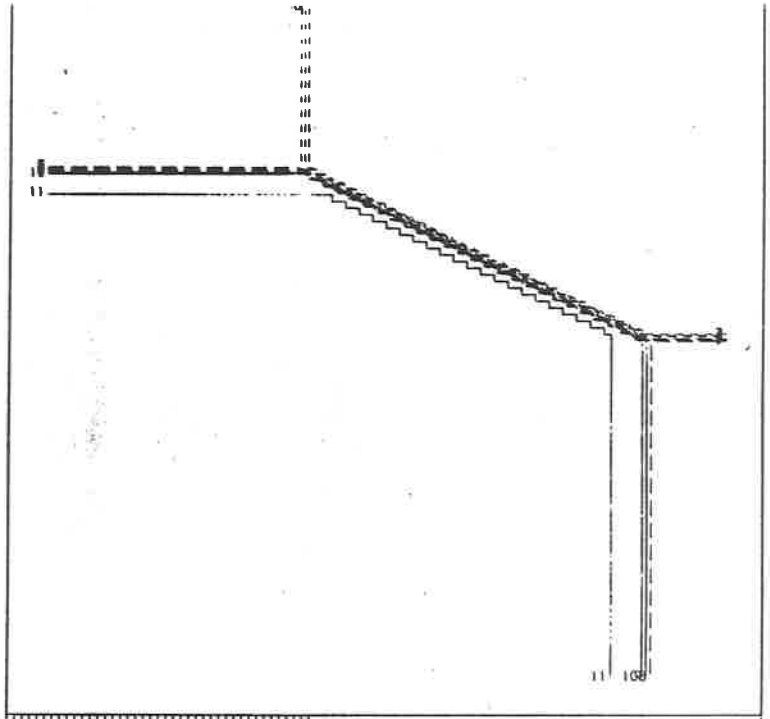

S 3 R P 2 2

CONTOUR HEIGHTS

| | | | |
|---|---|---|---|
| 1 | -0.5000 | 2 | -0.3500 |
| 3 | -0.2000 | 4 | -0.0500 |
| 5 | 0.1000 | 6 | 0.2500 |
| 7 | 0.4000 | 8 | 0.5500 |
| 9 | 0.7000 | 10 | 0.8500 |
| 11 | 1.0000 | | |

Figure 47

# TWO DIMENSIONAL RIEMANN PROBLEM

SOLN. AT TIME T = 0.50

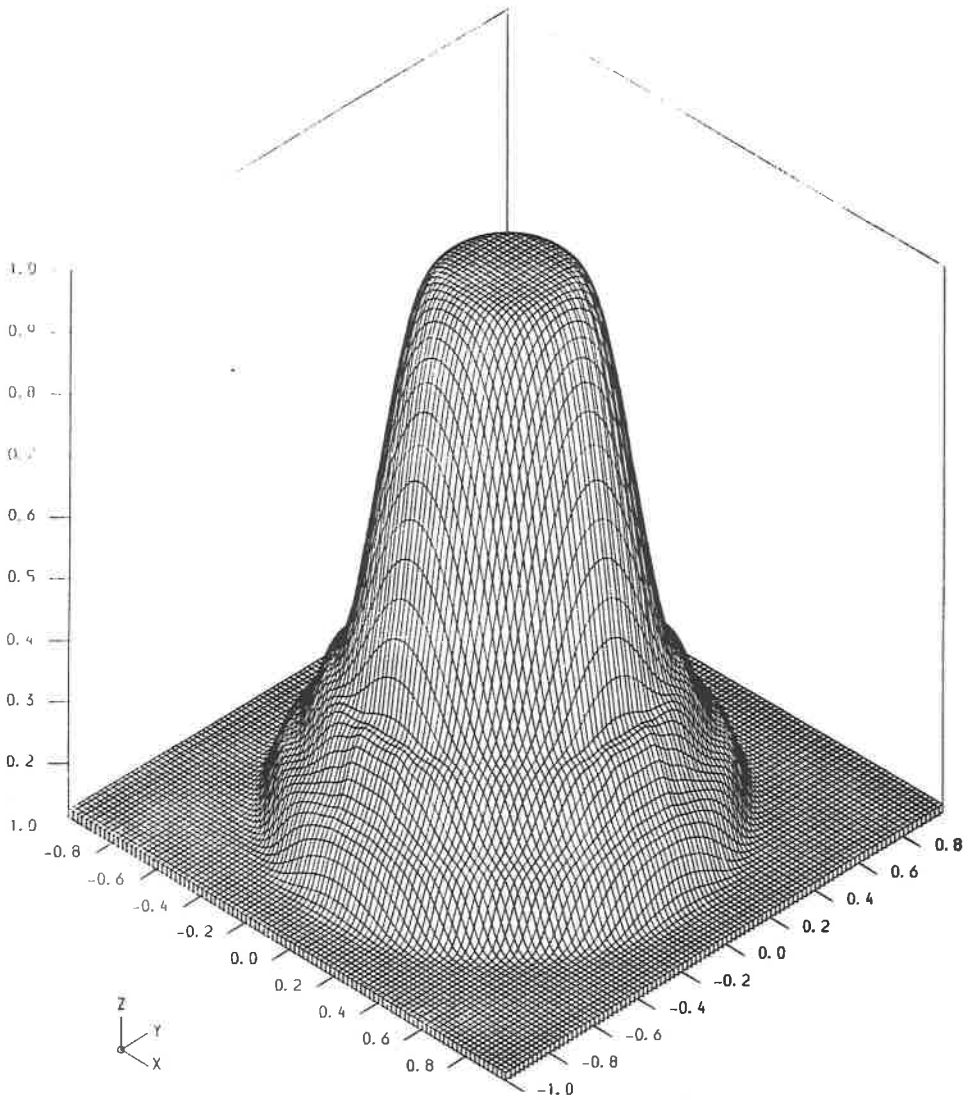


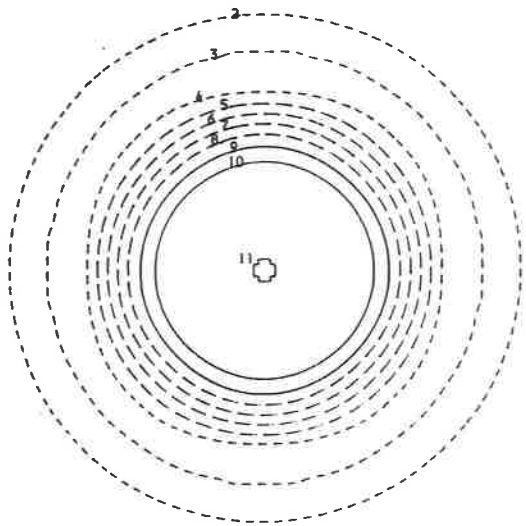


## DENSITY

CONTOUR HEIGHTS

| | | | |
|---|---|---|---|
| 1 | 0.1250 | 2 | 0.2125 |
| 3 | 0.3000 | 4 | 0.3875 |
| 5 | 0.4750 | 6 | 0.5625 |
| 7 | 0.6500 | 8 | 0.7375 |
| 9 | 0.8250 | 10 | 0.9125 |
| 11 | 1.0000 | | |

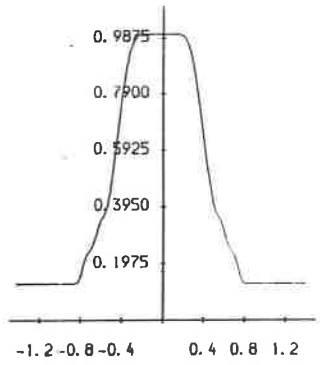


# CYLINDRICALLY DIVERGENT SHOCK (SOD)

SOLN. AT TIME T = 0.14

Figure 48 FIRST ORDER S1

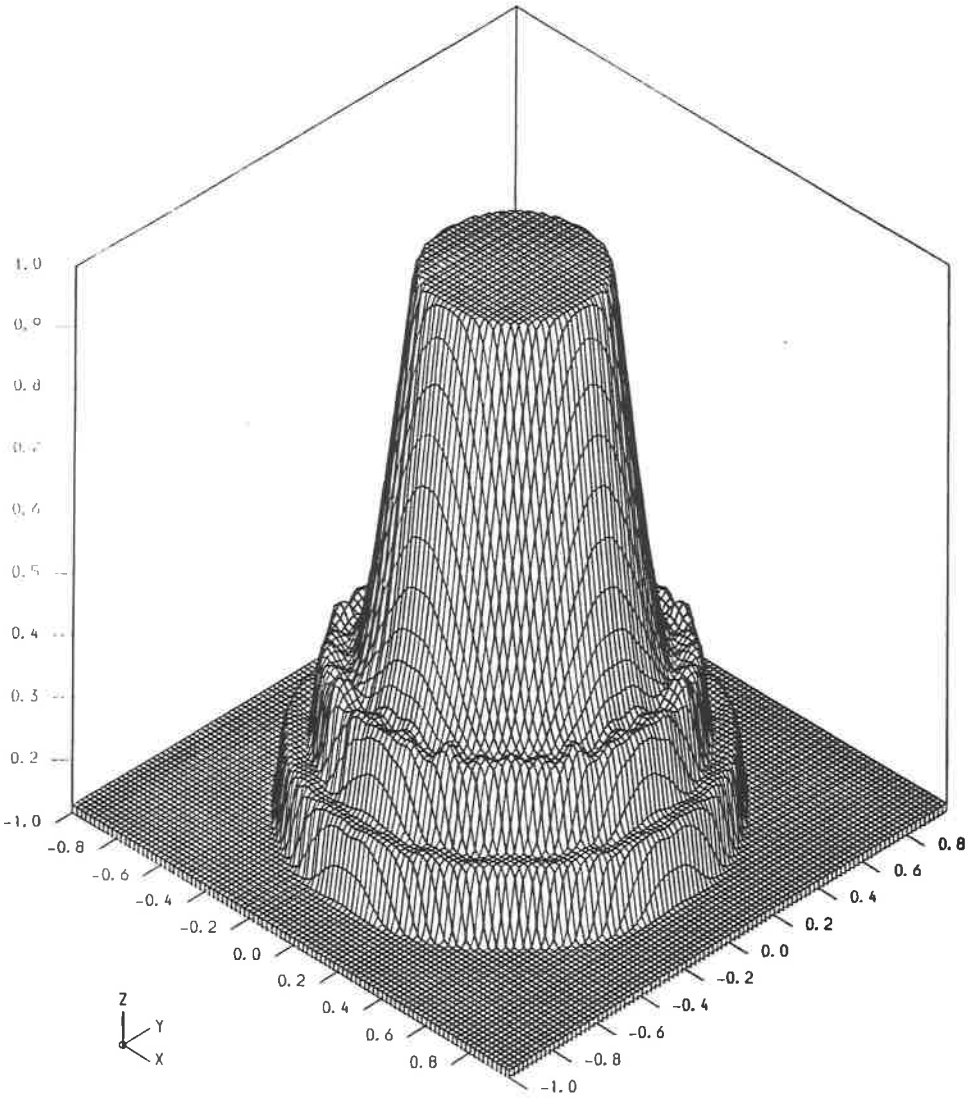


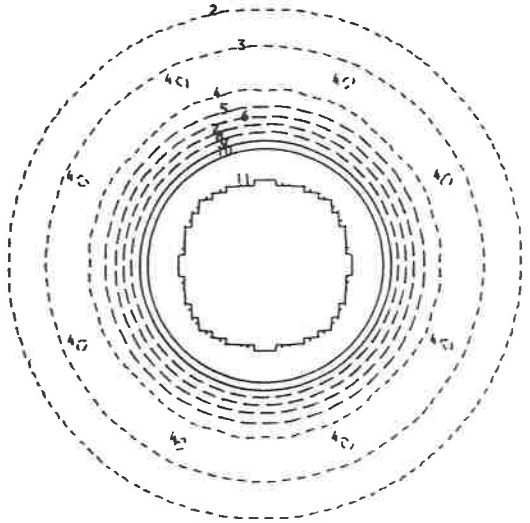

| DENSITY | | | |
|---|---|---|---|
| CONTOUR HEIGHTS | | | |
| 1 | 0.1250 | 2 | 0.2125 |
| 3 | 0.3000 | 4 | 0.3875 |
| 5 | 0.4750 | 6 | 0.5625 |
| 7 | 0.6500 | 8 | 0.7375 |
| 9 | 0.8250 | 10 | 0.9125 |
| 11 | 1.0000 | | |

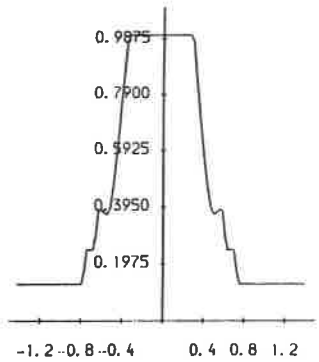


# CYLINDRICALLY DIVERGENT SHOCK (SOD)

SOLN. AT TIME T = 0.14

Figure 49 SECOND ORDER S1 'SUPERBEE' LIMITER USED

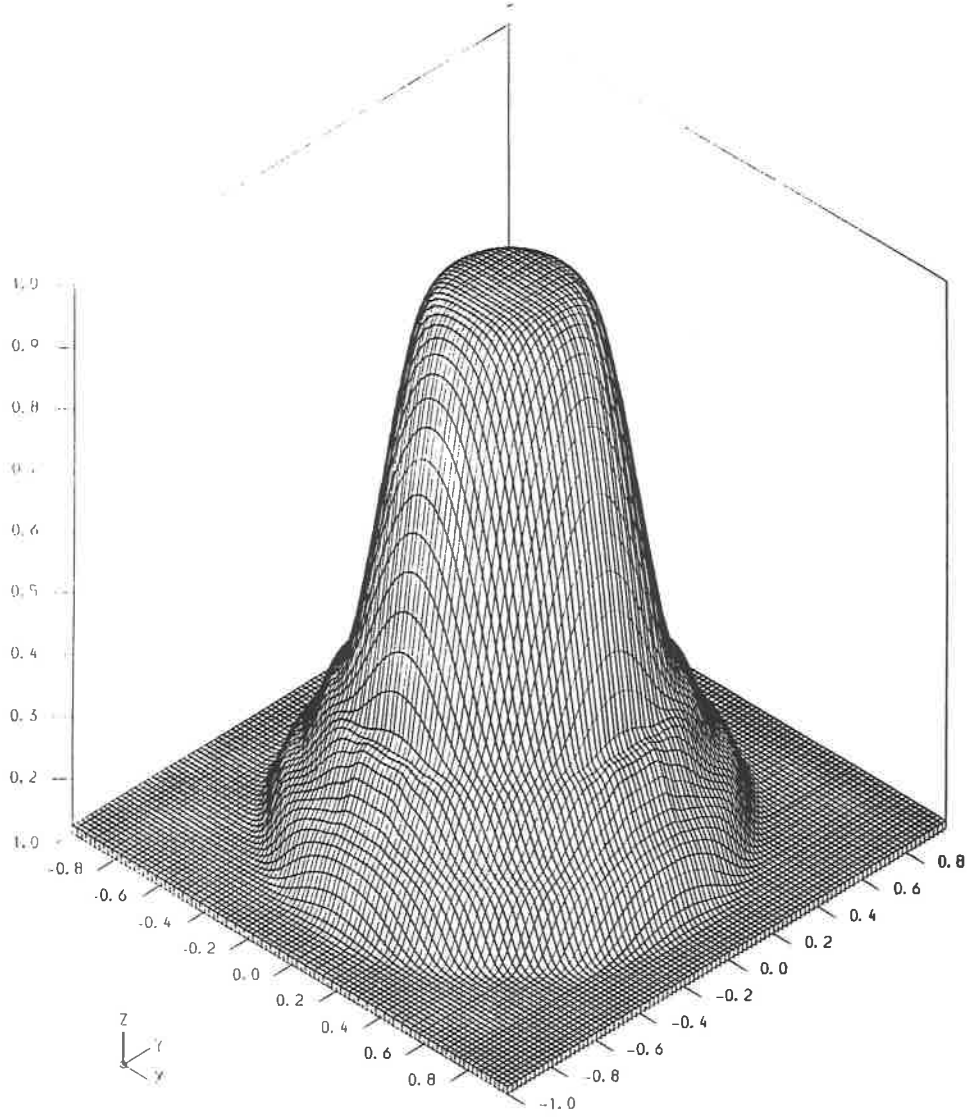


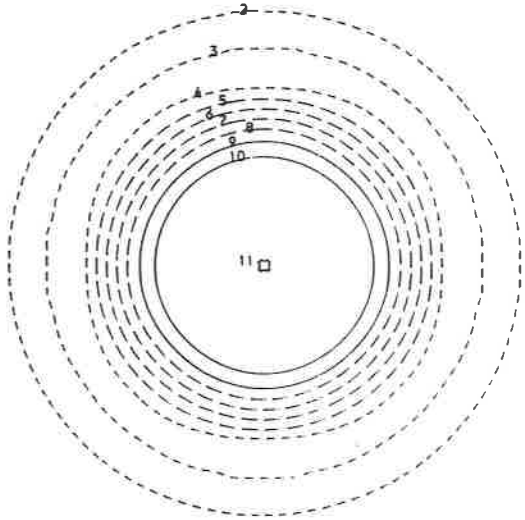


DENSITY

CONTOUR HEIGHTS

| | | | |
|---|---|---|---|
| 1 | 0.1250 | 2 | 0.2125 |
| 3 | 0.3000 | 4 | 0.3875 |
| 5 | 0.4750 | 6 | 0.5625 |
| 7 | 0.6500 | 8 | 0.7375 |
| 9 | 0.8250 | 10 | 0.9125 |
| 11 | 1.0000 | | |

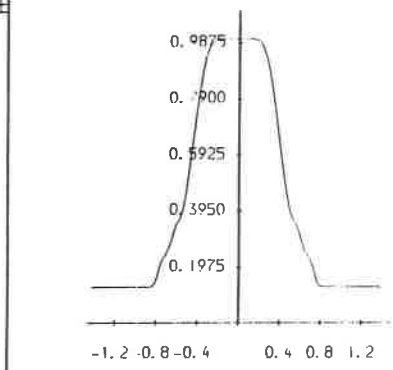


# CYLINDRICALLY DIVERGENT SHOCK (SOD)

SOLN. AT TIME T = 0.14

Figure 50 FIRST ORDER S2

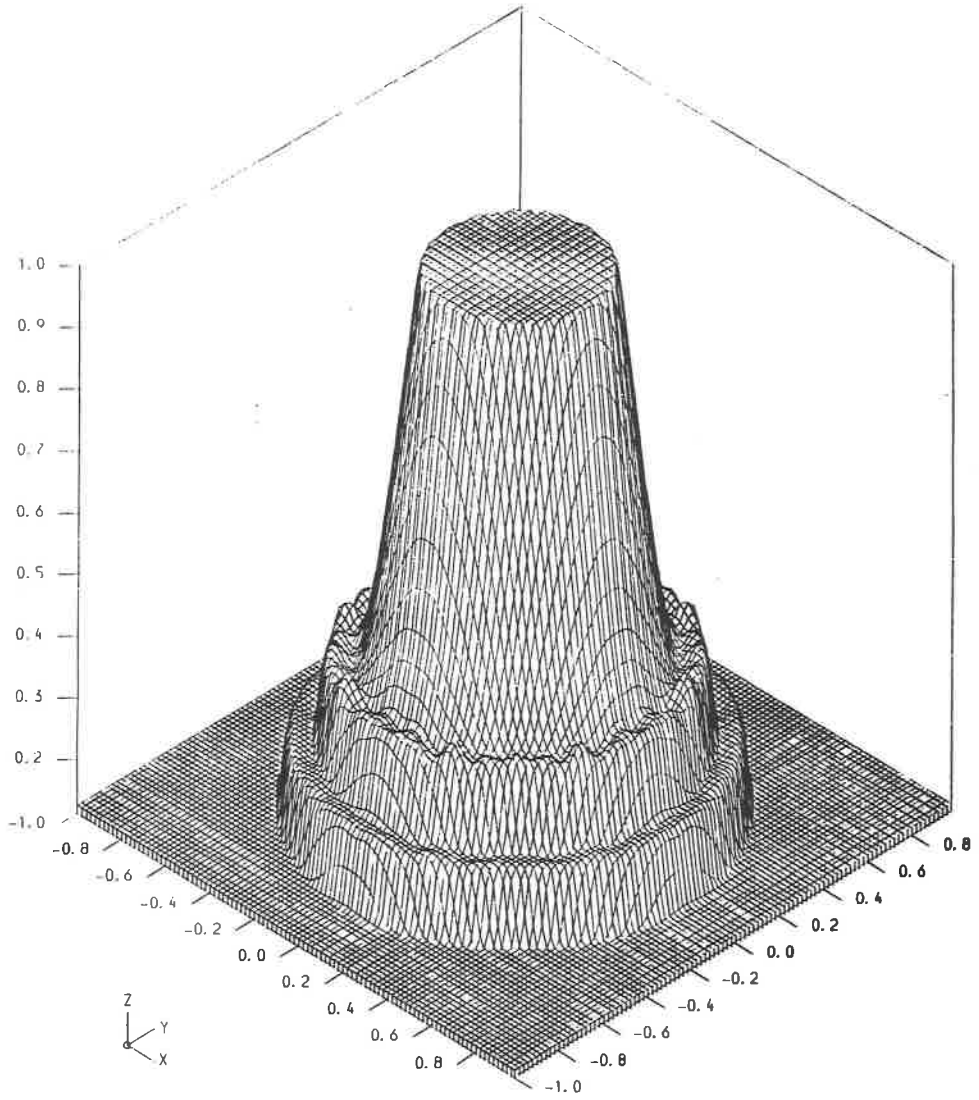


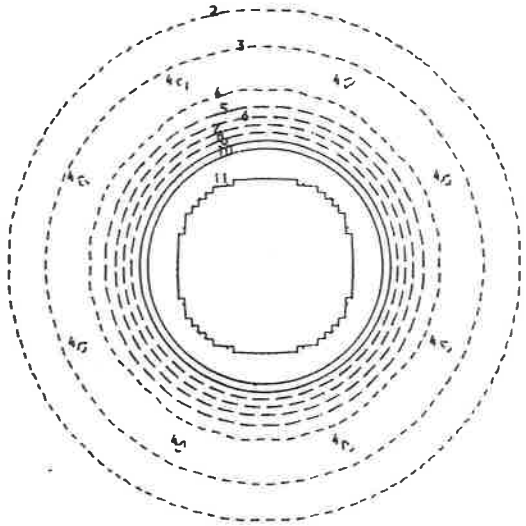

DENSITY

CONTOUR HEIGHTS

| | | | |
|---|---|---|---|
| 1 | 0.1250 | 2 | 0.2125 |
| 3 | 0.3000 | 4 | 0.3875 |
| 5 | 0.4750 | 6 | 0.5625 |
| 7 | 0.6500 | 8 | 0.7375 |
| 9 | 0.8250 | 10 | 0.9125 |
| 11 | 1.0000 | | |

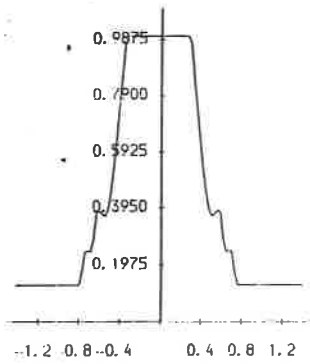


# CYLINDRICALLY DIVERGENT SHOCK (SOD)

SOLN. AT TIME T = 0.14

FIGURE 51 SECOND ORDER S2 'SUPERBEE' LIMITER USED

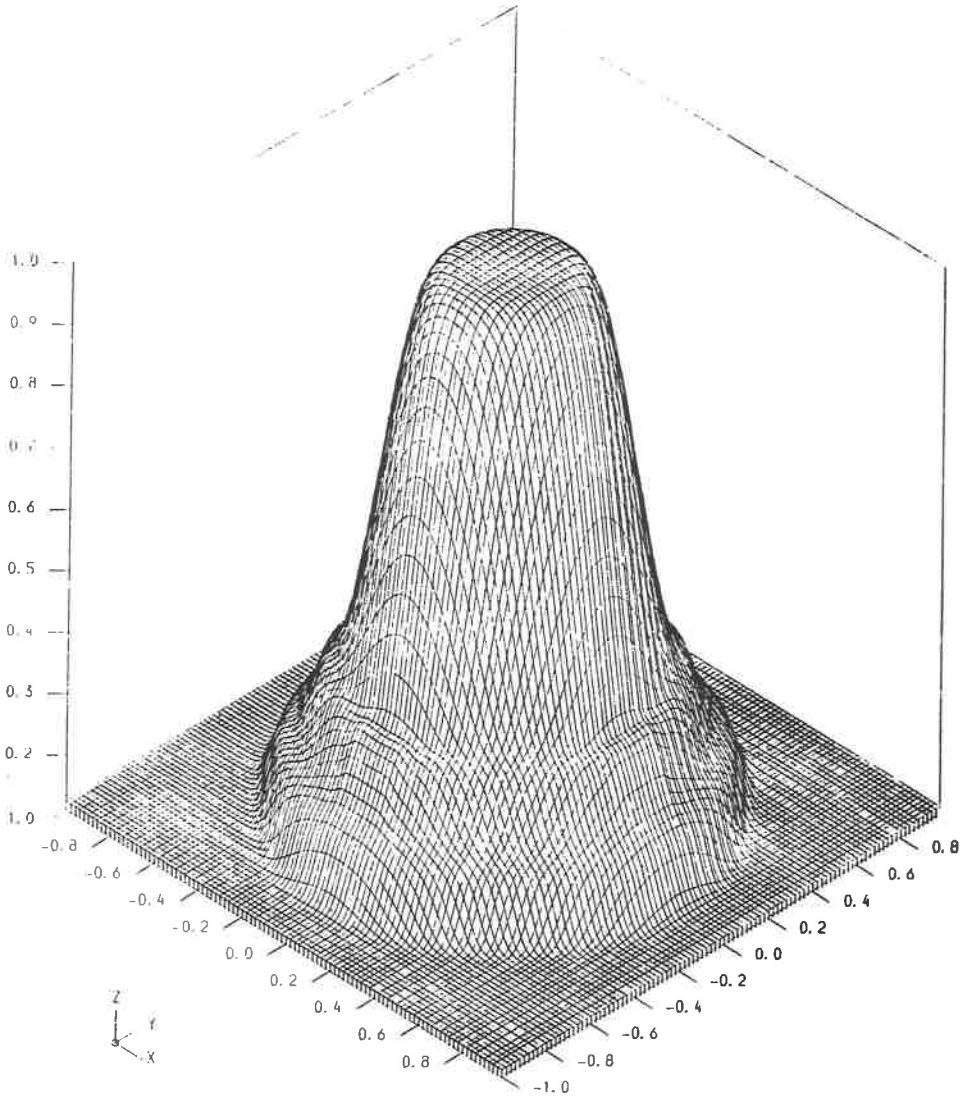


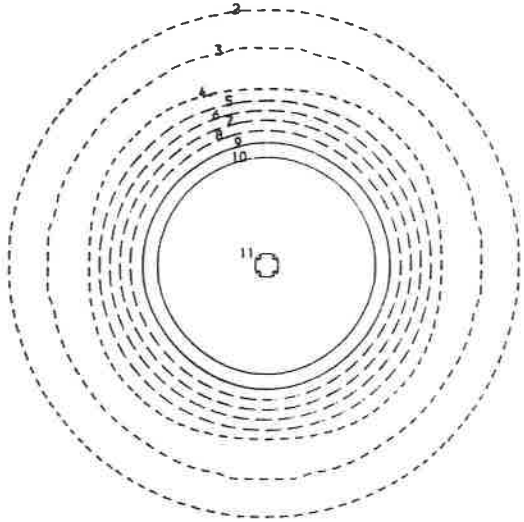



## DENSITY

CONTOUR HEIGHTS

| | | | |
|---|---|---|---|
| 1 | 0.1250 | 2 | 0.2125 |
| 3 | 0.3000 | 4 | 0.3875 |
| 5 | 0.4750 | 6 | 0.5625 |
| 7 | 0.6500 | 8 | 0.7375 |
| 9 | 0.8250 | 10 | 0.9125 |
| 11 | 1.0000 | | |

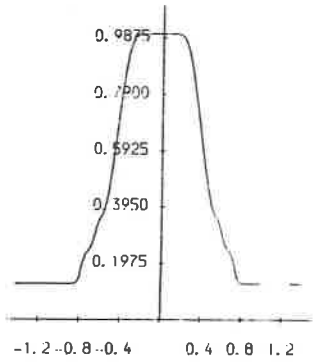


# CYLINDRICALLY DIVERGENT SHOCK (SOD)

SOLN. AT TIME T = 0.14

FIGURE 52 FIRST ORDER S3

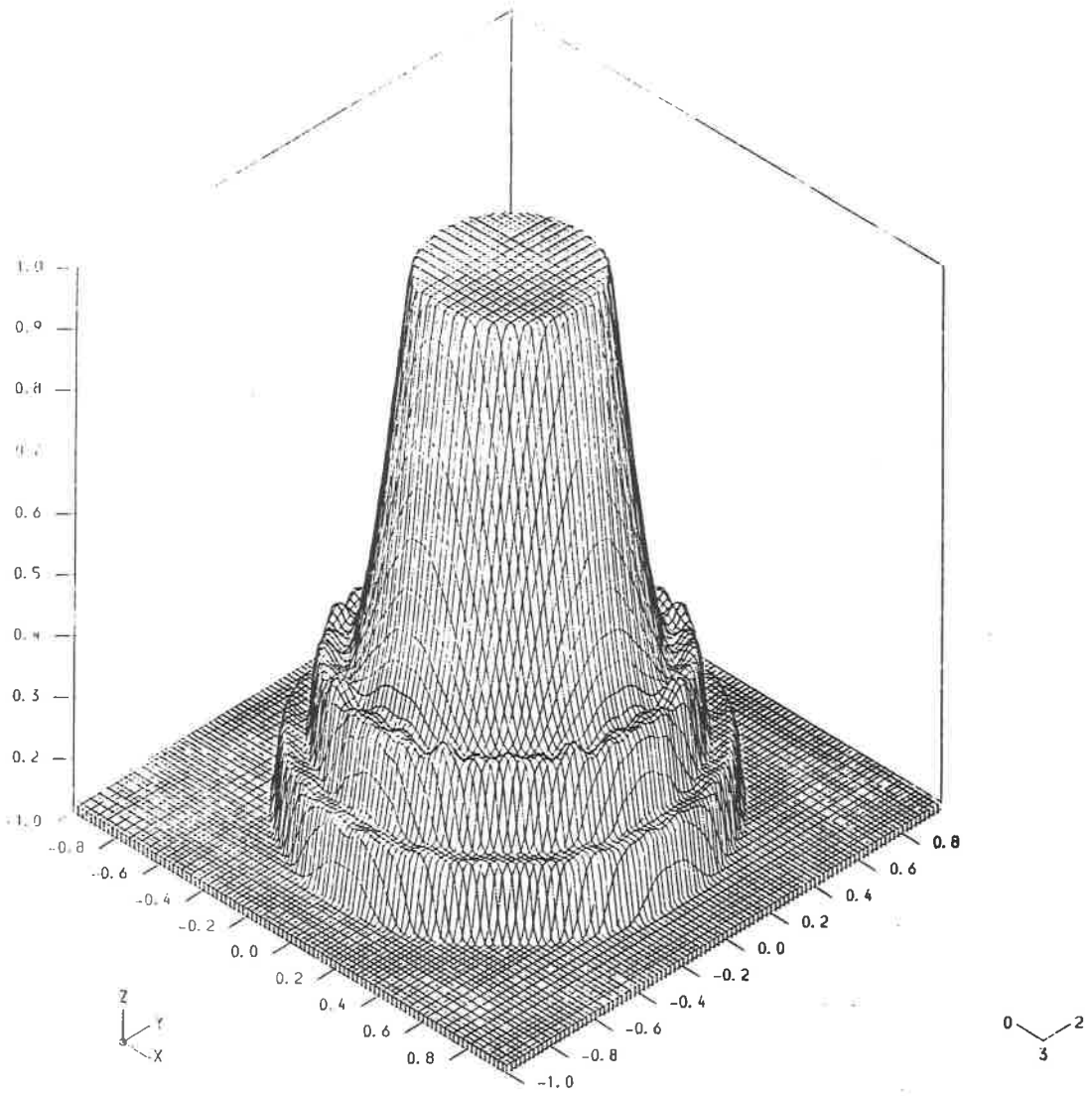


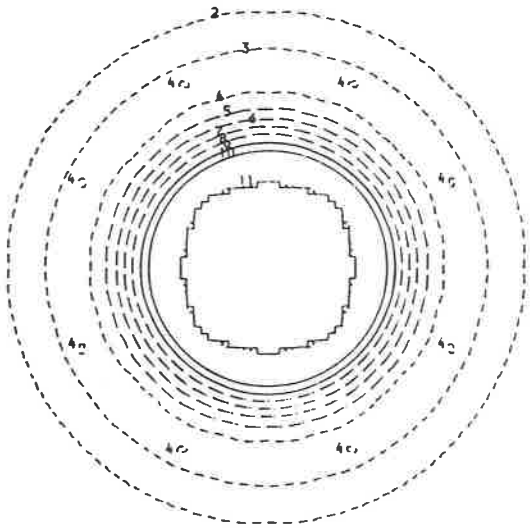

DENSITY

CONTOUR HEIGHTS

| | | | |
|---|---|---|---|
| 1 | 0.1250 | 2 | 0.2125 |
| 3 | 0.3000 | 4 | 0.3875 |
| 5 | 0.4750 | 6 | 0.5625 |
| 7 | 0.6500 | 8 | 0.7375 |
| 9 | 0.8250 | 10 | 0.9125 |
| 11 | 1.0000 | | |

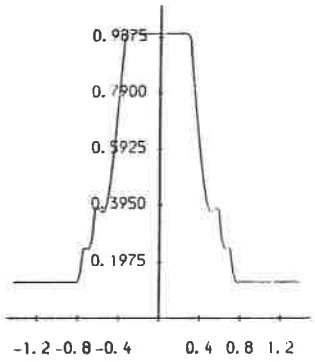


# CYLINDRICALLY DIVERGENT SHOCK (SOD)

SOLN. AT TIME T = 0.14

FIGURE 53 SECOND ORDER S3 'SUPERBEE' LIMITER USED